

2

AD-A214 460

**DEPARTMENT OF
MATERIALS SCIENCE AND MINERAL ENGINEERING**

AIRBORNE ELECTROMAGNETIC SENSING OF SEA ICE THICKNESS

Final Report
prepared for NORDA
Under U.C.B. contract #N00014-87-K-6005
482456-25867 (GF-25867)

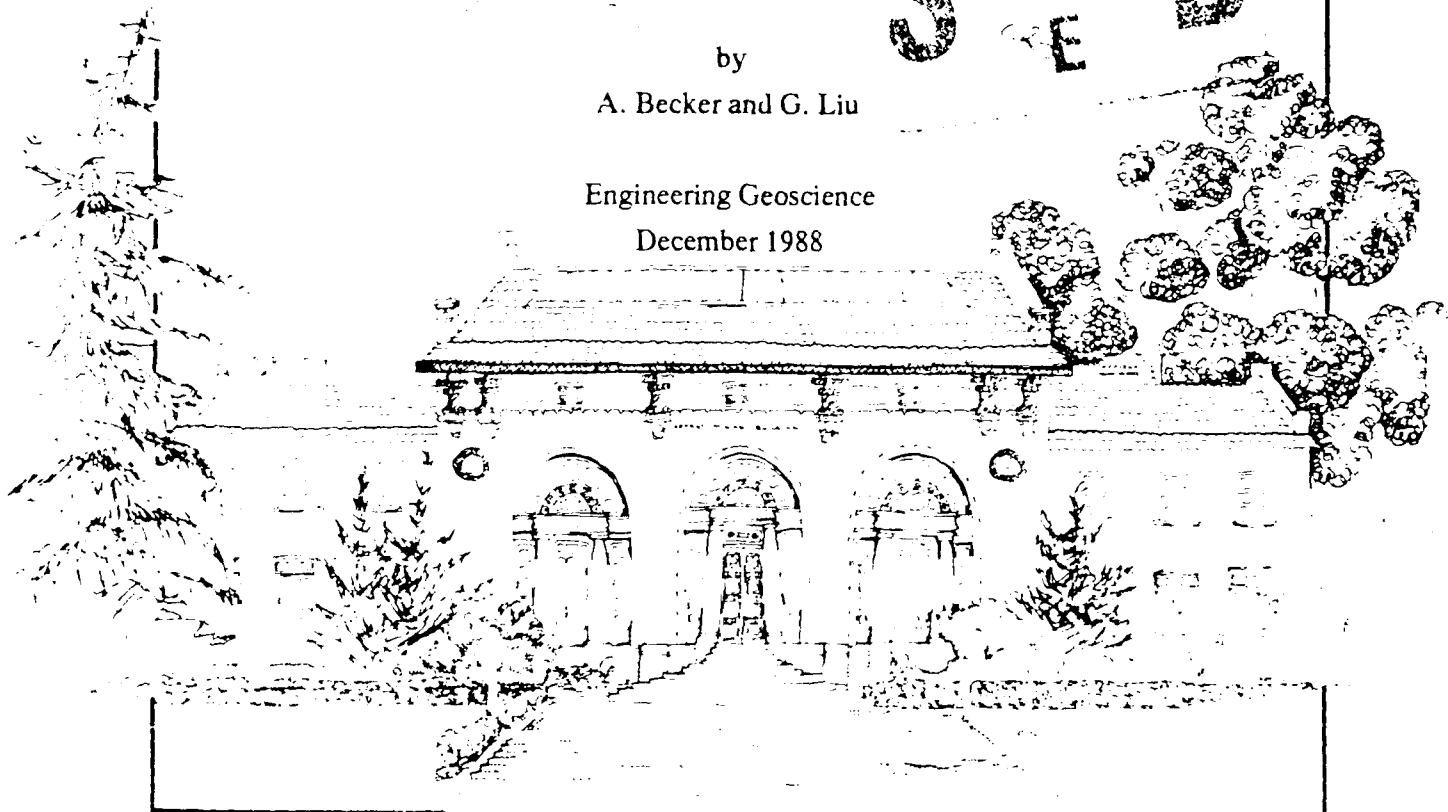
DEPARTMENT OF MATERIALS SCIENCE AND MINERAL ENGINEERING
UNIVERSITY OF CALIFORNIA, BERKELEY

DTIC
PUBLISHED
NOV 16 1989
S E D

by

A. Becker and G. Liu

Engineering Geoscience
December 1988



Hearst Mining Building
University of California, Berkeley

89 11 16 114

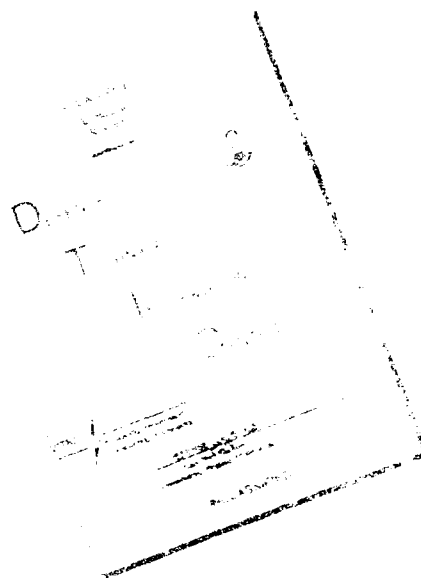
REPORT DOCUMENTATION PAGE			Form Approved OMB No. 0704-0188	
<small>Public reporting burden for this collection of information is estimated to average 1 hour per response, including the time for reviewing instructions, searching existing data sources, gathering and maintaining the data needed, and completing and reviewing the collection of information. Send comments regarding this burden estimate or any other aspect of this collection of information, including suggestions for reducing this burden, to Washington Headquarters Services, Directorate for Information Operations and Reports, 1215 Jefferson Davis Highway, Suite 1204, Arlington, VA 22202-4302, and to the Office of Management and Budget, Paperwork Reduction Project (0704-0188), Washington, DC 20503.</small>				
1. Agency Use Only (Leave blank).	2. Report Date. Dec. 14, 1988	3. Report Type and Dates Covered. Final		
4. Title and Subtitle. Airborne Electromagnetic Sensing of Sea Ice Thickness		5. Funding Numbers. Program Element No. DE63704 Project No. R129905 Task No. 300 Accession No. DN257087		
6. Author(s). A. Becker and G. Fire				
7. Performing Organization Name(s) and Address(es). Department of Materials Science and Mineral Engineering Hearst Mining Building University of California, Berkeley		8. Performing Organization Report Number. CR N00014-87-K-6005		
9. Sponsoring/Monitoring Agency Name(s) and Address(es). Naval Ocean Research and Development Activity Code 311 SSC, MS 09729-5004		10. Sponsoring/Monitoring Agency Report Number. CR N00014-87-K-6005		
11. Supplementary Notes.				
12a. Distribution/Availability Statement. Approved for public release; distribution is unlimited.		12b. Distribution Code.		
13. Abstract (Maximum 200 words).				
14. Subject Terms. electronic/electrical engineering, physical oceanography snow ice and permatrost			15. Number of Pages. 121	
			16. Price Code.	
17. Security Classification of Report. Unclassified	18. Security Classification of This Page. Unclassified	19. Security Classification of Abstract. Unclassified	20. Limitation of Abstract.	

Summary

A conventional frequency domain helicopter-borne electromagnetic (HEM) system can be used to map sea ice keels with a reasonable degree of accuracy. A preliminary interpretation of the acquired data can be made manually with the help of a nomogram or automated with the use of a table look-up routine on a small computer. Such data may also be more accurately interpreted with the use of an adaptation of Occam's inversion. This scheme allows for the practical non-uniqueness of the inverse solution but selects the smoothest keel shape that is consistent with the field data. The inversion method is much more computationally intensive than the table look-up technique. While the latter can be implemented on a small computer to form an interactive in-flight interpretation system, the inversion technique involves many forward computations and, for the present, is best reserved for post flight data analysis. It is possible that this difficulty can be resolved with the use of specialized computing equipment.

In the strict sense both the proposed interpretation techniques are only suitable for use on data acquired over two dimensional features whose strike length (measured in a direction perpendicular to the flight line) is much greater than the flight height. An examination of the anomalies for three-dimensional keels however, reveals that good data interpretation is possible whenever the keel strike length exceeds the system height by a factor of three.

DISCLAIMER NOTICE



THIS DOCUMENT IS BEST
QUALITY AVAILABLE. THE COPY
FURNISHED TO DTIC CONTAINED
A SIGNIFICANT NUMBER OF
PAGES WHICH DO NOT
REPRODUCE LEGIBLY.

Table of Contents

Table of Illustrations.....	i
1.0 Introduction.....	1
2.0 AEM Anomalies for Ice Keels.....	2
3.0 Charts for Data Interpretation.....	4
4.0 Inversion of AEM Data.....	7
4.1 Theory.....	8
4.2 Inversion of synthetic data.....	13
4.3 Application to low frequency data.....	17
4.4 Discussion.....	20
5.0 The Three Dimensional Keel.....	21
5.1 The keel model.....	22
5.2 Airborne electromagnetic profiles.....	22
5.3 Discussion.....	26
References.....	26
Appendix A Computational Methods	55
Appendix B Computer Programs	67

Accession For	
NTIS GRA&I	<input checked="" type="checkbox"/>
DTIC TAB	<input type="checkbox"/>
Unannounced	<input type="checkbox"/>
Justification	
By	
Distribution/	
Availability Codes	
Dist	Avail and/or Special
A-1	23

Table of Illustrations

	page
Figure 1 HX and HZ systems over sea ice.....	29
Figure 2 System geometry and the traversed feature ($A = 3.4\text{m}$, $w = 21\text{m}$)	30
Figure 3 HX system response for two different ice keels (solid line: $A = 12\text{m}$, $W = 28\text{m}$. dashed line: $A = 12\text{m}$, $W = 14\text{m}$) ..	31
Figure 4 HZ system response for the same ice keels as shown in Figure 3	32
Figure 5 HX system response for two different ice keels (solid line: $A = 12\text{m}$, $W = 28\text{m}$. dashed line: $A = 6\text{m}$, $W = 28\text{m}$)	33
Figure 6 HZ system response for the same ice keels as shown in Figure 5	34
Figure 7 (a) HX system responses. (b) Cross sections of the model keel (solid line) and the interpreted keel (dashed line)	35
Figure 8 Two-dimensional interpretation chart for the HX system response. Point C for the theoretical data shown in Figure 8, point D for the 930 Hz field data shown in Figure 11	36
Figure 9 Two-dimensional interpretation chart for the HZ system response	37
Figure 10 Field data for a part of line F6L3	38
Figure 11 Comparison of the interpreted result of field data with the drill-hole measurements	39

Figure 12	(a) Synthetic data for the HX system and inversion results. Model 1. (b) Synthetic data for the HZ system and inversion results. Model 1	4 0
Figure 13	(a) Synthetic data for the HX system and inversion results. Model 2. (b) Synthetic data for the HZ system and inversion results. Model 2	4 1
Figure 14	(a) Synthetic data with 5% added noise and inversion results for the HX system. Model 1. (b) Synthetic data with 5% added noise and inversion results for the HZ system. Model 1	4 2
Figure 15	(a) Synthetic data with 10% added noise and inversion results for the HX system. Model 1. (b) Synthetic data with 10% added noise and inversion results for the HZ system. Model 1	4 3
Figure 16	(a) Synthetic data with 5% added noise and inversion results for the HX system. Model 2. (b) Synthetic data with 5% added noise and inversion results for the HZ system. Model 2	4 4
Figure 17	(a) Height of the system over the ice/water interface during the flight. (b) Synthetic data and inversion results for the HX system. Model 3. (c) Synthetic data and inversion results for the HZ system. Model 3	4 5
Figure 18	Synthetic data at 2500Hz and inversion results for the HX system. Model 4. The data shown are the scaled sum of the in-phase and quadrature components of the secondary magnetic field	4 6
Figure 19	Scaled in-phase data at 16,290Hz and the inversion results for the HZ system	4 7
Figure 20	Sea ice keels of Model Set 1. A=3m, w=24m. (a) s= inf.; (b) s=96m; (c) s=48m; (d) s=24m; (e) s=12m	4 8

- Figure 21 (a) HX system response over the ice keels shown in Figure 20. (b) HZ system response. (c) Cross section of the ice directly below the flight line 49
- Figure 22 Current flow pattern on a flat water surface below a horizontal-axis transmitter. The length of the arrows corresponds to the strength of the current 50
- Figure 23 Sea ice keels of Model Set 2. $A=6\text{m}$, $w=24\text{m}$. (a) $s=\text{inf.}$; (b) $s=96\text{m}$; (c) $s=48\text{m}$; (d) $s=24\text{m}$ 51
- Figure 24 (a) HX system response over the ice keels shown in Figure 23. (b) HZ system response. (c) Cross section of the ice directly below the flight line 52
- Figure 25 Sea ice keels of Model Set 3. $A=3\text{m}$, $w=12\text{m}$. (a) $s=\text{inf.}$; (b) $s=96\text{m}$; (c) $s=48\text{m}$; (d) $s=24\text{m}$; (e) $s=12\text{m}$ 53
- Figure 26 (a) HX system response over the ice keels shown in Figure 25. (b) HZ system response. (c) Cross section of the ice directly below the flight line 54

Airborne Electromagnetic Mapping of Sea Ice Keels

Alex Becker and Guimin Liu

1.0 Introduction

Sea ice is a unique environment encountered in most Arctic work. This includes the transportation of vehicles through ice-covered waters, the construction of offshore drilling structures, and the safe operation of submarines. In such circumstances, knowledge of the thickness and properties of sea ice is important. This is true especially for ice keels, which constitute a local downward indentation of the ice-water interface.

Recently, Canpolar consultants (1985) reviewed the possible techniques for remotely measuring sea ice thickness, among these they included airborne impulse radar and airborne electromagnetics. The impulse radar technique has been very successful in some areas (Kovacs and Morey, 1985). It may however, occasionally yield erroneous data when saline moisture zones exist within the ice cover. Becker et al. (1983), on the other hand, examined the feasibility of using frequency-domain airborne electromagnetics to determine sea ice thickness. At low frequencies, sea ice is practically transparent to electromagnetic waves and the observed secondary magnetic field can be used to estimate the distance from the EM system boom to the ice-water interface. At the same time, a laser altimeter installed on the boom measures the distance to the surface of the ice, so that the difference of these two distances is the sea ice thickness. This technique was successfully used in mapping the average sea ice thickness in Prudhoe Bay, Alaska, but it failed in an area of a multi-year pressure keel because of the inappropriate one-dimensional (1-D) techniques used to interpret data (Kovacs, et al., 1986; Becker, et al., 1987). In order to recover

the geometry of the keel, two- or three-dimensional interpretation techniques are required.

In this report we primarily concern ourselves with the development of techniques for interpreting AEM data for two-dimensional keels which are assumed to be infinitely long in a direction perpendicular to the flight line. The computational methods used to construct the necessary forward solutions are outlined in the Appendix. These serve either for the construction of interpretation nomograms or in the implementation of a numerical inversion scheme. In order to establish the validity of the two-dimensional interpretation scheme we also examine the effects of finite keel length on the observable anomalies.

In terms of computer time, the modeling technique we employ is particularly well suited for the interpretation of the AEM data collected over sea ice keels. Using the conventional finite element method, 30 minutes CRAY II CPU time is required to compute the AEM system response along a traverse line over an ice keel. However, for a similar problem, using an approach rooted in potential theory, the computation takes about 10 seconds on IBM 3090 (equivalent to about 3 seconds on CRAY) with a gain more than two orders of magnitude in speed. We will show that the assumption of a perfectly conducting sea water model is not a significant drawback since it can be used for any system operation frequency greater than 30 KHz.

2.0 AEM Anomalies for Ice Keels

Let us first briefly examine the airborne electromagnetic response to two-dimensional sea ice keels as a function of their size and shape (cf. Fig.1). For these calculations, the electromagnetic system has a coil separation of 6.5m and is "flown" 25m above the upper ice surface which is flat. With the exception of the zone containing the keel, the sea ice is 5m thick and is assumed to have negligible electrical conductivity. The data is calculated for both the vertical-coaxial coil configuration (HX system) and the horizontal-coplanar one (HZ system). The keel is assumed to have

the shape of a Gaussian curve and its parameters and geometry are shown in Figure 2.

Figure 3 shows the HX system response for two different keels with parameters $A = 12\text{m}$, and $W = 28\text{m}$ (solid line) or 14m (dashed line). The observed secondary magnetic field is expressed in parts per million (ppm) of the primary field at the receiver. There is a big anomaly in the system response due to either of these ice keels. For a keel width $W = 28\text{m}$, the maximum anomaly is about 35% of the background response and we define this to be the "percent anomaly". In order to characterize the shape of the observed anomaly, we define the "anomaly width", q , to be the width of the anomaly at one half of its maximum value. For a keel width $W = 28\text{m}$, the anomaly width q is 45m . When the keel width W is halved and other conditions are kept unchanged, the HX system anomaly is significantly reduced. In this case, the maximum anomaly (or percent anomaly) decreases by 37%, and the anomaly width decreases by 33%.

The situation for the HZ system is similar. Figure 4 shows the HZ system response due to the same two ice keels that were previously examined. For a keel defined by $A = 12\text{m}$ and $W = 28\text{m}$, the percent anomaly for the HZ system response is 32%. The anomaly width q is 66m in this case, which is much larger than that seen for the HX system. When the keel width is halved, the HZ system anomaly also decreases greatly. In this case, the anomaly amplitude (or percent anomaly) drops by 32% and the anomaly width decreases by 20%. From the comparison of Figures 3 and 4, we can see that the HX system response tracks the shape of the keel closely, while the HZ system anomaly is much wider.

Next, the keel drawdown A is halved while the keel width is kept constant at $W = 28\text{m}$. The corresponding HX system response is shown in Figure 5 (dashed line), and HZ system response is shown in Figure 6 (dashed line). The anomaly amplitude contracts by 29% for the HX system and by 37% for the HZ system. However, the

corresponding decrease in the anomaly width is small, 8% for the HX system, and 3% for the HZ system.

From the above model studies, we find that the amplitude of the anomaly (or accordingly the percent anomaly) is sensitive to both the thickness and the width of the keel. Thus, it is essentially a function of the area of the cross section of the keel. In contrast, the anomaly width is primarily related to the keel width. It is not sensitive to the keel thickness as long as the shape of the keel does not change. It is also noticed that the HX system response is more sensitive to keel shape than the HZ system response. The curve of HX system response resembles the keel shape and the change in the anomaly width due to the change of the keel width is much larger than that for the HZ system (33% compared to 20%).

It is worthwhile to compare the result calculated with the above technique to that obtained by the finite element method (Lee and Morrison, 1985) that allows a finite conductivity for both the sea ice and the sea water as well as a low operation frequency. This is done in Figure 7 for a triangular sea ice keel. The ice is uniformly 5m thick except for the keel area and it has a conductivity of 0.002 S/m. The conductivity of the sea water is 4 S/m and the HX system flies at 30m above the surface of the ice and operates at 2500 Hz. The dashed line in Figure 7 (upper part) represents the in-phase component of the response, and the solid line corresponds to the system response that would be observed if the sea water conductivity were infinite and sea ice conductivity were zero. Notice the similarity of these two curves and that the percent anomalies and anomaly widths are almost identical for these two curves. Thus it appears appropriate to use the perfect conductor model to interpret low frequency data observed in practice.

3.0 Charts for Data Interpretation

From the above analysis of numerical data, it is seen that the percent anomaly is a function of the cross area of a sea ice keel and the anomaly width is primarily a function of the keel width. To

interpret field data, we need a strategy to relate the observed electromagnetic anomaly to the keel geometry. In terms of the smooth keel used in this analysis (see Figure 2), we need to estimate the two keel parameters A and W from the observed anomaly of the system response. In the following, we are going to concentrate on the HX system configuration which appears superior in terms of sensitivity of the keel geometry. Parallel analysis can be carried out for the HZ system. .

From the computation and analysis of the HX system response for model keels with systematic values of A and W , one can construct an interpretation chart as shown in Figure 8. The vertical axis of the chart is the percent anomaly, while the horizontal axis represents the ratio of the anomaly width q to the flight height h above the flat part of the ice-water interface. Here, the two sets of parametric curves intersect each other clearly and are well separated. The solid lines are for constant values of the drawdown A , and the dashed lines are for constant keel width W . The charted values of a and w are the keel drawdown " A " and width " W " normalized by h , the system height above the flat seawater surface. As shown, the percent anomaly decreases with the decrease of the keel drawdown and keel width. In fact, the line $a = 0.8$ tends to zero fast and intersects the lines $a = 0.4$, $a = 0.2$, etc.. For purpose of clarity, this is not shown in Figure 8. Nonetheless, this does not pose a serious problem in practice since such narrow and sharp keels are highly improbable. Although the interpretation chart is constructed for $h = 30\text{m}$, it can be used for the range $h = 25\text{m} - 50\text{m}$ with an error less than $\pm 4\%$. .

As pointed out at the end of last section, the anomaly shape for low frequency data is almost identical to that obtained in case of the perfect conductor model. This makes the interpretation chart shown in Figure 8 applicable for a wide range of frequencies. We expect that the interpretation chart is useful for the frequency range between 1 - 100 kHz. A similar interpretation chart can be constructed for the HZ system response. It is shown in Figure 9.

Now consider the 2500 Hz theoretical data shown in Figure 7 (dashed line) for an asymmetric triangular keel. From the in-phase component of the AEM response, the percent anomaly and anomaly width are calculated to be 7% and 27m respectively. Thus $q/h = 27/35 = 0.72$. We draw this point in the interpretation chart (point C in Figure 8) and find the corresponding values of a and w to be 0.1 and 0.35 respectively. Hence $A = a \times h = 3.5\text{m}$, and $W = w \times h = 12.3\text{m}$. The estimated keel is drawn (symmetrically about the maximum anomaly of the data) in the lower portion of the illustration (dashed line in Figure 7). We can see that the size of the interpreted keel is close to that of the model keel. But since we have assumed that the keel is symmetric in the interpretation, the position of the maximum of the interpreted keel is misplaced 3.5m to the right.

The field data collected over an ice keel in the Prudhoe Bay by Geotech Ltd. for CRREL (Kovacs et al., 1986) are interpreted next. The AEM system used consists of two pairs of vertical coaxial coils (HX system) and two pairs of horizontal coplanar coils (HZ system). The former operate at 930 Hz and 4158 Hz respectively, and the latter operate at 530 Hz and 16290 Hz respectively. The transmitter-receiver separation of each coil pair is about 6.5m.

A part of the 930 Hz and 16290 Hz data for line F6L3 is shown in Figure 10. The altitude is the distance from the system boom to the ice surface measured by a laser altimeter. Note that the quadrature component of the 16290 Hz data is of bad quality. As we can see in the figure, the data are highly correlated with the altitude as expected. First, we interpreted the data using a 1-D technique (Becker et al, 1987). The result shows an average of 3m thick ice (see Figure 11) but no ice keel is apparent in the interpretation. However, we notice that there is an anomaly in the system response from fiducial numbers 2668 - 2675, which can not be related to the small altitude variation in that area. Moreover, the 1-D interpreted results also show thicker ice in that region. For the 930 Hz data, the anomaly width q is found to be 31.4m and the percent anomaly is 6.5%. Since h is about 38.5m (altitude + average

ice thickness), $q/h = 0.83$. The corresponding point is found in the interpretation chart (point D in Figure 8), which gives $a = 0.08$ and $w = 0.42$. Hence $A = a \times h = 3.08\text{m}$, $W = w \times h = 16.2\text{m}$. The interpreted keel is plotted symmetrically about the maximum anomaly in Figure 11 (dashed line). The solid line in the figure is the average of the drill hole measurements along three parallel lines 11.5 meters apart. As we can see, the interpreted keel is an good approximation of the real feature. Note, however, that the effect of the variation of the altitude of the system boom has been neglected in the interpretation.

The interpretation of 4158 Hz data yields similar result to the above. But difficulty was encountered in interpreting the HZ system data which were acquired at 530 and 16290 Hz. As shown in Figure 10, there is also an anomaly in the 16290 Hz data from fiducial numbers 2668 - 2675. If we calculate the percent anomaly and anomaly width in this case, the corresponding point will fall off the interpretation chart shown in Figure 9 and can not be interpreted.

Generally speaking, the chart interpretation method gives an overall estimate of the size and shape of an ice keel. In order to recover the detail shape of an ice keel, we consider in the next section an iterative technique for data inversion. The chart interpretation can be used to obtain an initial model for the iterative technique where the variation of the system altitude can be easily accounted for.

4.0 inversion of AEM Data

Now consider the determination of sea ice keel shape by data inversion. In order to overcome the problem associated with 1-D data interpretation, we present a two-dimensional (2-D) AEM data inversion scheme where ice thickness may vary along the flight direction of the AEM system. In the perpendicular direction, however, the geometry of the ice/water interface is assumed to be invariant. Although the actual ice bottom topography is three dimensional (3-D), most ice keels do exhibit a dominant extension in

one direction which is called the strike because they are formed by the interaction of two ice plates (Canpolar, 1985). Indeed, as will be shown in the next section, if the strike length of an ice keel of Gaussian shape is greater than three times the AEM system flight height 2-D interpretation may be quite appropriate.

The interpretation scheme that we have developed is based on the principle of the Occam's inversion presented by Constable et al. (1987). Due to practical non-uniqueness of the inverse problem, there may be many sea ice keels that may fit the observed data within a specified error. This scheme yields the smoothest among these. The smooth keel shows the basic features of the actual keel although small bumps on its surface may not appear in the inversion results. Because the process of the data acquisition however constitutes a low-pass filter, it is also possible that the information needed to define the keel in detail is absent from the acquired data.

We first examine the theory of constrained smooth inversion and then use it to interpret synthetic field data which are generated with our numerical modeling program (cf. Appendix). Both noise free and artificially contaminated data are used to test the scheme. Finally we propose a procedure to apply this inversion scheme to low frequency data. In addition to this field data sets (collected in Prudhoe Bay by Geotech,Ltd. in 1985) are also interpreted using this procedure.

4.1 Theory

Let x denote the traverse direction of the AEM system, y the strike direction of the ice keel and z the downward pointing vertical. The interface of the ice and the water is described by $z = h(x)$. Our purpose here is to reconstruct this interface from the airborne electromagnetic data $d(x)$ while the upper surface of the ice is mapped by a laser device. The difference in elevation between the bottom and the top surface of the ice is the required ice thickness. The data $d(x)$ can be either the horizontal or/and the vertical secondary magnetic field recorded during the flight.

Now consider $h(x)$ as the only unknown. This is true when the two assumptions used in our previous modeling algorithm (see the Appendix) are valid. These are: 1) the sea ice is transparent to the electromagnetic wave, and 2) the sea water can be treated as a perfect electric conductor. With these considerations, the AEM data can be written as

$$d(x) = F[h(x)] \quad \dots (1)$$

where $F[]$ is the functional for forward modeling. Equation (1) immediately reveals that the inversion problem is actually one-dimensional (1-D) with the direction of variation along x instead of along z . Fortunately there is a large amount of geophysical literature dealing with 1-D inversion. One particular scheme that well suits our needs is Occam's inversion presented by Constable et al. (1987).

The basis for Occam's inversion is the search for the smoothest solution that fits the observed data within a specified tolerance. This principle applies particularly well to our work because electromagnetic wave propagation in sea water is a diffusion process, so that the resolution of sharp edges on the ice/water interface can not be expected from the data. Furthermore, any information on the sharp edges is contained in the high wave-number range of the data, which is contaminated by noise. Because inversion implies downward continuation (Parker, 1977), the attempts to reconstruct the fine structures of the interface will amplify any noise and result in unstable solutions. Hence a stable solution is necessarily smooth.

In order to find the smoothest solution, let us first define the roughness of the ice/water interface. Physically the rougher the interface is, the larger the magnitude of its derivatives. Thus we define

$$R = \int_{p_1}^{p_2} \left| \frac{dh(x)}{dx} \right|^2 dx$$

to be the roughness of the interface $h(x)$; (p_1, p_2) define the lateral keel extent outside of which the interface is assumed to be flat. In the discrete sense,

$$R = \sum_{i=2}^N (h_i - h_{i-1})^2 = \|\partial \mathbf{h}\|^2 \quad \dots (2)$$

where $h_i = h(x_i)$ and $\|\cdot\|$ denotes the l_2 norm, and

$$\partial = \begin{vmatrix} 0 & 0 & 0 & \dots & 0 \\ -1 & 1 & 0 & \dots & 0 \\ 0 & -1 & 1 & \dots & 0 \\ \vdots & \vdots & \vdots & \ddots & \vdots \\ 0 & 0 & \dots & -1 & 1 \end{vmatrix}$$

$$\mathbf{h} = (h_1, h_2, \dots, h_N)^T$$

Note that $p_1 = x_1$, $p_2 = x_N$ and that the points x_1, x_2, \dots, x_N are usually equally spaced.

Suppose that there are M data points recorded over an ice keel, $d_j = d(X_j)$, $j=1, 2, \dots, M$. The corresponding computed predictions from the discrete model \mathbf{h} are $F_j(\mathbf{h})$. The goodness of fit of the predictions to the actual data can be evaluated using the least-squares criterion

$$E = \sum_{j=1}^M [d_j - F_j(\mathbf{h})]^2 = \|\mathbf{d} - \mathbf{F}(\mathbf{h})\|^2 \quad \dots (3)$$

where

$$\mathbf{d} = (d_1, d_2, \dots, d_M)^T$$

$$\mathbf{F}(\mathbf{h}) = (F_1(\mathbf{h}), F_2(\mathbf{h}), \dots, F_M(\mathbf{h}))^T$$

The ice/water interface \mathbf{h} can only vary within some physical bounds. If we assume that the $z = 0$ plane is chosen such that it coincides with the flat part of that interface then a reasonable lower bound is:

$$h_i \geq 0, \quad i = 1, 2, \dots, N \quad \dots (4)$$

since the ice keel protrudes downward. An upper bound can also be set for each individual case

$$h_i \leq T_i, \quad i = 1, 2, \dots, N \quad \dots (5)$$

In the Arctic, small ice keels may protrude several meters into the water, whereas large keels can protrude tens of meters (Lowry and Wadhams, 1979). The values of T_i should be estimated for each specific ice keel encountered. Note that $h_1 = h_N = 0$ should be included in the constraints in order for the solution to be smooth at the two end points. This condition can be met by simply letting $T_1 = T_N = 0$.

Now the mathematical problem to be solved can be stated as follows: find a solution h which minimizes the roughness R and brings the misfit E within an acceptable tolerance, while the bound constraints (4) and (5) are satisfied. Without the bound conditions (4) and (5), this problem is exactly identical to the one solved by Constable et al. (1987).

The condition for the data misfit is

$$\|d - F(h)\|^2 \leq E_* \quad \dots (6)$$

where E_* is the tolerance. If we treat this inequality as an equality and apply the method of Lagrange multipliers, the above problem can be reduced to the minimization of

$$U = \|\partial h\|^2 + \mu^{-1} (\|d - F(h)\|^2 - E_*) \quad \dots (7)$$

with constraints (4) and (5). Here μ^{-1} is the Lagrange multiplier. As interpreted by Constable et al, μ is a smoothing parameter. The larger the μ is, the less the solution is affected by the misfit. On the contrary, if μ is small, the data misfit is minimized with little influence from the roughness term.

The original problem can now be solved with the following procedures: Solve the above minimization problem for a series of μ

values to obtain a set of solutions of the ice/water interface. Among these solutions, choose the one which satisfies the tolerance condition (6). If more than one solution satisfies (6), choose the one with the largest μ value for this corresponds to the smoothest solution desired.

Such solutions can not however be easily obtained by the direct minimization of the objective function U (equation (7)) since the minimization is non-linear. It is first necessary to transform the non-linear problem into a problem of quadratic programming, for which existing mathematical tools can be used.

Let us linearize the $F(h)$ about an initial model h^0

$$F(h) = F(h^0) + J \Delta \quad \dots (8)$$

Here $h = h^0 + \Delta$, and the Jacobian matrix is

$$J = \begin{bmatrix} \frac{\partial F_1}{\partial h_1} & \frac{\partial F_1}{\partial h_2} & \dots & \frac{\partial F_1}{\partial h_N} \\ \frac{\partial F_2}{\partial h_1} & \frac{\partial F_2}{\partial h_2} & \dots & \frac{\partial F_2}{\partial h_N} \\ \dots & \dots & \dots & \dots \\ \frac{\partial F_M}{\partial h_1} & \frac{\partial F_M}{\partial h_2} & \dots & \frac{\partial F_M}{\partial h_N} \end{bmatrix} \quad \dots (9)$$

Substituting (8) into (7) and dropping the constant term $\mu^{-1}E$, we obtain

$$U = ||\partial h||^2 + \mu^{-1} ||\tilde{d} - J h||^2$$

where $\tilde{d} = d - F(h^0) + J h^0$ is the modified data. Rearrangement of the above equation gives

$$V = \frac{1}{2} \mu U - \tilde{d}^T \tilde{d} = \frac{1}{2} h^T H h - C^T h \quad \dots (10)$$

Here V is the new objective function and

$$\mathbf{H} = \mu \partial^T \partial + \mathbf{J}^T \mathbf{J}$$

$$\mathbf{C} = \mathbf{J}^T \tilde{\mathbf{d}}$$

Note that \mathbf{H} is a symmetric positive-definite matrix. The minimization of the new objective function V is equivalent to the minimization of U for a fixed value of μ .

Now that the new objective function is in quadratic form the problem of optimization with bound constraints (4) and (5) can be solved using quadratic programming (Gill et al., 1981). There are subroutines available in existing mathematical software libraries which can be used for this purpose. These are E04AF in the NAG Fortran Library and VE04A in the Harwell Fortran Library. We selected VE04A because of its simplicity.

The smoothest solution can now be actually obtained in the following way. Starting from an initial model \mathbf{h}^0 , solve the minimization problem for different μ values. From these solutions choose the one that minimizes the actual misfit E instead of V . (Minimizing V may result in divergence of the solution (Constable et al., 1987)). Use this solution for the next initial model and iterate until the solution for the ice/water interface that brings the misfit below a specified tolerance is found.

The initial model \mathbf{h}^0 can be chosen arbitrarily since it does not affect the convergence of the inversion to the smoothest solution. This is one of the beauties of the smooth inversion scheme which sets out to seek a unique solution. In our problem we set the initial model to be a flat ice cake, i.e., $\mathbf{h}^0 = (0, 0, \dots, 0)^T$.

4.2 Inversion of synthetic data

In this section we will apply the above scheme to invert some synthetic data which are generated with the fast modeling algorithm (see Appendix). To test the stability of the inversion scheme white

noise will also be added to the numerical data. Most inversion schemes require the knowledge of solutions to the forward problem in the computation of the Jacobian matrix. Here these are obtained with the fast forward modeling algorithm. The partial derivatives in the Jacobian are computed using the forward finite-difference of two numerical solutions. Thus one iteration of the inversion process requires $N+1$ forward calculations for M data points.

Before considering the inversion results let us first describe the geometry of the problem for all the synthetic models. Unless otherwise specified, the transmitter and the receiver are both small circular loops separated by 6.5 meters, and both are maintained at 25 meters above the upper ice surface. For convenience the vertical co-axial coil system is referred to as the HX system because the axes of the coils are in the x direction while the horizontal co-planar coil system is referred to as the HZ system. The receiver measures the secondary magnetic field which is expressed in parts per million of the received primary field. The inversion is performed for the HX and the HZ system data independently although the joint inversion can be easily accomplished. Except in the keel area the ice thickness is assumed to be five meters. Note that for the synthetic data generation we assume the induction limit to hold so that the system frequency is not involved. Applications to low frequency data, however, will be shown in the next section.

The position of the end points p_1 and p_2 of the ice keel must now be chosen. These can be arbitrary as long as they are located outside the range of the keel. They should not be too far apart however, because the computation of the Jacobian matrix can be quite expensive and convergence of the inversion may be slow. From our experience, locating these two points at the one quarter of the peak HX system anomaly points, and at the two points at half of the peak HZ system anomaly yields good results. Note that this condition may need to be relaxed for field data because they may be acquired at fluctuating flight heights, which will distort the shape of the observed anomaly.

The sampling interval of $h(x)$, Δx , is taken to be 3 meters for all the examples shown in this report. The data $d(x)$ is sampled at an interval of 3.5 meters unless otherwise specified, which at a helicopter speed of 68 knots corresponds to a recording rate of 10 samples/second.

Figure 12(a) shows the inversion results of the HX system data for a triangular model keel (Model 1), which is symmetric and is located between 60 and 90 meters along the profile. The keel drawdown at the peak is 5 meters and its two sides slope at 18 degrees from the horizontal. The solid line in the upper graph is the synthetic data corresponding to the ice keel shown in solid line in the lower graph, while the dashed line is the system response from the inverted keel shown in dashed line in the lower graph. Similar results for the HZ system data are shown in Figure 12(b). In the inversion the two end points p_1 and p_2 are taken at 45 and 105 meters respectively. The tolerance criterion for convergence is set at 1 ppm for the HX system data and 2 ppm for the HZ system data. Three iterations in the inversion yield the convergent solutions shown in Figure 12 from an initial guess of a flat ice cake that is 5 meters thick. As we can see the interpreted keels have smooth vertices as can be expected for the constrained smooth inversion. The interpreted keels are about 1.5 meters too shallow, and the independent results for the HX and the HZ system data are almost identical.

In the next example we invert the synthetic data for an irregular trapezoidal ice keel (Model 2). The steep side of the keel is 34 degrees from the horizontal while the slope of the other side is 16 degrees (Figure 13). The keel protrudes 6 meters down into the water with a flat bottom of 12 meters. Again both the HX and the HZ system data are inverted independently and the results shown were obtained after three iterations. Misfit for the HX system data is again held below 1ppm, and that for the HZ system data is below 2ppm. For the HX system the inverted maximum keel thickness is correct although the two vertices on the steep side are smoothed out. The

other side however is imaged correctly. For the HZ system, the results are similar except that the maximum keel thickness is a half meter too small.

Now white noise of 5% to 10% of the peak anomaly is added to the Model 1 and Model 2 theoretical data. Here system noise may be small but "geological noise" is estimated to be about 5 percent of the anomaly amplitude. The tolerance criterion for the inversion is set at the RMS noise level and the convergence is usually achieved within 4-5 iterations. The inversion results are shown in Figures 14 - 16. As demonstrated in these figures the inversion still yields good results except at the 10% noise level where the keel interpreted from the HZ system data is flat at the bottom (Figure 15). Our experience with noisy data shows that the inversion results obtained from the HX system data are usually better than those obtained from the HZ system data. In practice 5% noise is probably excessive.

We next examine the case where the height of the system varies during a flight, as is usually the case in practice. The model keel is a symmetric trapezoid in shape with a maximum drawdown of 3 meters (Model 3). The flat bottom is 12 meters wide and the two sides of the keel slope at 12 degrees from the horizontal (Figure 17). The system height over the flat part of the ice/water interface, shown in Figure 17(a), varies between 37 and 41 meters. This height variation was taken from a test flight in Prudhoe Bay. Here it is assumed that the transmitter and the receiver are always at the same level although in practice the instrument pod may tilt in space. The inversion results for the HX and the HZ system response are shown in Figures 17(b) and (c). As can be seen the inverted keels agree very well with the model keel in this case. The final data misfit is 0.3ppm for the HX system and 0.8ppm for the HZ system.

4.3 Application to low frequency data

The inversion procedure can also be extended to the interpretation of low frequency field data. As mentioned earlier, the synthetic data used above were generated in the induction limit where the secondary field only exhibits an in-phase component. In practice however, this can not be realized because the sea water is not a superconductor and the operating frequency of the system must be low enough for the EM wave to penetrate the ice freely. Hence the measured secondary magnetic field has both an in-phase and a quadrature component. Ideally the in-phase and quadrature components can be inverted simultaneously using the above scheme if a fast modeling algorithm for a general conductivity distribution exists. The finite-element and finite-difference methods have been very successful in solving such problems (Lee and Morrison, 1985; Stoyer and Greenfield, 1983). The computational costs associated with these methods however, are prohibitive so that they can not be used in solving this problem as too many forward computations must to be carried out even for one iteration.

Although the fast modeling algorithm that we developed generates theoretical data at the induction limit it can be used to invert low-frequency data. For data collected at 30 kHz the arithmetic sum of the in-phase and quadrature components gives a good approximation of the data that would be obtained at the induction limit (Becker et al, 1983). This sum can be directly interpreted using the previous scheme, but it must first be multiplied by a scale factor prior to interpretation. The same scheme can be used since the anomaly shape changes but little with frequency (Becker and Liu, 1987). The scale factor can be computed as the ratio of the response at the induction limit to the sum of the in-phase and quadrature components at that frequency for a 1-D model. Note that this factor varies with the system altitude. If the altitude does not change much in a flight over the ice keel this factor can be taken as a constant.

Let us now consider an example of synthetic data of the HX system at the frequency of 2500 Hz which was generated by the finite-element method (Lee and Morrison, 1985). The conductivities of the ice and water are 0.002 S/m and 4 S/m respectively. The ice is uniformly 5 meters thick except at the keel area where it protrudes 5 meters into the sea water. The shape of the keel is step-triangular as shown in Figure 18 and the HX system is flown at 30 meters above the ice surface. The scaled sum of the in-phase and quadrature components of the theoretical data and the inversion results are also shown in Figure 18. There are ten unevenly spaced data points and the scale factor is 1.044 in this case. As we can see the inverted ice keel is close to the model although it is somewhat shallower. We consider this an encouraging success of the application of the above proposed procedure.

We have not yet had the opportunity to experiment with large quantities of low frequency data. Thus it is not clear in which frequency range the above procedure can be used to yield reasonable results. Furthermore the role of the water conductivity has not yet been investigated although we suspect that its main effect is to decrease the resolution of the inversion results expected from the superconductor assumption. It is worthwhile however to attempt an inversion of the data collected in the Prudhoe Bay by Geotech Ltd. in 1985 (Kovacs, et al., 1987). The data is for line F6L3 collected with the HZ system at the frequency of 16290 Hz. Because the quadrature component is of very poor quality only the in-phase component was scaled by a factor of 1.104 and interpreted. The system altitude, the scaled in-phase component and the inversion results are all shown in Figure 19. The inversion was performed with the two end points of the ice keel fixed at $p_1 = 54$ meters and $p_2 = 102$ meters. The background ice thickness was fixed at 3.3 meters which is the average from the 1-D interpretation.

The interpreted ice thickness is 1.5 meters too shallow as compared to the drill-hole measurements (solid line in the bottom of Figure 19) in the keel area. However the keel is clearly visible in the

inversion result, which is encouraging since it is much better than the 1-D inversion that shows but little of the keel (Becker et al., 1987). The inversion was stopped at an RMS data misfit of 15 ppm since more iterations could not reduce the misfit. There may be several causes for such a large misfit:

- 1) The effects of the pitch and roll of the system during the flight was not accounted for in this inversion.
- 2) The time constant of the instrument may be too large for such a small keel to be fully represented in the data. The inversion treats the data as being recorded with a zero time constant, which ignores the integral effect due to the instrument. This effect has been carefully studied by Becker and Cheng (1987).
- 3) The top surface of the ice was treated as a flat plane and the effect of the associated ridge was not considered.
- 4) The assumed 2-D structure of the ice may be incorrect.
- 5) For this frequency channel the operational system noise was large. The quadrature component was quite erratic and was not used in the inversion.

Errors due to 1) can be diminished by improving the computer code. Errors due to 2) and 5) can be reduced to a large extent by improving the instrument. But errors due to 4) can not be reduced in the present 2-D inversion scheme. To do this a 3-D inversion algorithm needs to be developed which can be an extension of the present scheme. The process will be computer intensive and furthermore, the data acquisition will necessarily cover an area instead of a line over the keel. This will be very costly and may not be worthwhile.

Errors due to 3) need to be further investigated. Treating the ice top as a flat plane has an effect of pressing the ridge down into the sea water. The ice thickness probably may not be largely

affected. But it remains to be seen whether a topographic correction is necessary before a 2-D inversion is attempted.

Applying the constrained smooth inversion to the scaled sum of the in-phase and quadrature components of the real data appears to be an attractive simple scheme. If the phase of the response does not change, this is identical to scaling the in-phase component only. The performance, mainly the resolution, of this scheme will deteriorate with lowering the operation frequency. The range of the frequency, in which the above procedure can be applied, needs to be defined by further investigation. Effects of the conductivities of the sea ice and water will also reduce the resolution of the keel geometry expected from the assumption of transparent ice and superconducting sea water, which need be studied in the future.

All the computations in the above inversion have been done on a IBM RT PC computer, which has a comparable speed as the Microvax. An typical case of inversion of $M = N = 20$ takes about 4 hours of the CPU time. At the present the computer code is not optimized and it can be shown that its optimization may sharply reduce the CPU time by a factor of 5. It appears that in flight data interpretation will require some highly specialized computing equipment.

In all our examples the ice keel position was assumed known. In practice the position of the ice keel may be obtained from the videocamera record of the associated ridge. If this is not possible the AEM data itself can be used to estimate the position of the ice keel prior to the inversion. To do this the influence of the altitude should first be removed from the data so that the remaining anomaly will indicate the position of the keel.

4.4 Discussion

The 2-D inversion scheme can successfully recover the ice keel information, which is usually lost in 1-D inversion. Because the electromagnetic induction is a diffusion process, sharp edges can not

be resolved from the data and we set out to seek a smooth ice keel, which retains the major features of the true ice keel. Although the scheme is designed to work for data collected in the induction limit with transparent ice and superconducting sea water, it can be applied to low frequency data, where the sum of the in-phase and quadrature components is scaled to approximate the required data. At the present the range of the frequency, in which this procedure can be applied, remains unclear and needs further investigation. With refinements and optimization of the computer program however, there is no doubt that this algorithm can be used routinely to process field data.

5.0 The Three-Dimensional Keel

Under usual circumstances the ice-water interface in arctic seas exhibits the same irregular topography that is normally associated with land forms. In areas covered by young ice however, the topographic features are minimal and a one-dimensional data interpretation technique for the average thickness of the ice sheet from airborne electromagnetic data (Kovacs, et. al. , 1987) can be used. This technique fails in areas of even moderate ice-water interface topography (Kovacs, et al, 1987). In cases where the axial length of the keel is very large (compared to the AEM system altitude) it is possible to remedy this situation with the use of interpretation charts that allow for a two-dimensional description of the keel. If necessary, a 2-D data inversion outlined above may be carried out to delineate ice keels in more details. Because the two-dimensional data interpretation method appears to produce adequately accurate results it appears worthwhile to find the minimal keel axis length that is necessary for its proper application. This is done below where theoretical data for three-dimensional (3-D) keels is presented. In all 14 different keel models are considered.

5.1 The keel model

Cartesian coordinates are used and the XY plane is chosen to coincide with the flat part of the ice-water interface so that the Z axis points vertically down into the sea water. The ice is assumed to be transparent to electromagnetic waves and sea water is assumed to be a perfect electric conductor. Both the co-axial (HX) and co-planar (HZ) coil systems are considered.

The 3-D Gaussian keel model is an extension of the 2-D model described above. Its shape is given by

$$t(x,y) = A e^{-\frac{y^2}{0.361 s^2} - \frac{x^2}{0.361 w^2}} \quad (1)$$

where

$t(x,y)$ is the protruding depth of the ice keel into the sea water,

A is the keel drawdown or maximum keel thickness,

w is the keel width at $t = A/2$ on the cross section $y = 0$,

s is the keel width at $t = A/2$ on the cross section $x = 0$.

Here we define the y direction as the strike direction of the ice keel and hence designate s as the strike length of the keel. An infinite value of s corresponds to a 2-D ice keel. When $s = w$, the keel is a body of revolution. The numerical calculations were carried out as outlined in the Appendix.

5.2 Airborne electromagnetic profiles

In this section, we examine AEM profiles over three sets of model ice keels. Except in the keel area, the sea ice is assumed to have a uniform thickness of 5 meters. The keel parameters A , w , and s are varied to demonstrate the corresponding changes in the AEM system response. For each model set, the keel drawdown A and keel width w are fixed, while the keel strike length is varied. Model Set 1 represents a shallow keel, where $A = 3\text{m}$, $w = 24\text{m}$, and keel

strike lengths of 12, 24, 48, 96, and inf. meters respectively (Figure 20). The corresponding theoretical AEM response for the HX and HZ system over the center of these features along a line perpendicular to the keel strike is shown in Figure 21, where curves 1, 2, 3, 4, and 5 correspond to $s = 12, 24, 48, 96$, and inf. meters respectively. Both the transmitter and the receiver, which are separated by 6.5m, are "flew" 25m above the upper ice surface. The system response is plotted at a point located mid-way between the transmitter and receiver, and is expressed in parts per million of the primary field at the receiver. Figure 21 (c) shows the the cross section of the ice directly below the flight line.

It is evident in Figure 21(a) that as the strike length s decreases the HX system anomaly becomes smaller but the general shape of the anomaly curve changes little. If these system anomalies for 3-D ice keels are interpreted using the 2-D chart given in our previous report, the interpreted cross section of the keel will be smaller than that in the 3-D model. The significant effect here is a reduction of the interpreted keel drawdown. The keel width however is less affected since the anomaly width does not contract significantly with the keel strike.

As shown in Figure 21(a), the HX system response for a keel strike length s of 96m (curve 4) closely resembles the response for an infinitely long keel (curve 5). In fact the maximum difference in the relative amplitude or percent anomaly (c.f. Becker and Liu) is of the order of 1.5% and would result in an under-estimation of the keel depth of about 10%. In fact the relative error in the percent anomaly size is also of this order and suggests that a 10% value for this quantity be used as a threshold value for the definition of a two-dimensional keel. Thus, If the maximum relative difference in the relative anomaly is less than 10%, the finite strike keel can be effectively considered as two-dimensional, and hence 2-D interpretation techniques can be applied.

Using this criterion, any ice keel whose strike length exceeds 96m can be effectively considered as two-dimensional for the purpose of data interpretation. In general, the ratio of the strike length to the system height over the ice-water interface must be larger than 96/30. This value is much greater than the value expected from the footprint for the HX system (see Becker, et al., 1987), which is 1.4. At the first sight, this may seem puzzling. A careful look at the current distribution on the water surface, however, will yield the explanation.

The current pattern for a horizontal-axis transmitter is shown in Figure 22 (from Becker, et al., 1987). It consists of two circular current rings while most of the current flows in a direction parallel to the strike of the ice keel. For a keel of finite-strike, this major current flow is distorted. The footprint however was computed on the basis of the unaltered current flow so that it is not surprising to find that the strike/height ratio needed for 2-D interpretation is much larger than the footprint of the HX system.

Now let us look at the HZ system response and see how it changes as the keel strike length is varied. Curves 1, 2, 3, 4, and 5 in Figure 21(b) correspond to $s = 12, 24, 48, 96$, and ∞ meters respectively. As expected, the HZ system response also decreases when the strike length of the keel is reduced. The major change is the decrease of the anomaly amplitude. The anomaly width, in contrast, stays almost constant. Nonetheless, as the keel strike is further decreased, the anomaly shape also changes and the lower part of the anomaly flattens out.

The HZ system response for $s = 96\text{m}$ is also close to that for the 2-D keel. The maximum relative difference in the relative anomaly in this case is about 12%. Thus taking 10% as the threshold, the keel strike should be somewhat longer than 96m in order to use the 2-D interpretation. Roughly speaking, we may again take the strike/height ratio to be approximately $96/30 = 3.2$ for the 2-D interpretation to be valid. This is the same as that for the HX system

and is very close to the value obtained from the footprint of HZ system which is 3.7 . As a matter of fact, the current pattern on a flat water surface for a vertical-axis transmitter consists of concentric circles so that a 3-D ice keel will distort this pattern as much as a 2-D ice keel does.

Now let us increase the keel drawdown A to 6m and keep the keel width at $w = 24$ m. Figure 23 shows the deeper ice keels with different strike lengths (Model Set 2). The corresponding HX and HZ system responses are shown in Figure 24 (a) and (b) respectively. Now both the HX and HZ system responses are much larger than those for Model Set 1 due to the larger cross section of these keels. But the characteristics of these anomalies are similar to those discussed for Model Set 1. Therefore, the analysis for Model Set 1 still holds in this case.

Figure 25 shows the narrower keels that make up Model Set 3, where $A = 3$ m and $w = 12$ m. The keel strike, again, is 12, 24, 48, 96, and inf. meters respectively. Figure 26 (a) and (b) displays the HX and HZ system response and curves 1, 2, 3, 4, and 5 correspond to $s = 12, 24, 48, 96,$ and inf. meters. Figure 26 (c) shows the cross section of the keel below the flight line.

Now the HX system response is much smaller than those shown in Figure 21 (a) because of the smaller size of the ice keels. But the relative characteristics remain unaltered and the analysis for Model Set 1 still applies here.

The HZ system anomaly also reduces with the decrease of the strike length of the keel. Furthermore, it is observed that a minor feature begins to appear at the center of the anomaly when the keel strike is small. This feature, however, may not be real as it may be caused by numerical errors in the calculation. At present, we are unable to make this point clear due to computational limitations.

5.3 Discussion

- 1) The strike length of an ice keel must be at least three times the flight height of the AEM system in order to successfully use the 2-D techniques to interpret both HX and HZ systems response.
- 2) For the HX system, the anomaly amplitude decreases as the keel strike shortens, but the anomaly width changes little.
- 3) For the HZ system, the anomaly amplitude also decreases as the keel strike contracts. At the same time, the lower part of the anomaly tends to become flat.

References

- Becker, A., Morrison, H.F., and Smits, K., 1983, Analysis of airborne electromagnetic systems for mapping thickness of sea ice: NORDA technical note 261.
- Becker and Cheng, 1987, Detection of repetitive electromagnetic signals, *Electromagnetic Methods in Applied Geophysics*, Vol. 1, Edited by M.N. Nabighian, pp.443-465.
- Becker, A., and Liu, G., 1987, Airborne electromagnetic mapping of sea ice keels, First Interim Report to NORDA.
- Becker, A., Liu, G., and Morrison, H.F., 1987, Airborne electromagnetic sensing of sea ice thickness: Report prepared for CRREL under UCB contract #DACA89-85-K-0008.
- Bergeron, C.J., Juliette, W.I., and Gus, A.M., 1987, Lateral resolution of the modified image method for sea-ice thickness, Extended Abstracts of the SEG 57th International Meeting, New Orleans.
- CANPOLAR Consultants Ltd., 1985, Review of floating ice thickness measurement: Report prepared for the Department of Fisheries and Oceans, Canada under contract 01SE.FP921-3-0624.

Gill, P.E., Murray, W., and Wright, M.H., 1981, *Practical Optimization*, Academic Press, Inc..

Graham, I.G., 1980, Some application areas for Fredholm integral equations of the second kind: The Application and Numerical Solution of Integral Equations, Anderssen et al. ed., 75-101.

Kovacs, A., and R. Morey, 1985, Electromagnetic measurements of multi-year sea ice using impulse radar: CRREL Report 85-13.

Kovacs, A., Valteau, N., and Holladay, J.S., 1987, Airborne electromagnetic sounding of sea ice thickness and sub-ice bathymetry, CRREL Report 87-23, pp.1-40.

Kovacs, A., Morey, R.M., Gordon, F.N.C., and Valteau, N.C., 1986, Modeling the electromagnetic property trends in sea ice and example impulse radar and frequency-domain electromagnetic ice thickness sounding results: CRREL report in preparation.

Lee, K.H., and Morrison, H.F., 1985, A numerical solution for the electromagnetic scattering by a two-dimensional inhomogeneity: *Geophysics*, 50, 466-472.

Liu, G., and Becker, A., 1988, Effect of three-dimensional sea ice keels on airborne electromagnetic system response, Second Quarterly Report to NORDA.

Liu, G., and Becker, A., 1987, Airborne electromagnetic sensing of sea ice thickness, presented at the 57th SEG Annual International Meeting.

Lowry, R.T., and Wadhams, P., 1979, On the statistical distribution of pressure ridges in sea ice, *Journal of Geophysical Research*, Vol.84, No. C5, pp.2487-2494.

Mikhlin, S.G., 1964, *Integral equations*: Pergamon Press, 7-15.

Parker, R.L., 1977, Understanding inverse theory, *Ann. Rev. Earth Sci.*, vol.5, pp35-64.

Parry, J.R., and Ward, S.H., 1971, Electromagnetic scattering from cylinders of arbitrary cross-section in a conductive half-space. Geophysics, 36, 67-100.

Rikitake, I.K., and K. Whitham, 1964, Interpretation of the Alert anomaly in geomagnetic variations: Canadian Journal of Earth Sciences, vol.1, 35-62.

Rossiter, J.R., and Lalumiere, L.A., 1988, Evaluation of sea ice thickness sensors, Canpolar Inc., Toronto, Project 1027.

Stoyer, C.H., and Greenfield, R.J., 1976, Numerical solutions of the response of a two-dimensional earth to an oscillating magnetic dipole source, Geophysics, Vol.41, No.3, pp.519-530.

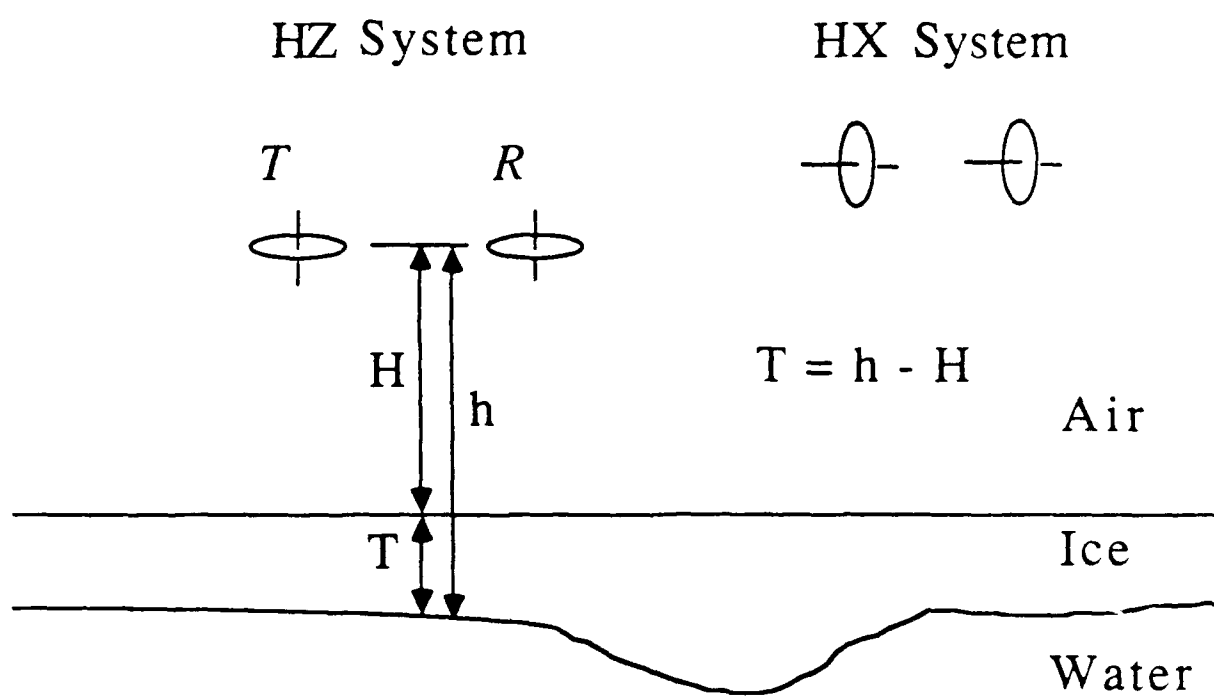


Fig.1 HX and HZ systems over sea ice

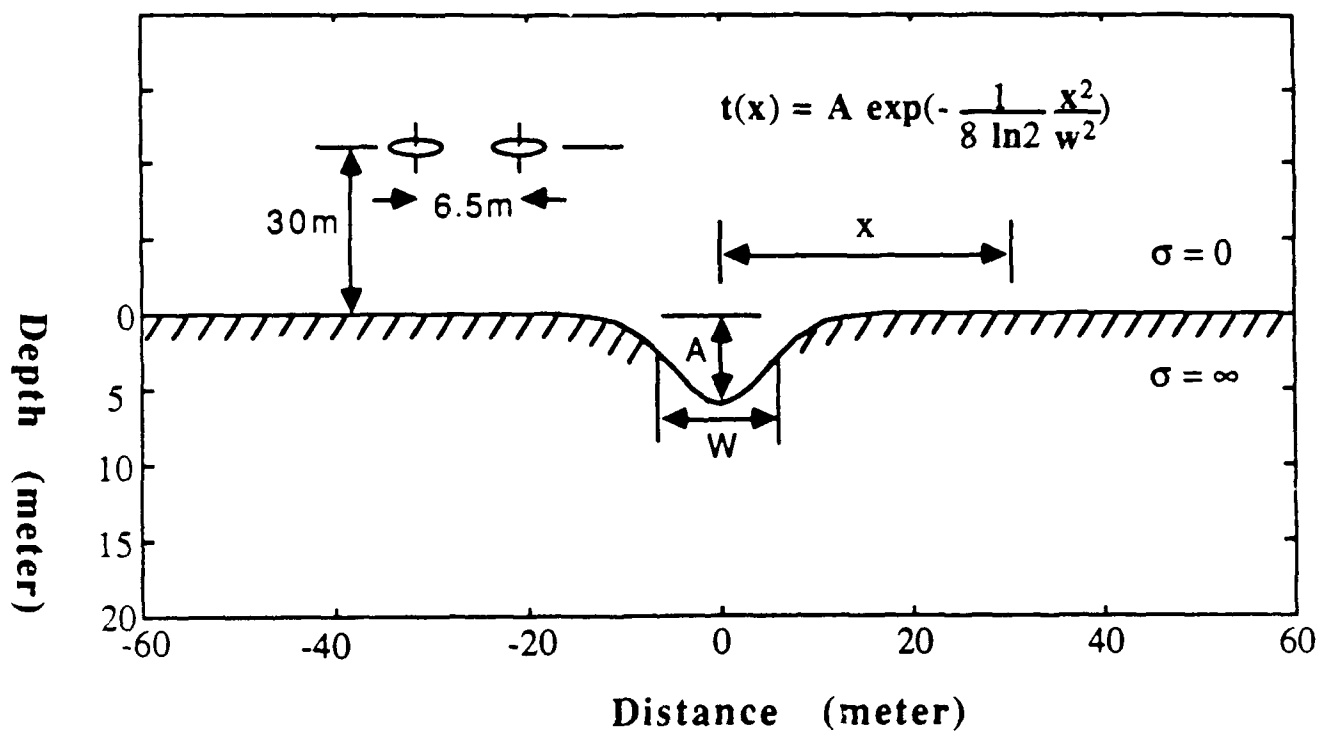


Fig.2 Cross section of a smooth keel

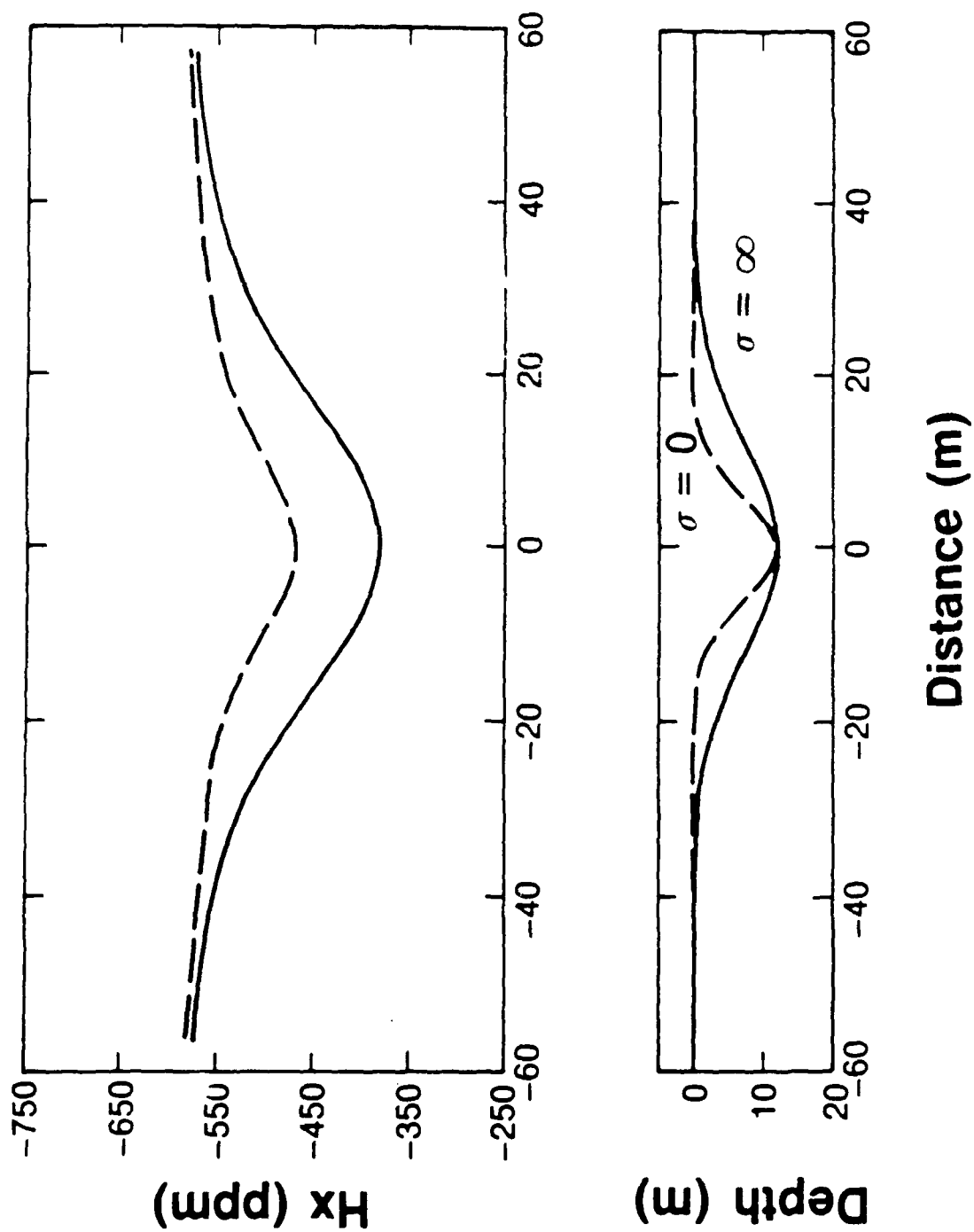


Fig.3 Effect of Keel Width on IIX System Reponse

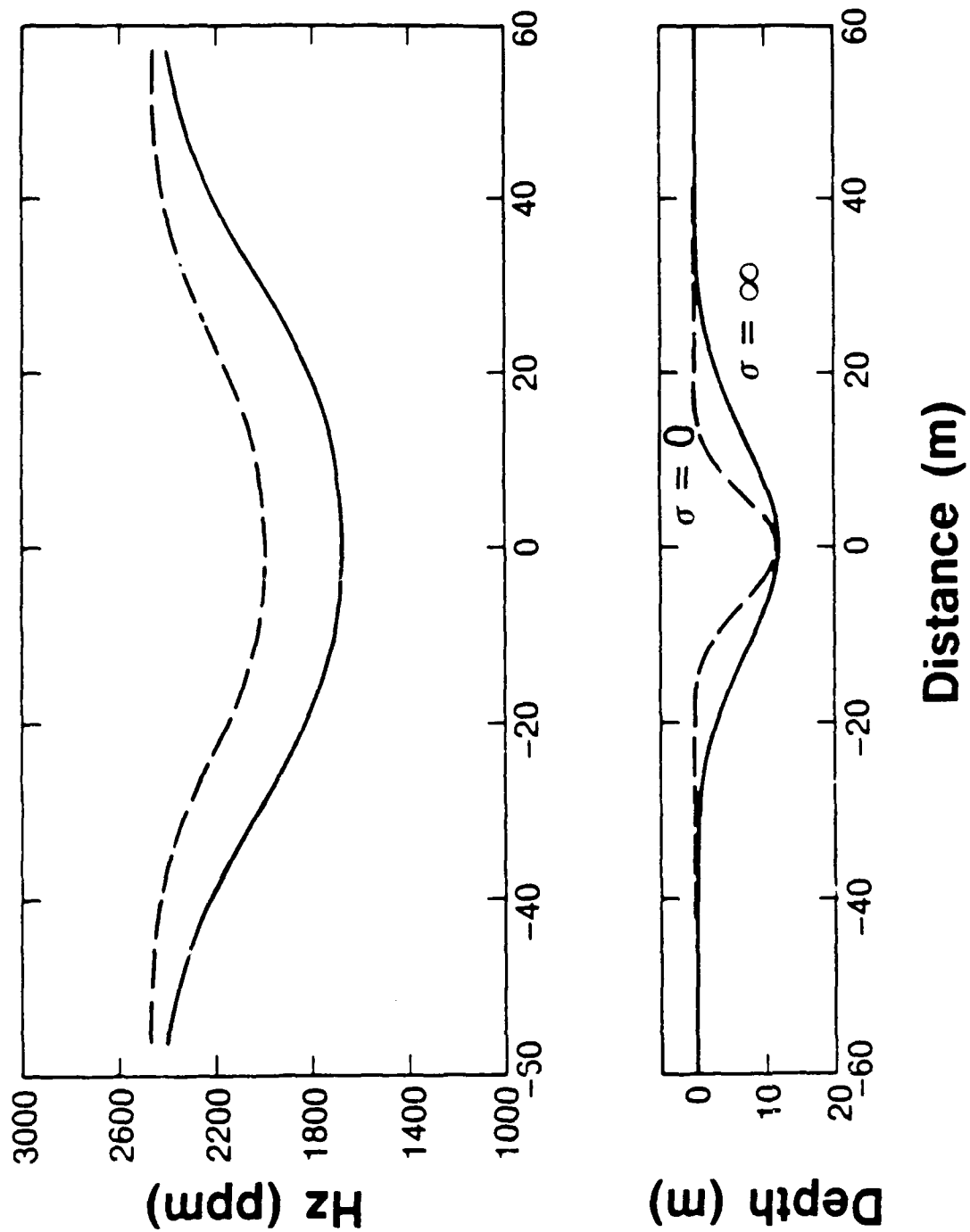


Fig.4 Effect of Keel Width on HZ System Response

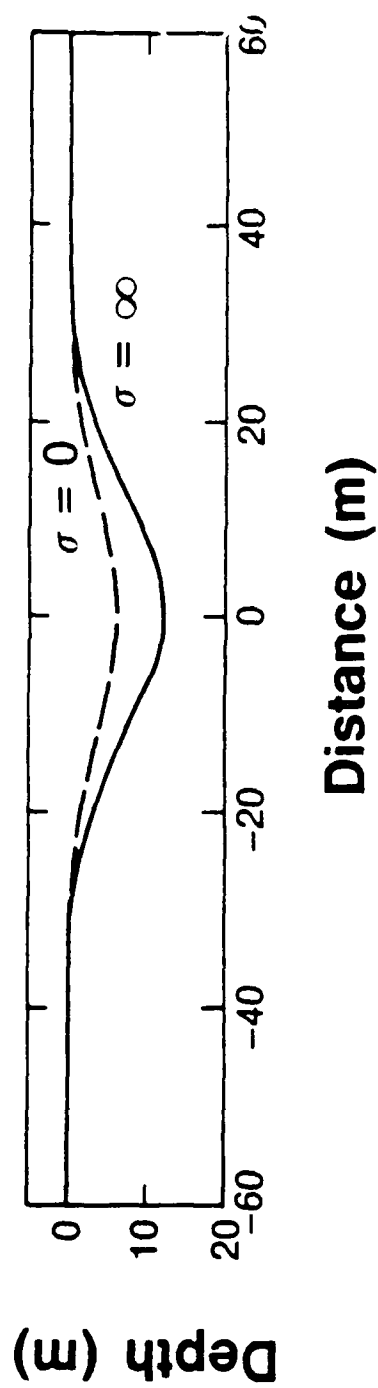
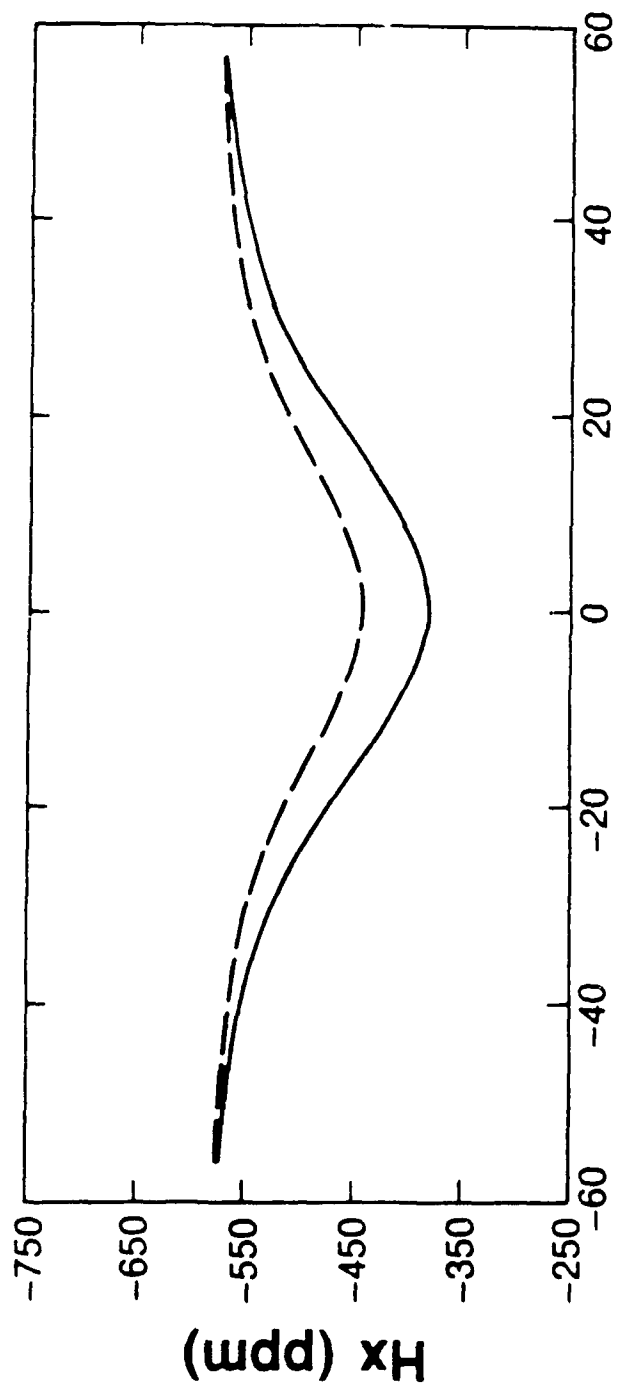


Fig.5 Effect of Keel Drawdown on HX System Response

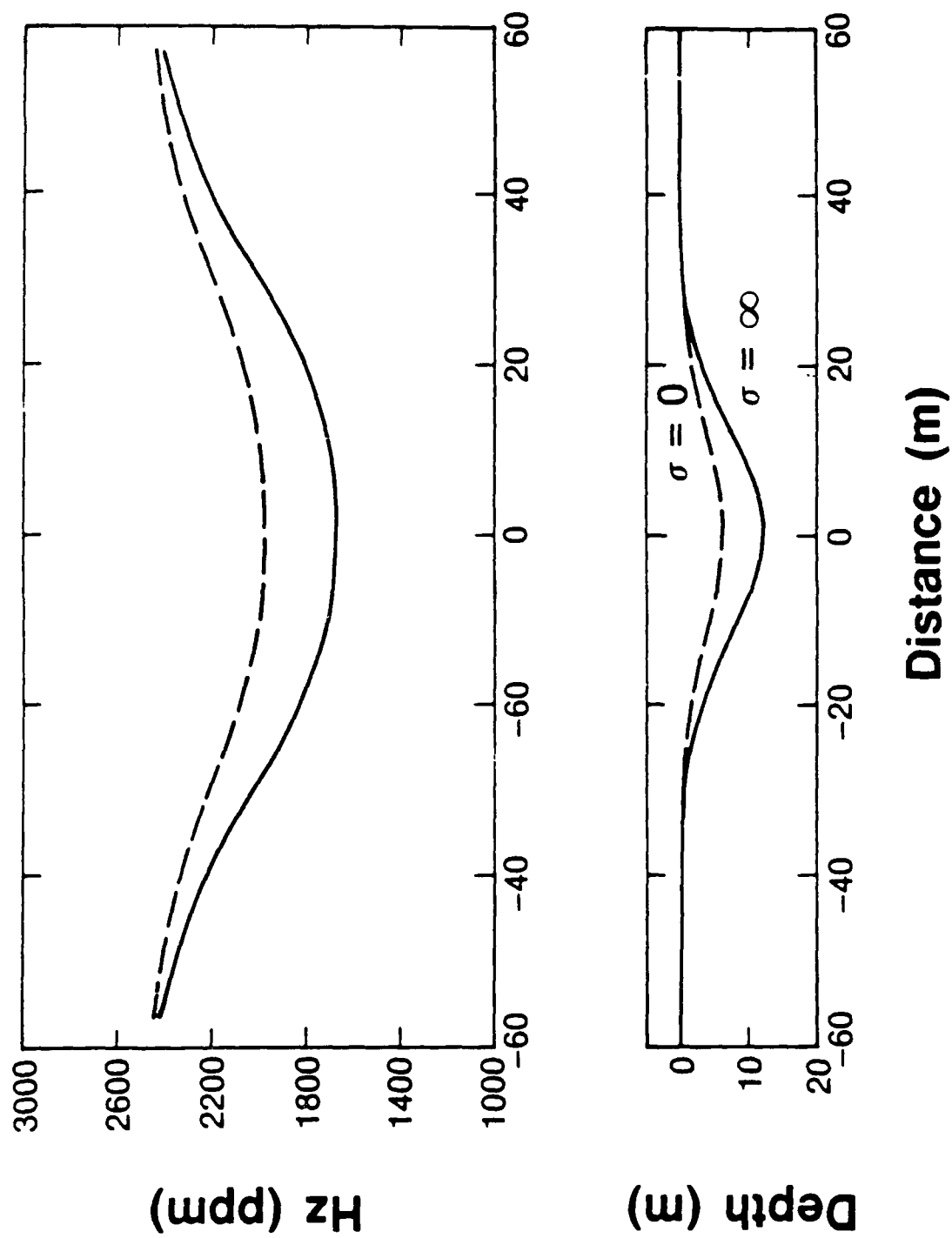


Fig.6 Effect of Keel Drawdown on HZ System Response

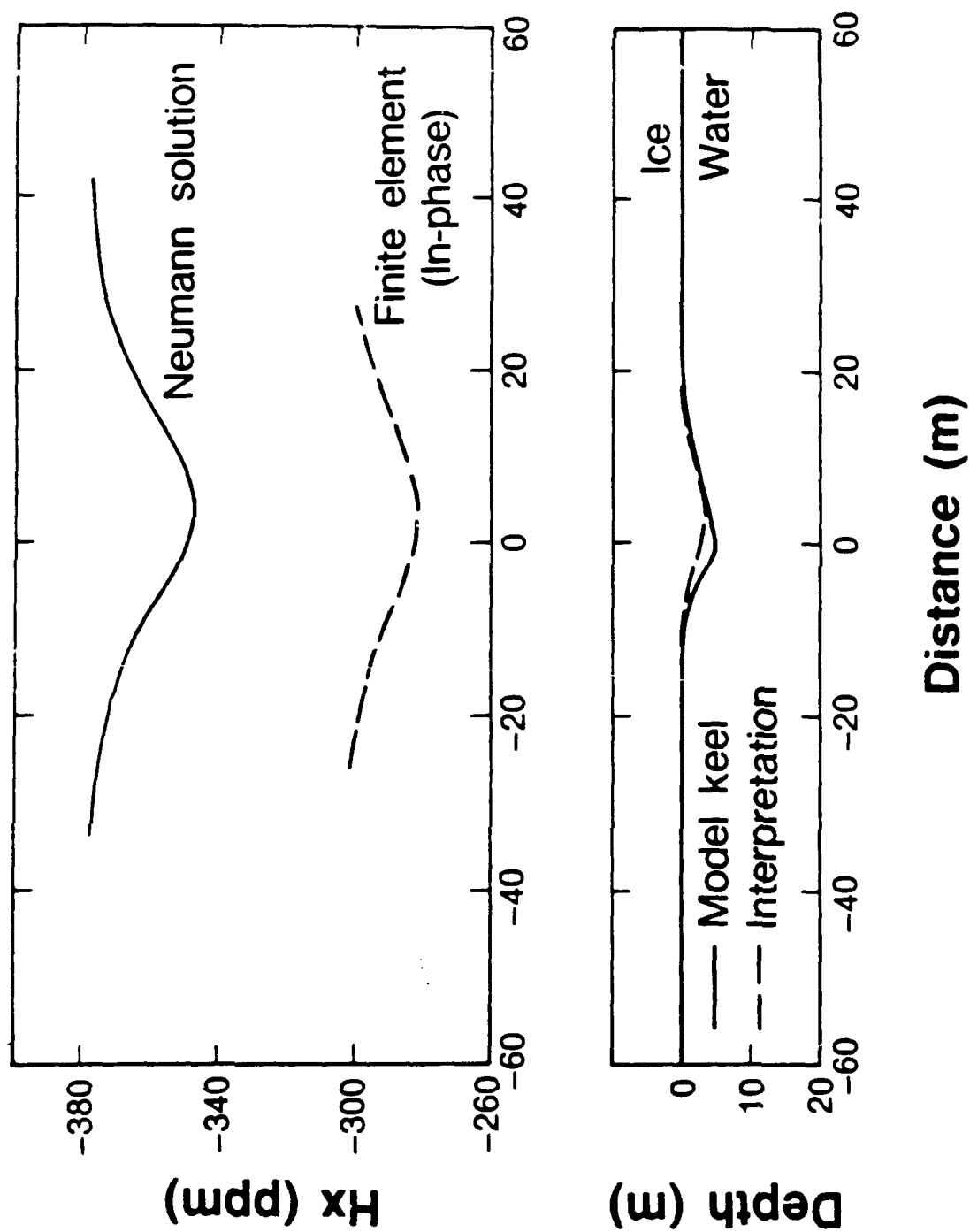


Fig.7 Model Response

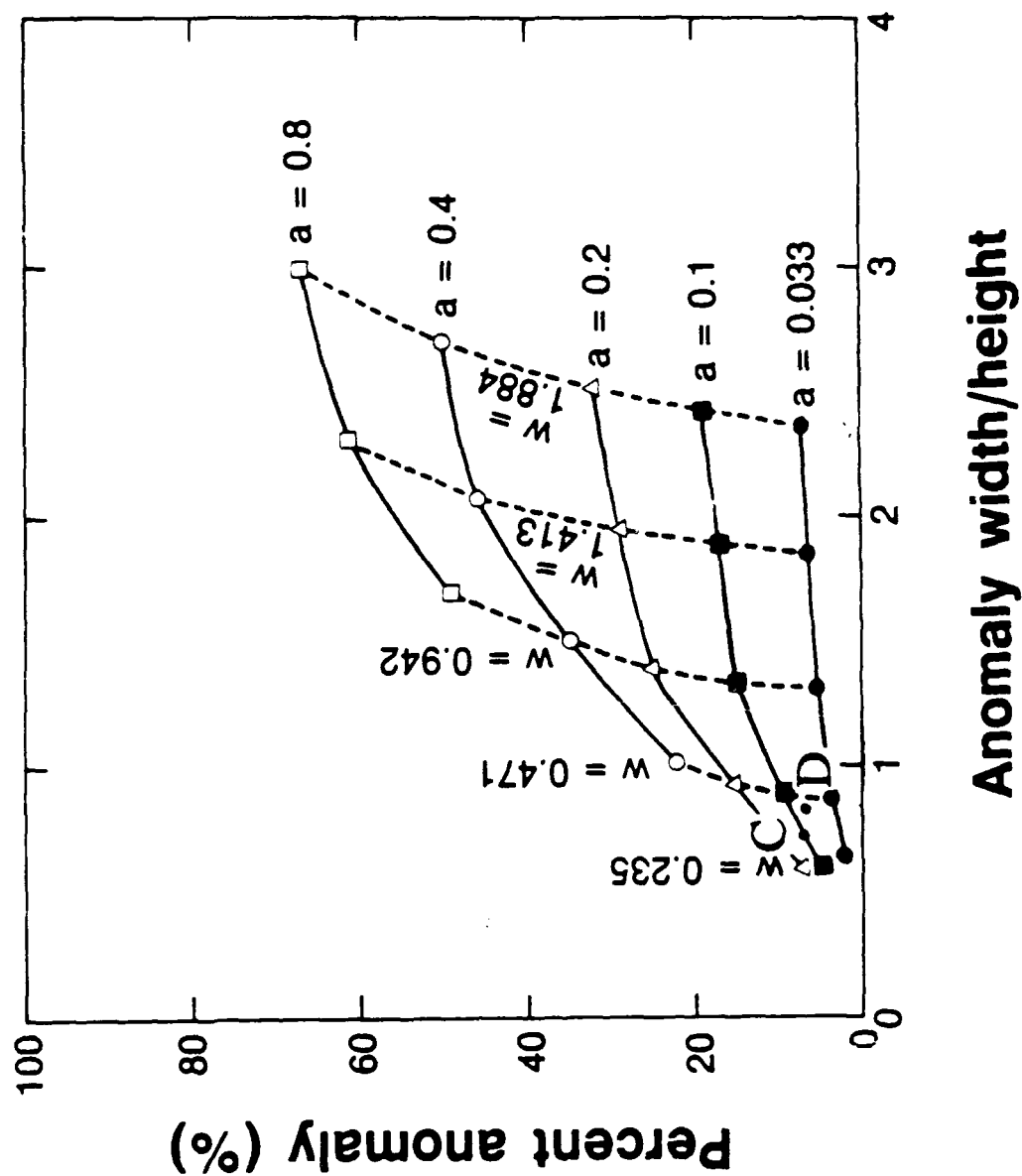


Fig.8 Interpretation Chart for HX System

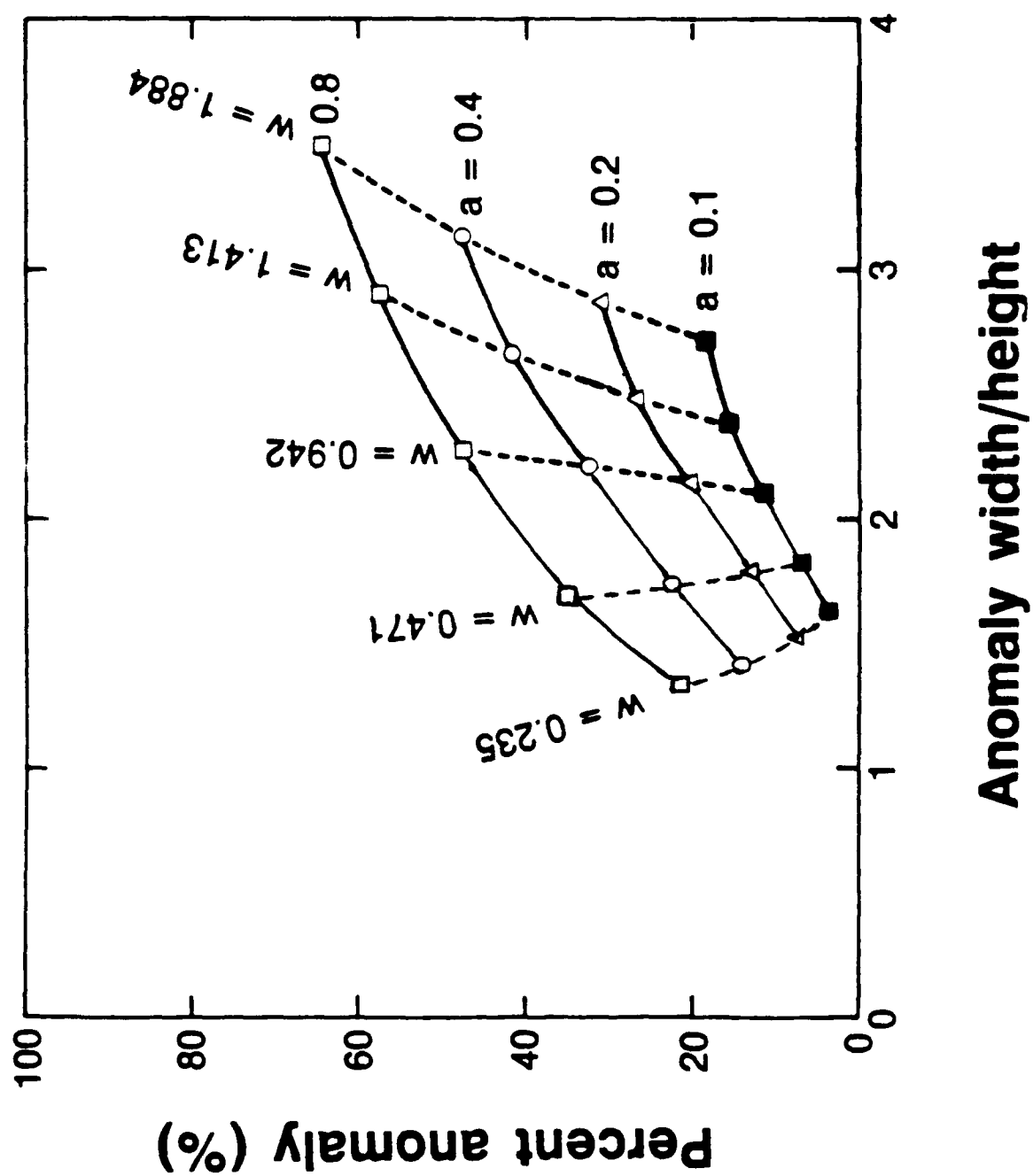


Fig.9 Interpretation Chart for HZ system

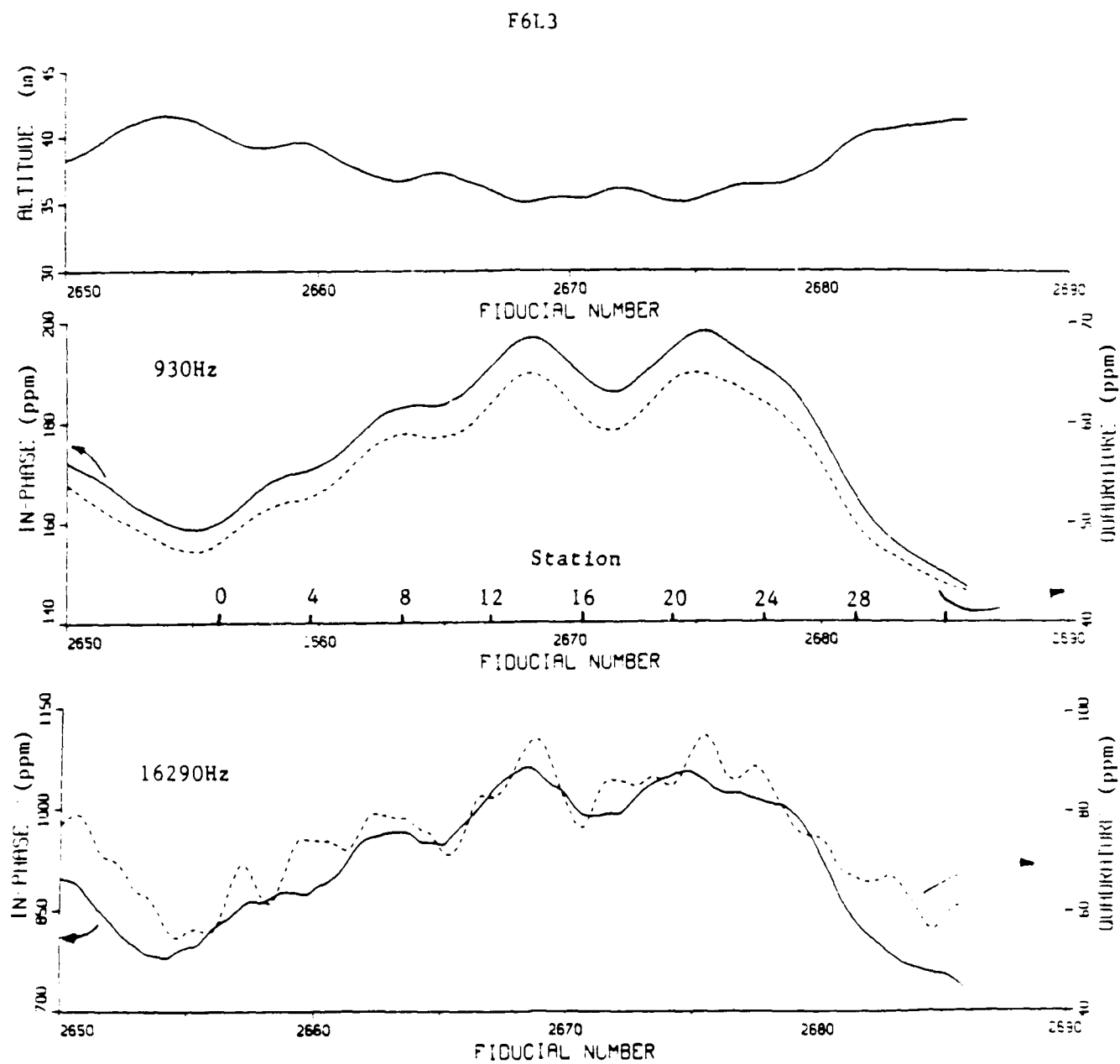


Fig.10 Field data. Line F6L3.

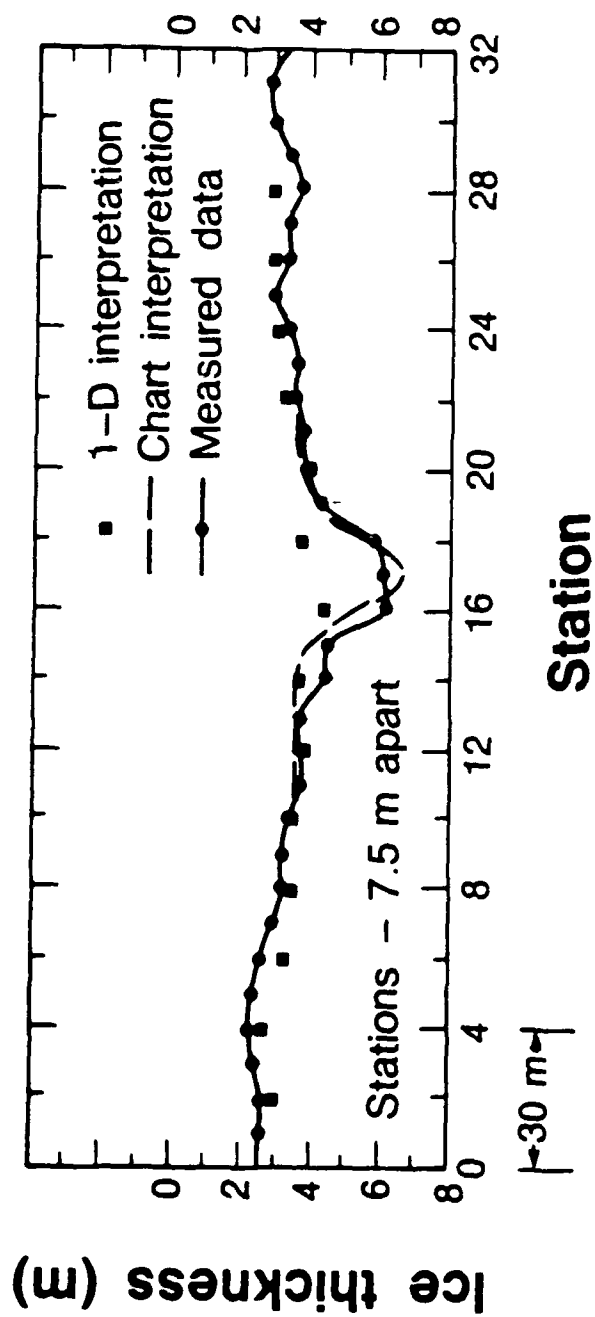


Fig.11 Interpretation of Field Data

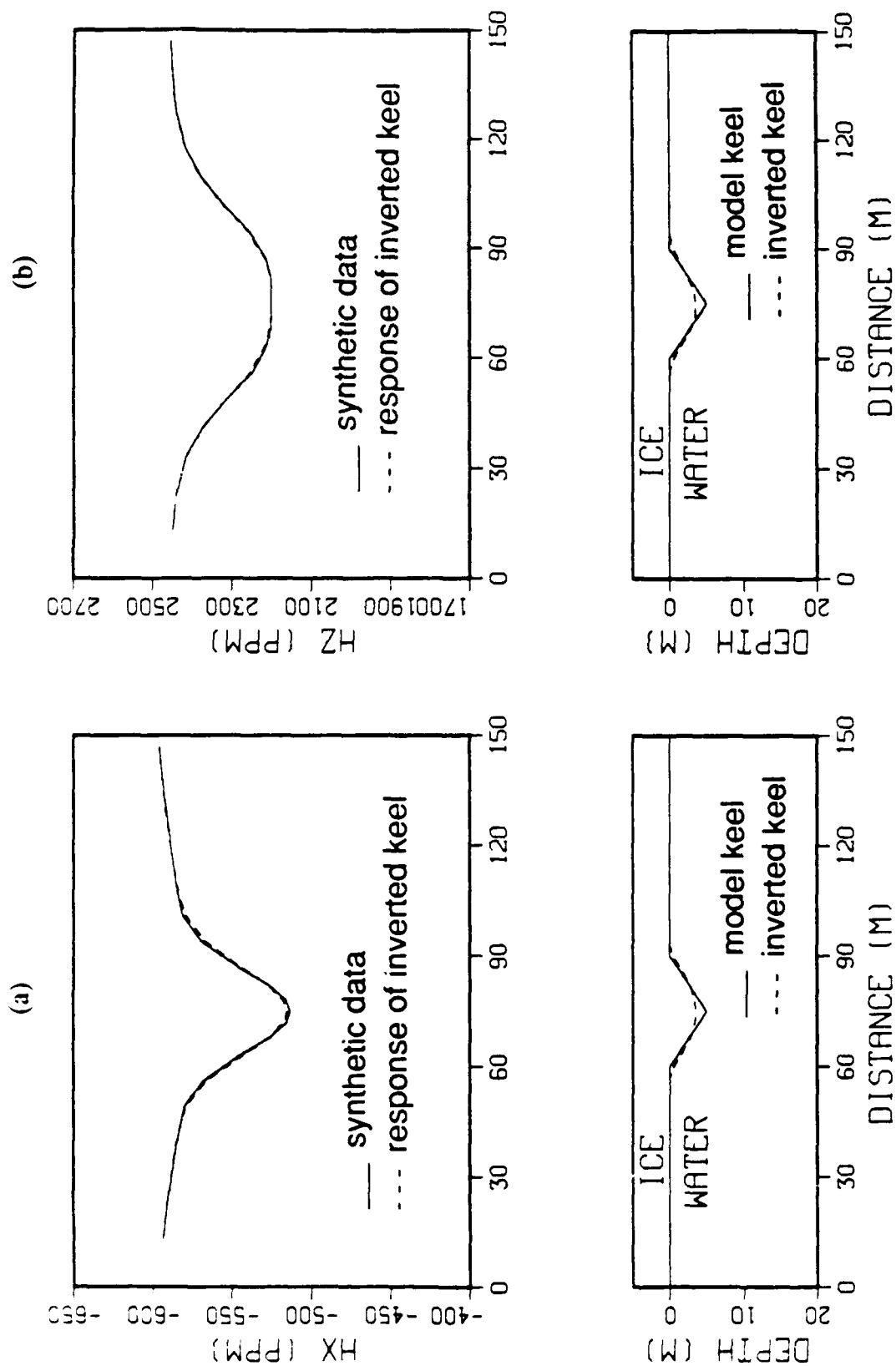


Figure 12 (a) Synthetic data for the HX system and inversion results, Model 1.

(b) Synthetic data for the HZ system and inversion results, Model 1.

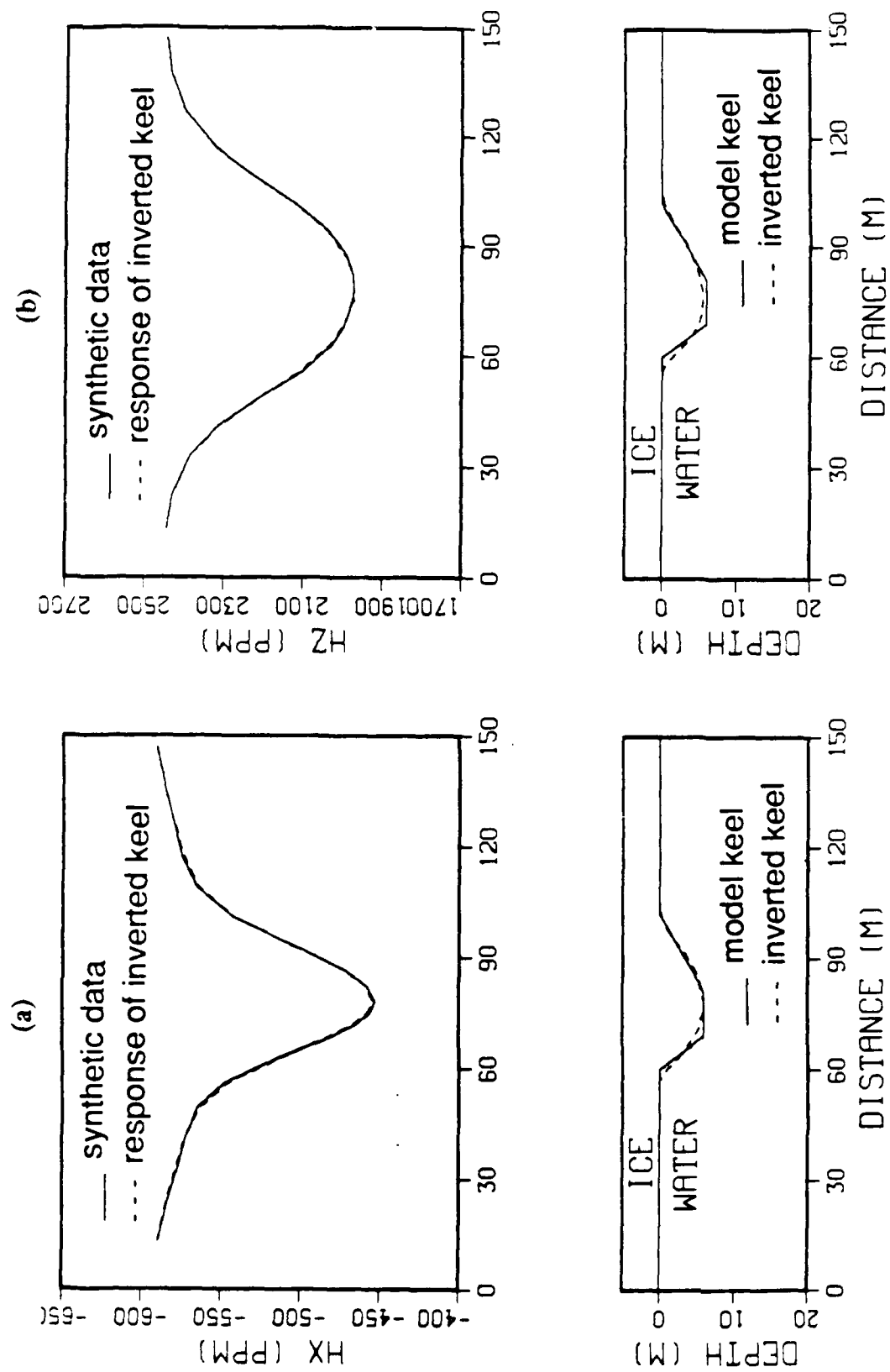


Figure 13 (a) Synthetic data for the IIX system and inversion results, Model 2.
 (b) Synthetic data for the IIZ system and inversion results, Model 2.

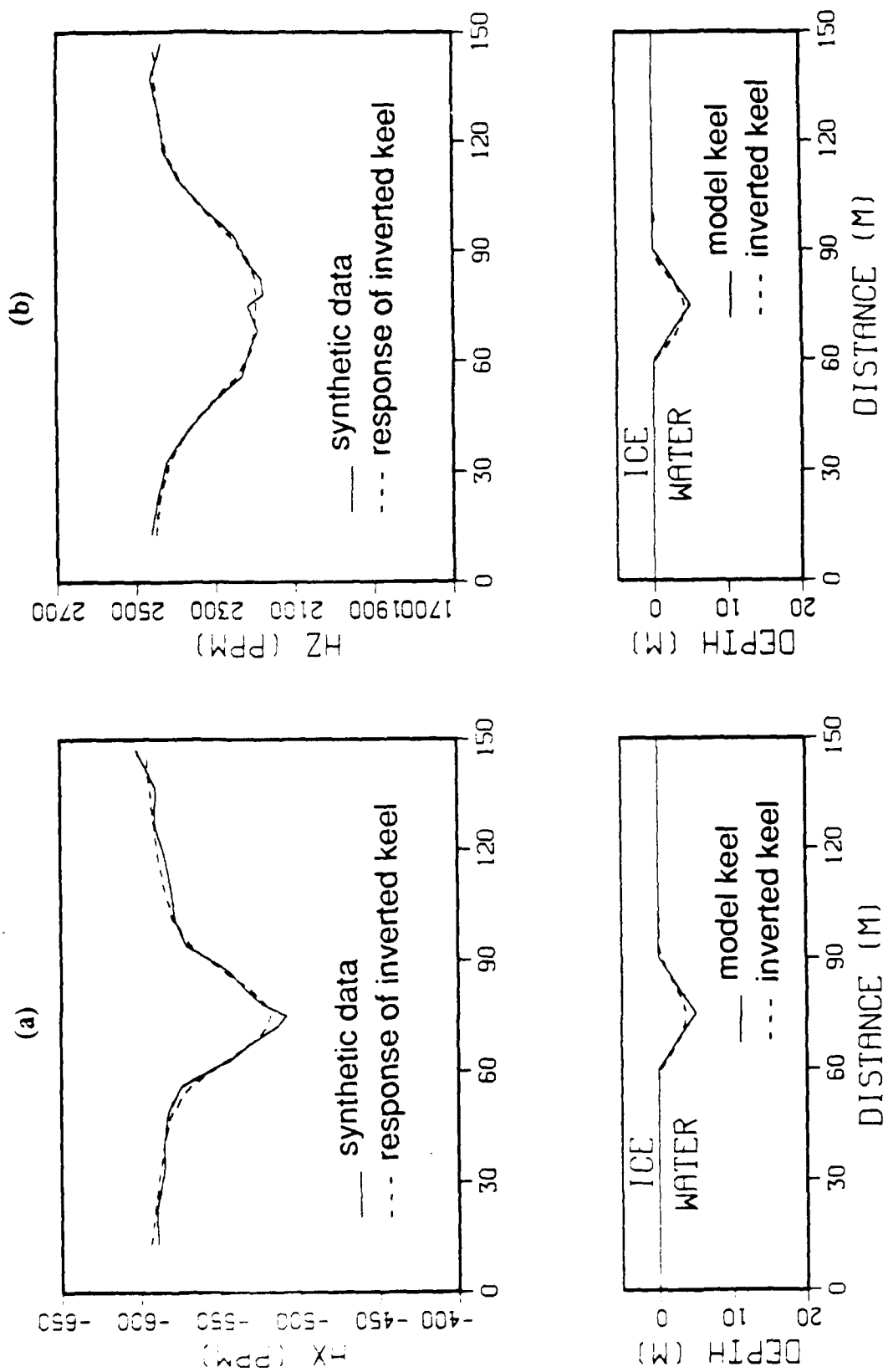


Figure 14 (a) Synthetic data with 5% added noise and inversion results for the HX system, Model 1. (b) Synthetic data with 5% added noise and inversion results for the IIZ system, Model 1.

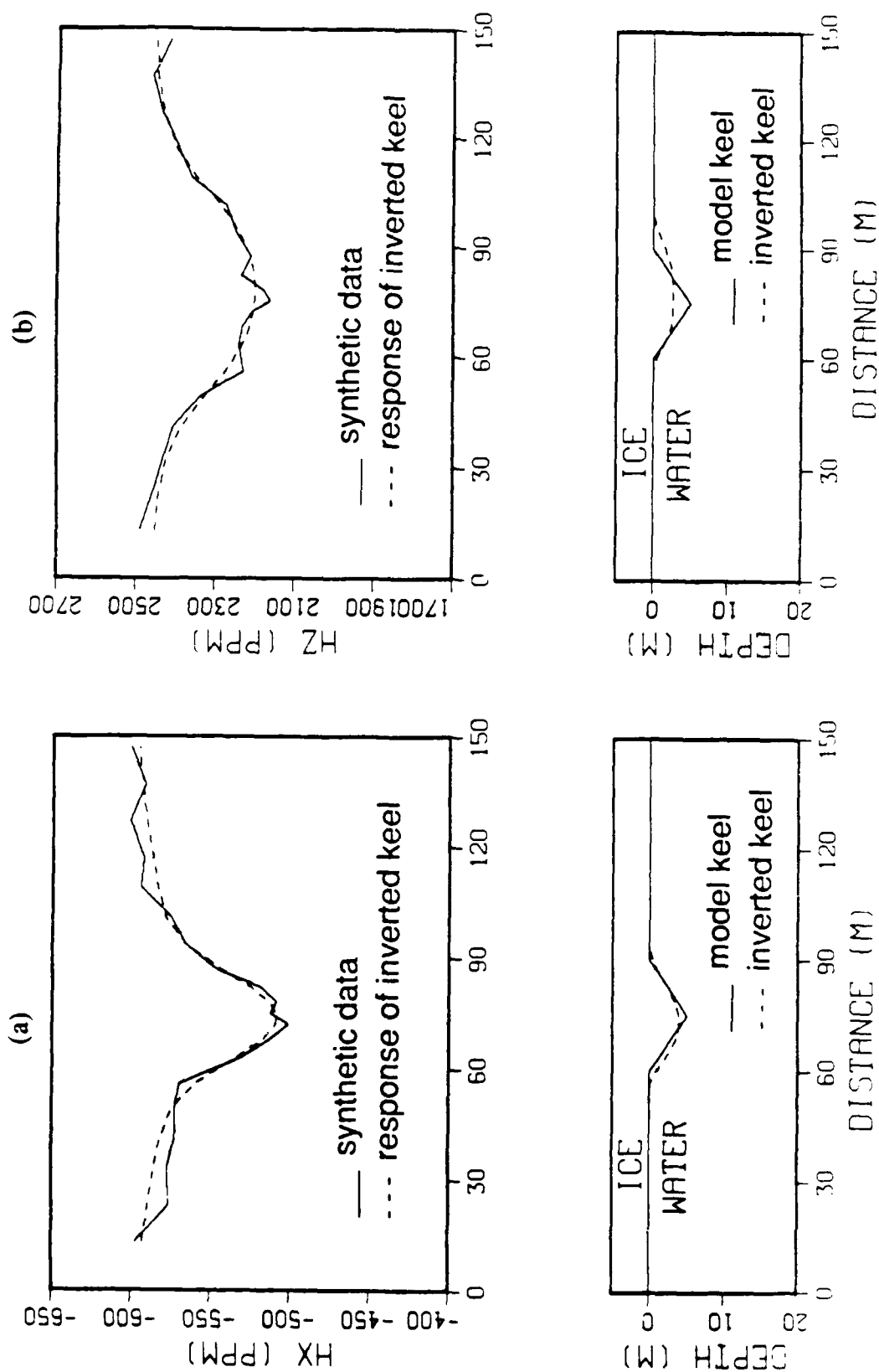


Figure 15 (a) Synthetic data with 10% added noise and inversion results for the HX system, Model 1. (b) Synthetic data with 10% added noise and inversion results for the HZ system, Model 1.

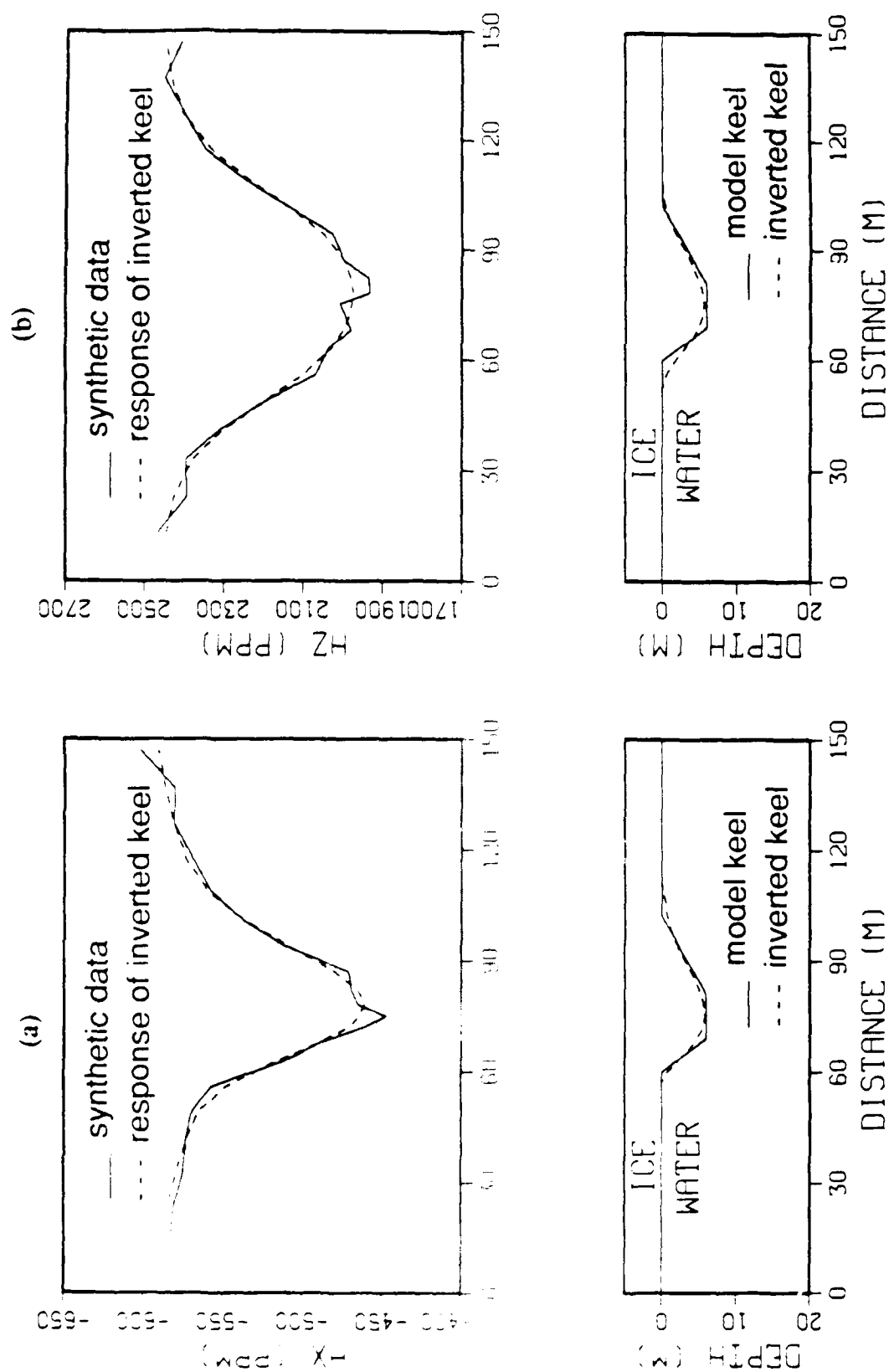


Figure 16 (a) Synthetic data with 5% added noise and inversion results for the HX system, Model 2. (b) Synthetic data with 5% added noise and inversion results for the HZ system, Model 2.

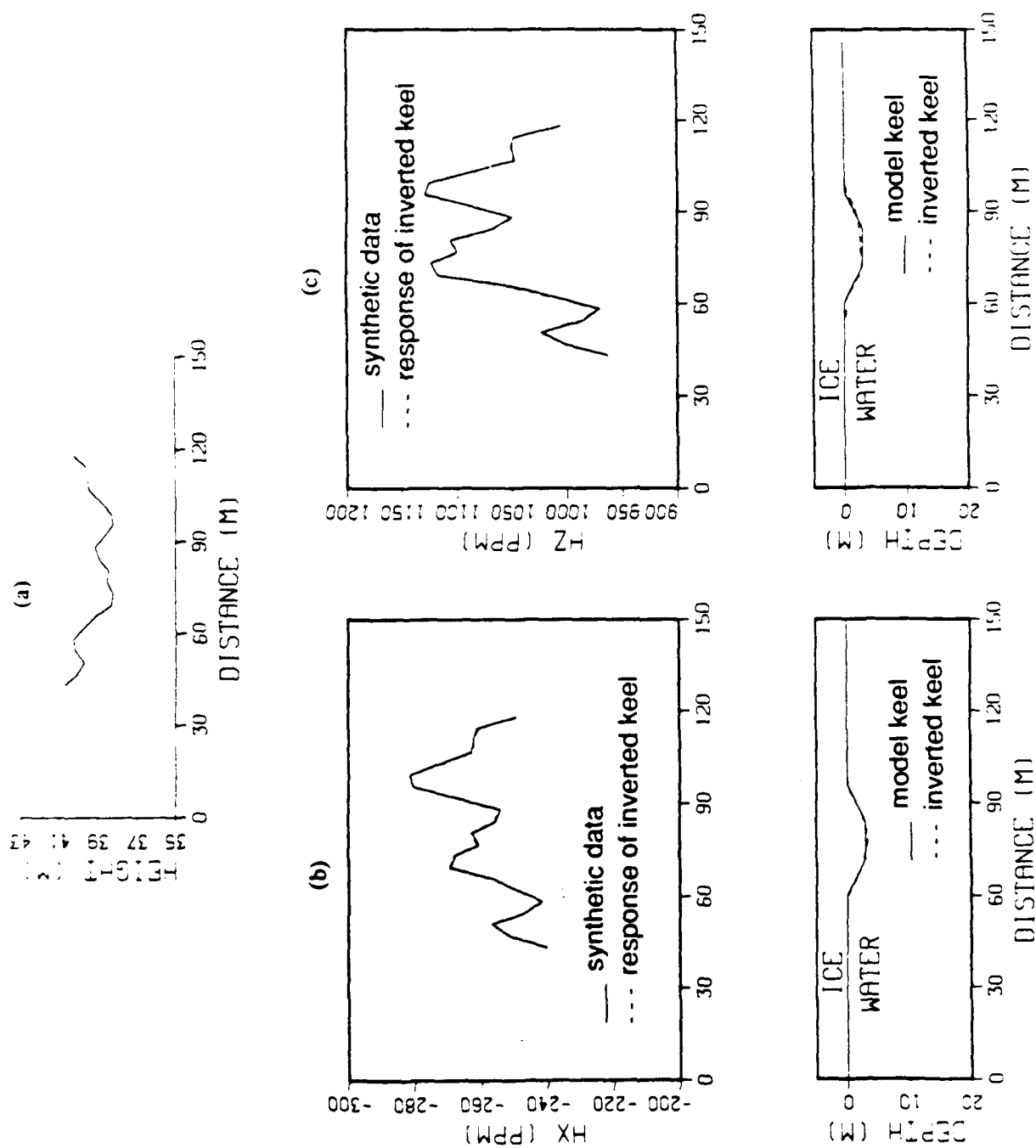


Figure 17 (a) Height of the system over the ice/water interface during the flight. (b) Synthetic data and inversion results for the IIX system, Model 3. (c) Synthetic data and inversion results for the IIZ system, Model 3.

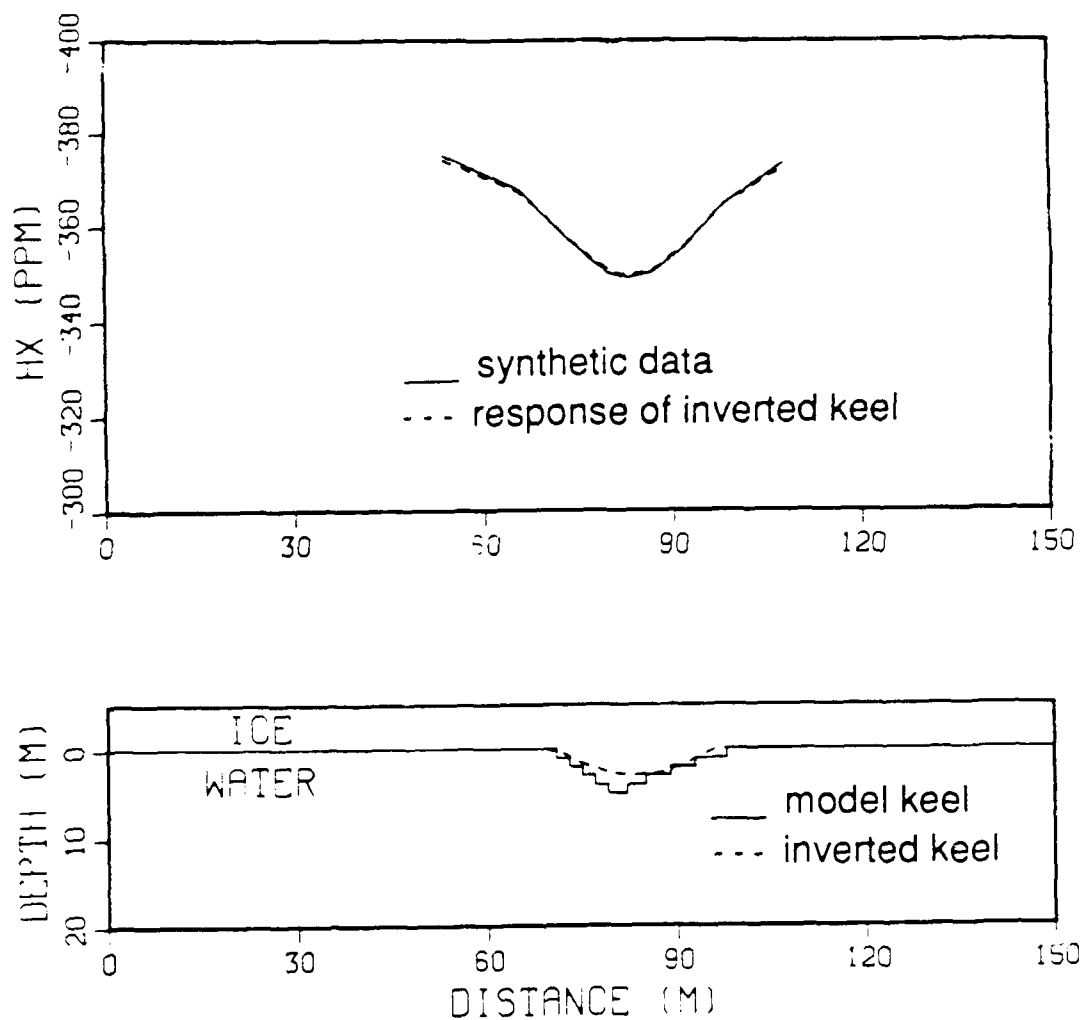


Figure 18 Synthetic data at 2500Hz and inversion results for the HX system, Model 4. The data shown are the scaled sum of the in-phase and quadrature components of the secondary magnetic field.

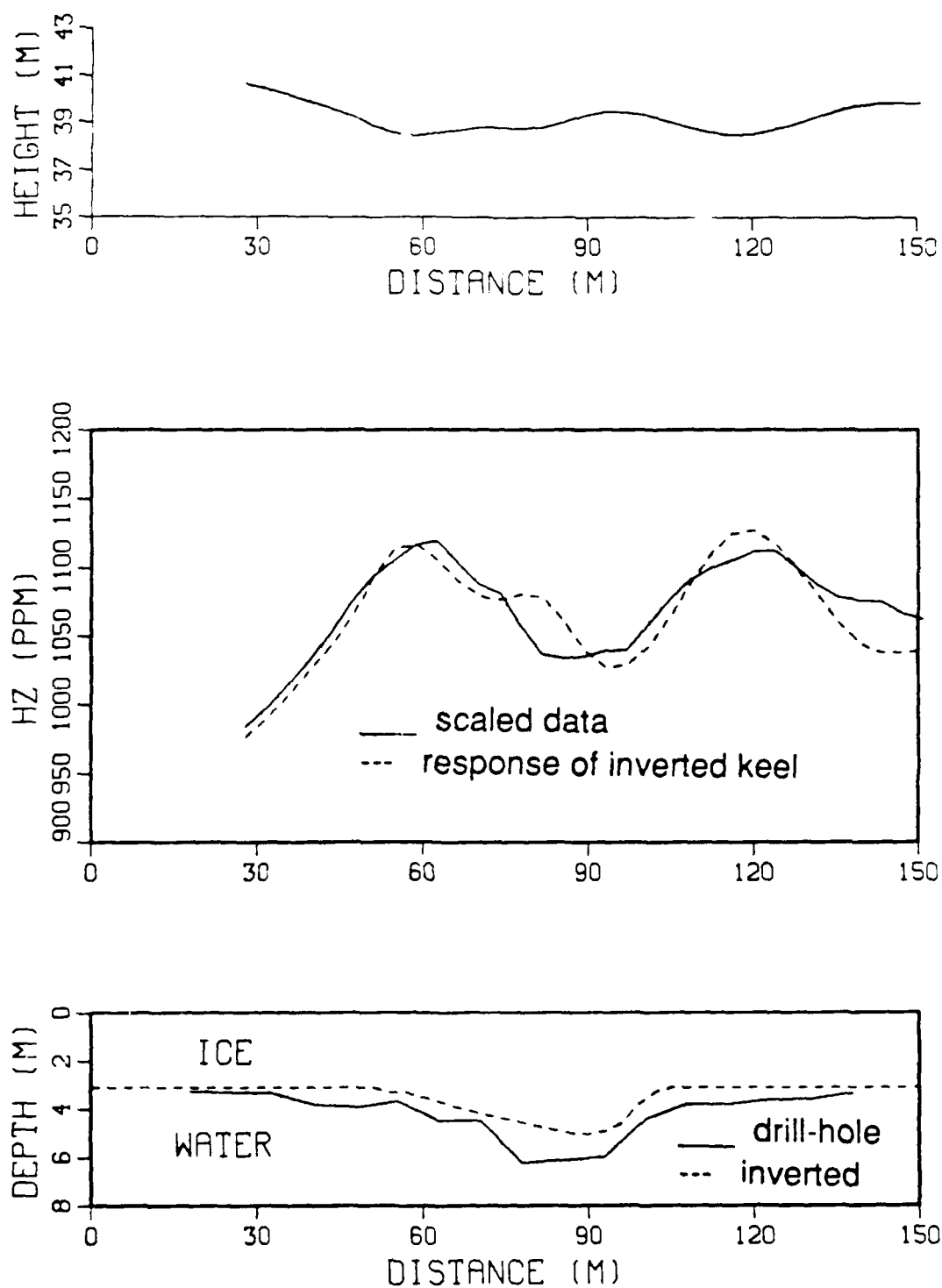


Figure 19 Scaled in-phase data at 16,290Hz and the inversion results for the HZ system. The data were collected at the Prudhoe Bay by Geotech Ltd. in 1985 on line F6L3.

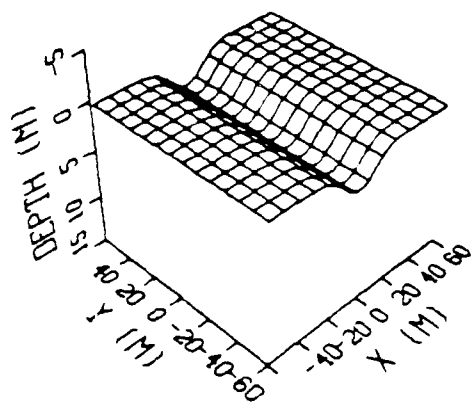
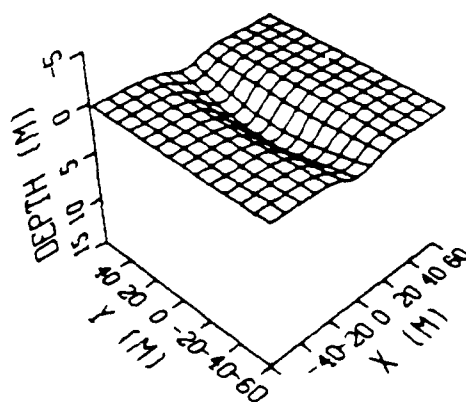
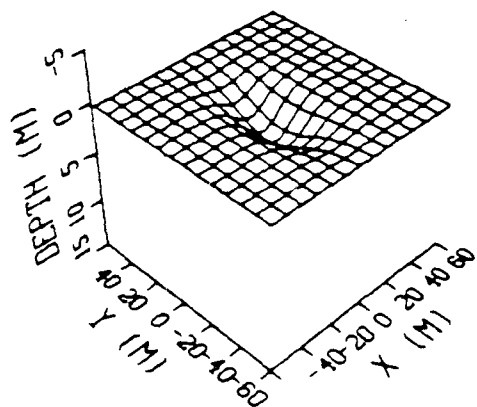
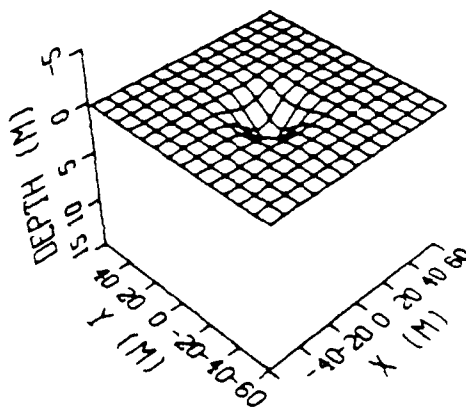
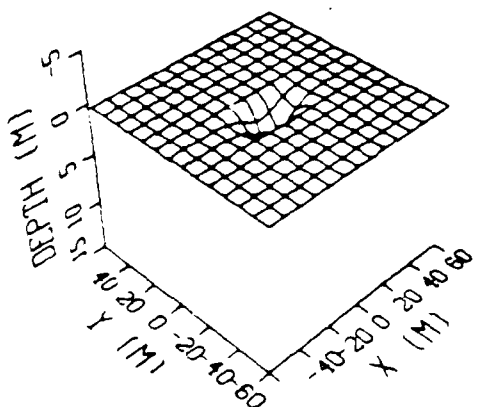
(a) $s = \text{inf.}$ (b) $s = 96\text{m}$ (c) $s = 48\text{m}$ (d) $s = 24\text{m}$ (e) $s = 12\text{m}$ 

Figure 20 Sea ice keels of Model Set 1.
 $A = 3\text{m}$, $w = 24\text{m}$.

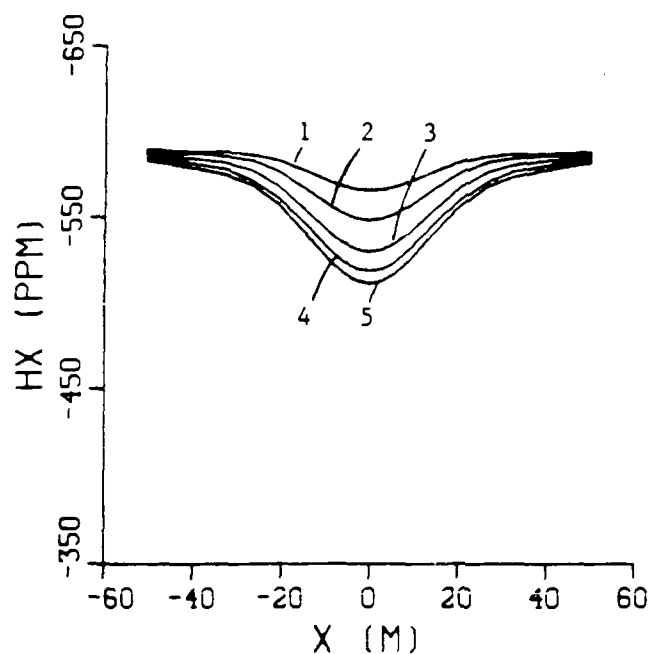


Figure 21(a) HX system response. Curves 1, 2, 3, 4, and 5 correspond to $s = 12, 24, 48, 96$, and infinity meters respectively.

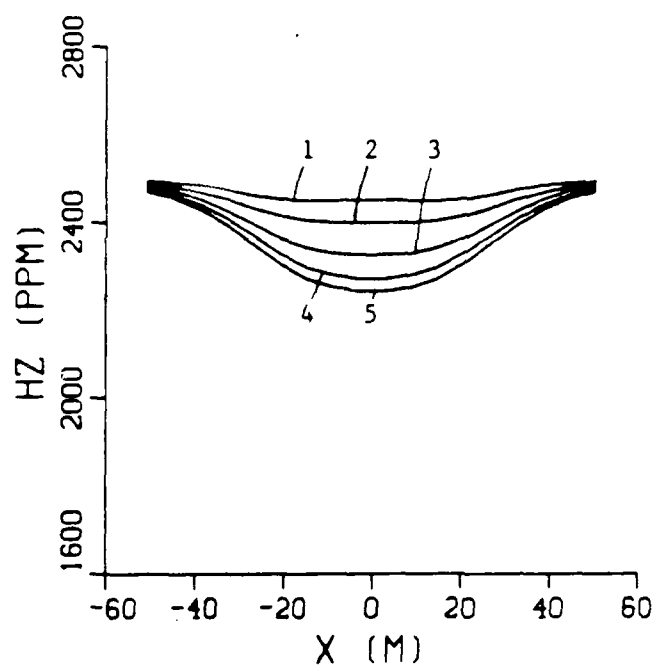


Figure 21(b) HZ system response. Curves 1, 2, 3, 4, and 5 correspond to $s = 12, 24, 48, 96$, and infinity meters respectively.

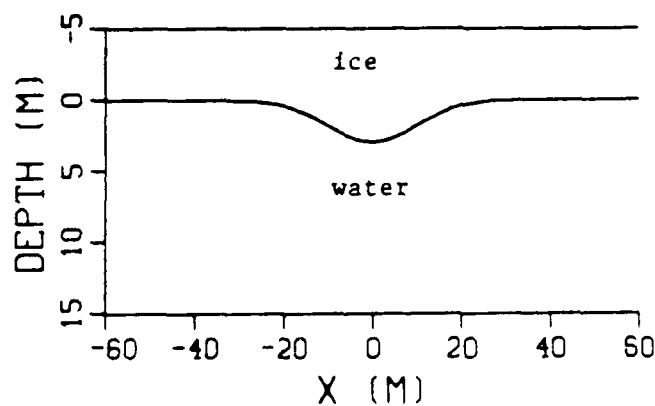


Figure 21(c) Cross section of the ice below the flight line.

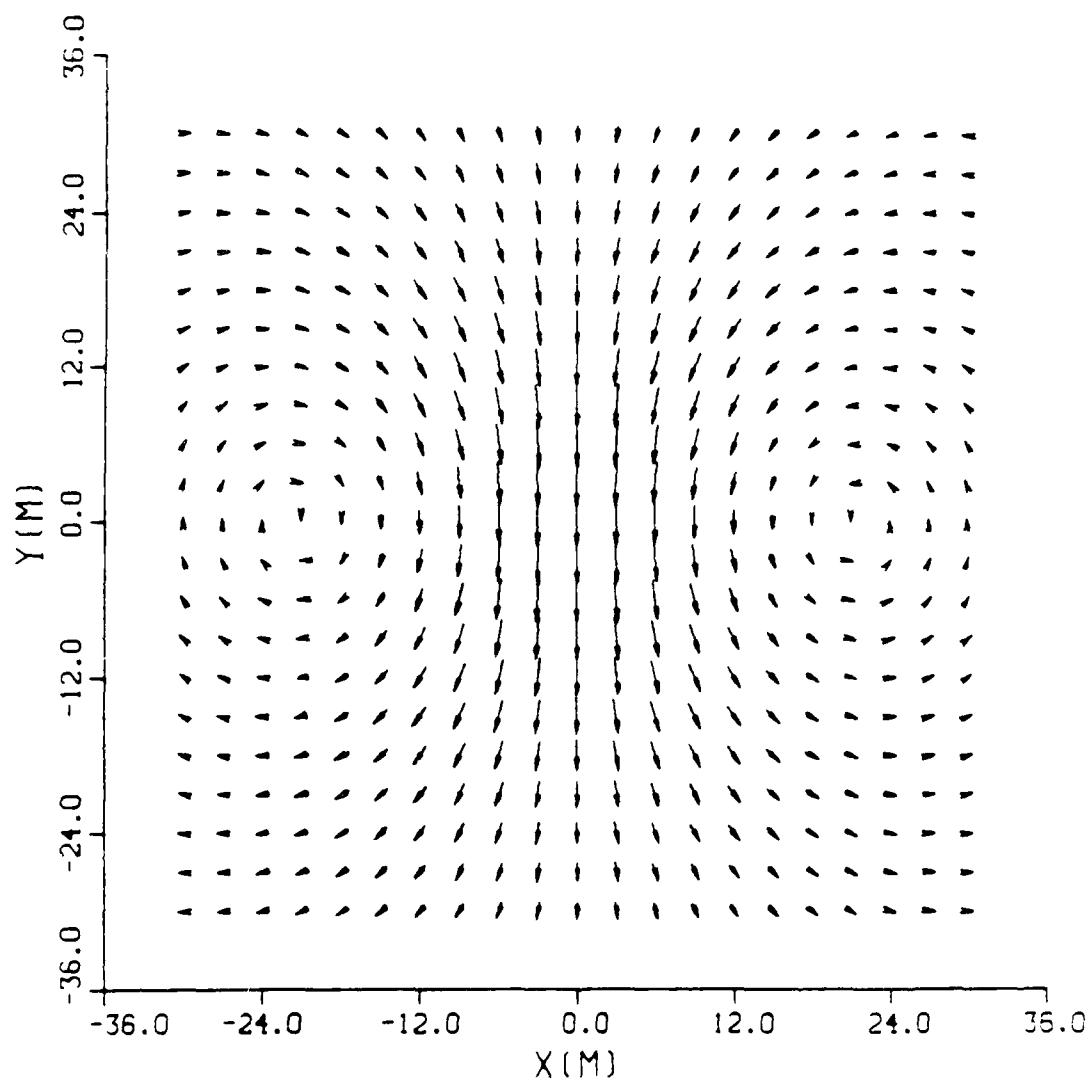


Figure 22 Surficial currents for a horizontal-axis transmitter, which is 30 meters above the center (0, 0).

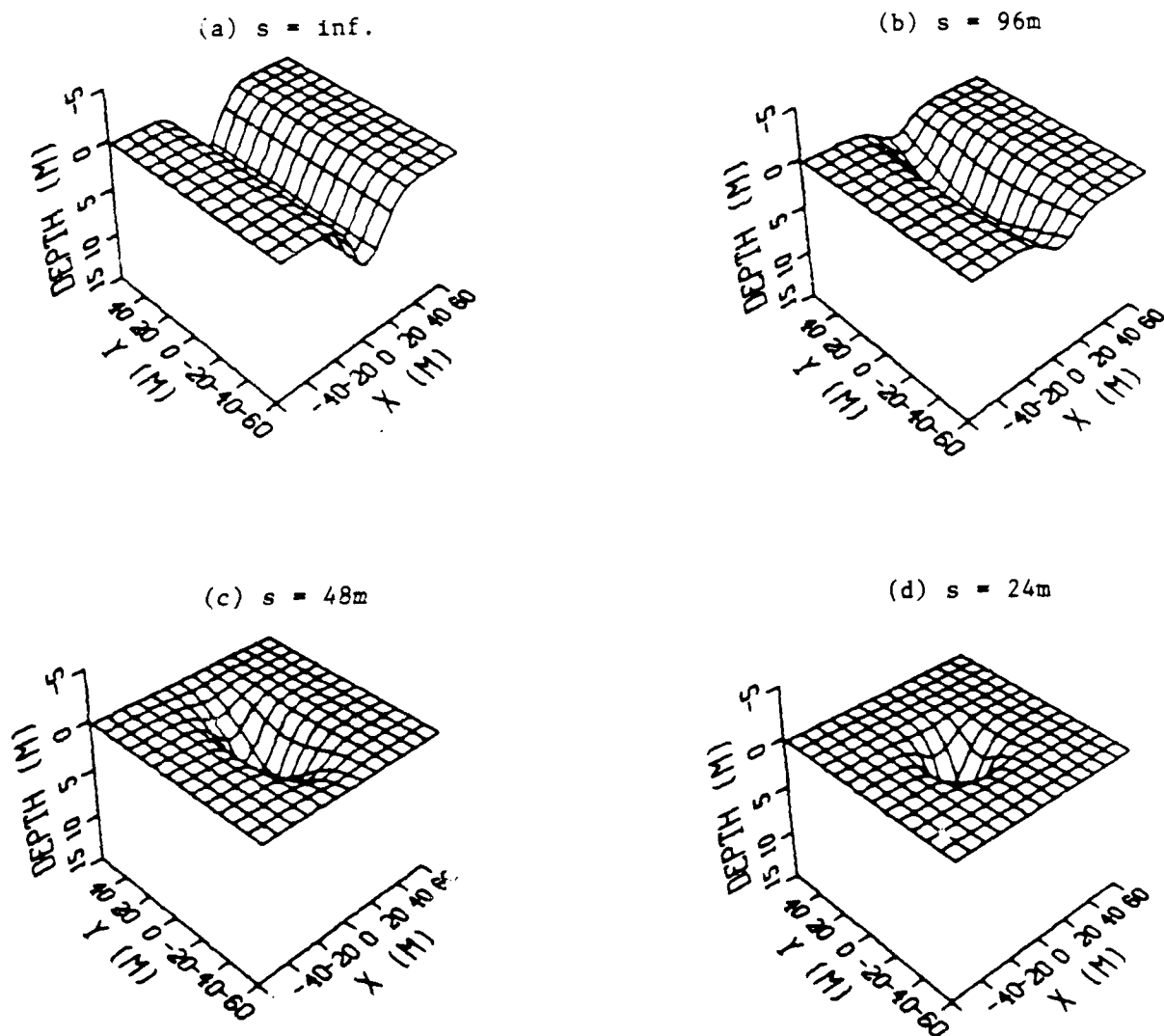


Figure 23 Sea ice keels of Model Set 2.
 $A = 6\text{m}$, $w = 24\text{m}$.

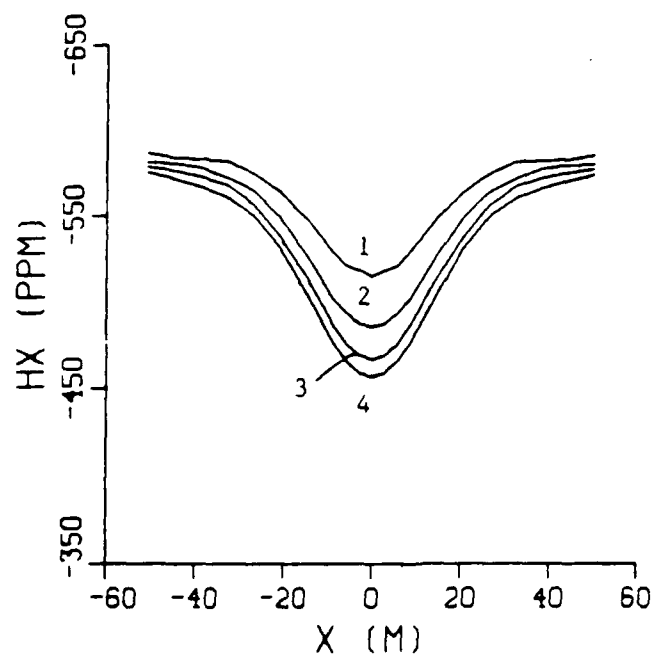


Figure 24(a) HX system response
Curves 1, 2, 3, 4 correspond to
 $s = 24, 48, 96$, and inf. meters
respectively.

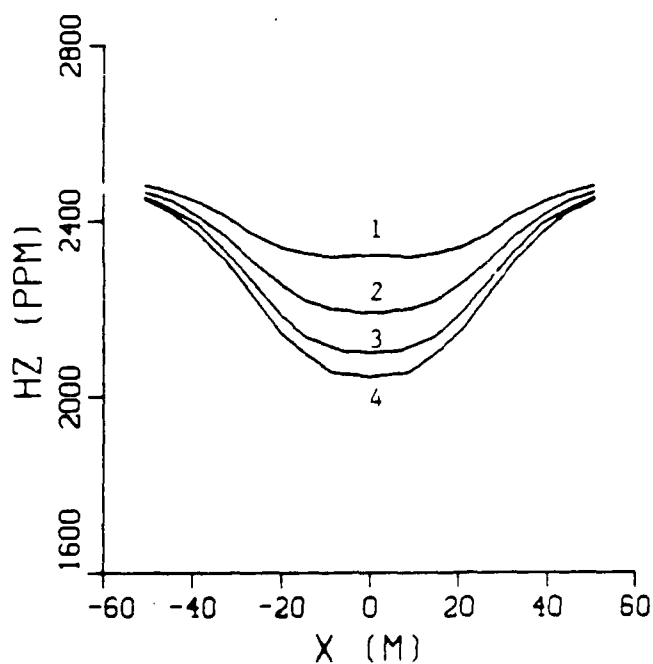


Figure 24(b) HZ system response
Curves 1, 2, 3, 4 correspond to
 $s = 24, 48, 96$, and inf. meters
respectively.

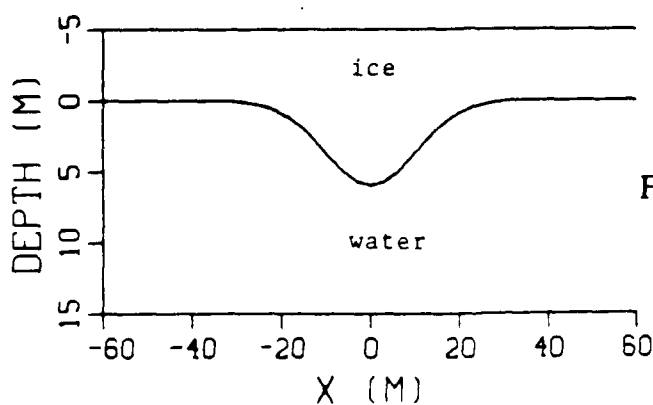


Figure 24(c) Cross section of the ice
below the flight line.

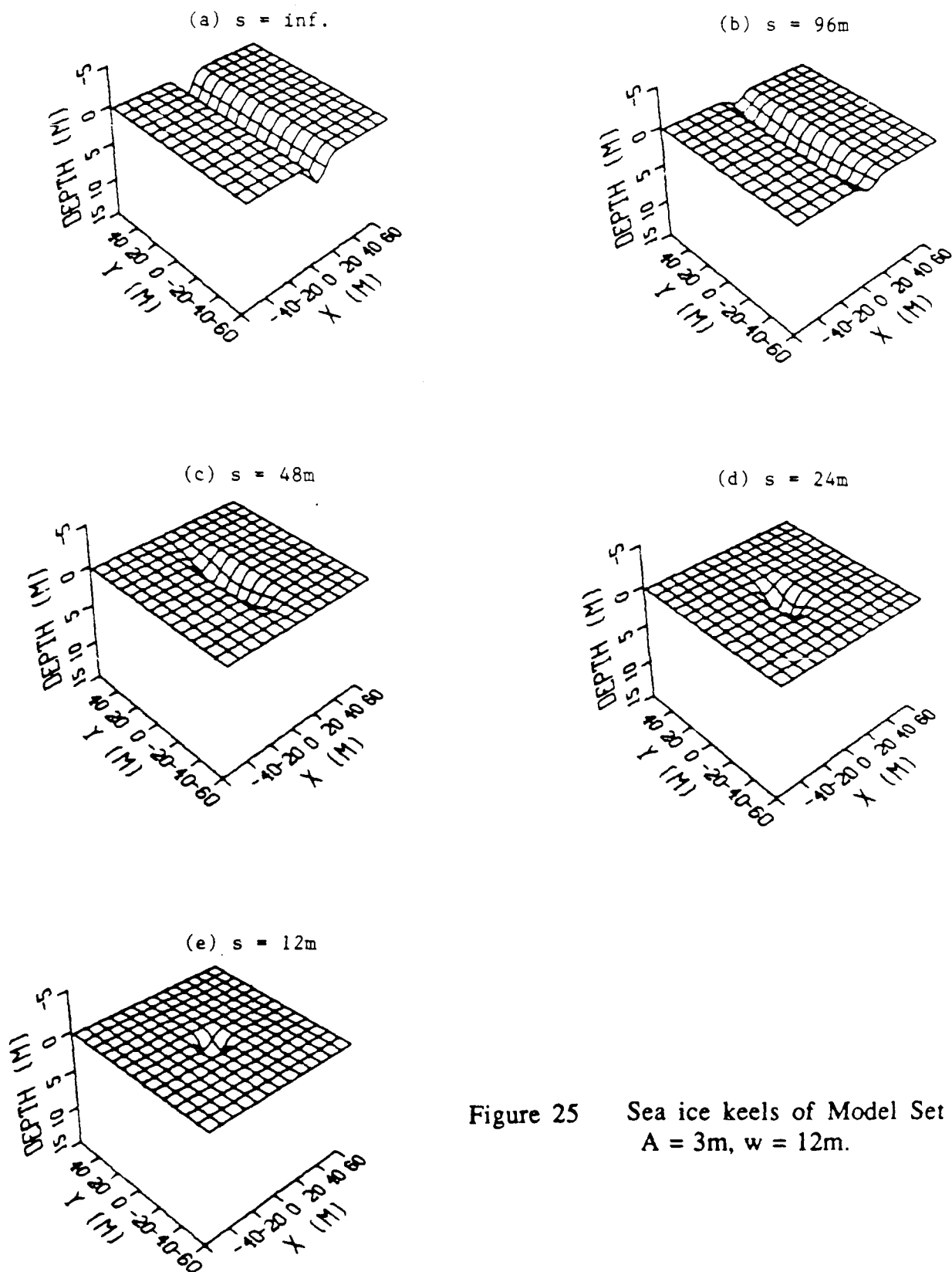


Figure 25 Sea ice keels of Model Set 3.
 $A = 3\text{m}$, $w = 12\text{m}$.

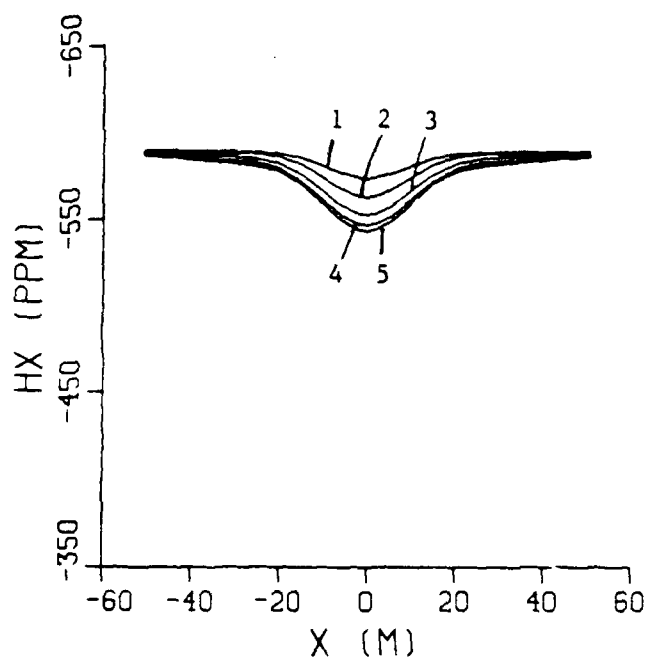


Figure 26(a) HX system response
Curves 1, 2, 3, 4 and 5 correspond to $s = 12, 24, 48, 96$, and 192 meters respectively.

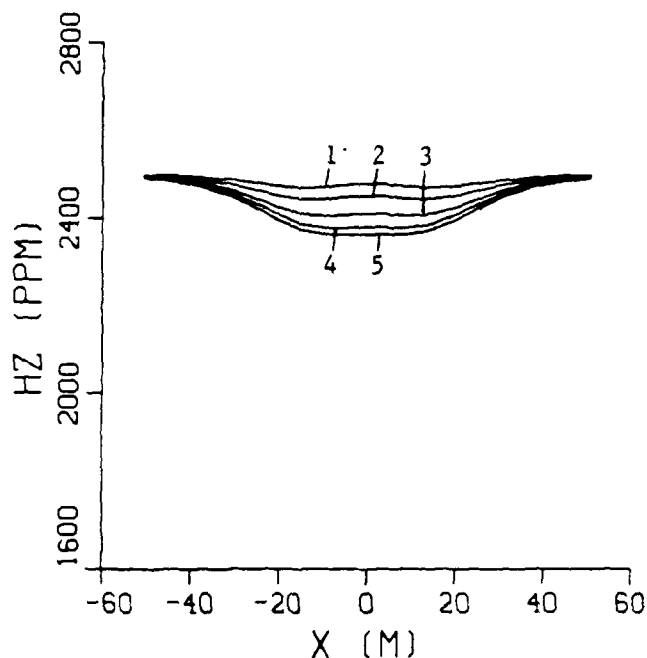


Figure 26(b) HZ system response
Curves 1, 2, 3, 4 and 5 correspond to $s = 12, 24, 48, 96$, and 192 meters respectively.

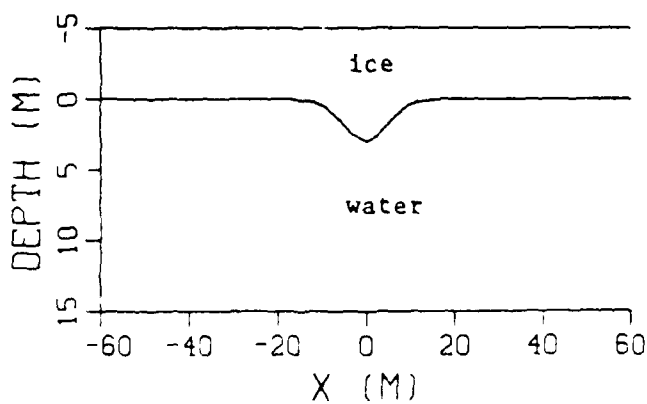


Figure 26(c) Cross section of the ice below the flight line.

Appendix A

Computational Methods

A.1 The General Case

Consider an alternating magnetic dipole (current loop) source T, located in free space as shown in Figure A1. Its orientation is arbitrary and it is positioned over a homogeneous, perfectly conductive medium with three-dimensional surface relief. Due to this source, electric currents are induced on the surface of the medium and they give rise to the secondary magnetic field \mathbf{H}_S in free space. It is our objective to calculate this quantity at any point above the surface S.

Here the height of the source above the medium is assumed to be small compared to the wavelength. The observation point is also assumed to be close to the source so that the electromagnetic field is quasi-static. In free space, $\nabla \times \mathbf{H}_S = 0$, and we may relate \mathbf{H}_S to a scalar magnetic potential ϕ

$$\mathbf{H}_S = -\nabla \phi \quad (1)$$

We also have $\nabla \cdot \mathbf{H}_S = 0$ and correspondingly

$$\nabla^2 \phi = 0 \quad (2)$$

Since the lower medium is assumed to be infinitely conductive, the normal component of the total magnetic field must vanish on the surface S, i.e.

$$H_{pn} + H_{sn} = 0 \quad \text{on } S \quad (3)$$

Here, H_{pn} and H_{sn} are the normal components of the secondary and primary magnetic fields respectively. Hence,

$$\left. \frac{\partial \phi}{\partial n} \right|_S = -H_{sn}|_S = H_{pn}|_S \quad (4)$$

The Laplace equation (2) and the boundary condition (4) constitute the Neumann boundary value problem. That is, given the normal derivative of the potential on a surface S , we wish to calculate the potential itself in the free space. Once ϕ is found, H_S may be calculated from equation (1).

The solution of the Neumann problem outside a closed surface can be expressed as the potential of a surface charge layer (Graham, 1980)

$$\phi(O) = \int_S \frac{\xi(P)}{r_{PO}} ds \quad (5)$$

where $\xi(P)$ is a fictitious charge density function, r_{OP} is the distance between points P and O (see Figure 1). The charge density satisfies a Fredholm integral equation of the second kind

$$\xi(M) = - \frac{1}{2\pi} \left. \frac{\partial \phi}{\partial n} \right|_S - \frac{1}{2\pi} \int_S \xi(P) \frac{\cos(r_{PM}, \mathbf{N})}{r_{PM}^2} ds \quad \text{on } S \quad (6)$$

where (r_{PM}, \mathbf{N}) is the angle between r_{PM} (the vector connecting P to M) and \mathbf{N} (the unit normal vector at M). In our problem, the surface S extends to infinity and equations (5) and (6) are still valid.

To solve the integral equation (6), we use the successive approximation method (Mikhlin, 1964). The initial solution (first iteration) is assumed to be the first term on the right hand side of equation (6), i.e.

$$\xi(M) = - \frac{1}{2\pi} \left. \frac{\partial \phi}{\partial n} \right|_S = - \frac{1}{2\pi} H_{pn}$$

We then use this value in the integral in the equation to compute an improved value of $\xi(M)$ and so on. Once the charge density is known,

the secondary magnetic field can be calculated from the following equation, which is obtained by combining equations (1) and (5)

$$\mathbf{H}_s = \int_S \frac{\xi(p)}{r_{PO}^3} \mathbf{r}_{PO} ds \quad (7)$$

Here \mathbf{r}_{PO} is the vector connecting P to O.

In the above context, the electrodynamic problem is reduced to a potential problem under the quasi-static field assumption. The charge distribution on the surface of the conductive medium is computed first. The secondary magnetic field in the free space is then found by summing up the contributions from the individual charges. This is analogous to the integral equation approach for solving electromagnetic scattering problem (Parry and Ward, 1970), where the equivalent electric and magnetic currents are first sought; the electromagnetic field are then obtained by integrating the contributions from the current distribution.

In the special case where the surface S forms a plane, the solution given by equation (7) for an oscillating magnetic dipole source is identical to that obtained by the method of images (Jackson, 1975). To illustrate our computational method, we now show this to be true for a vertical magnetic dipole source. The coordinate system is chosen such that the z axis is pointing vertically downward. The XOY plane is on the surface of the conductor which occupies the half space $z > 0$. The dipole source is h meters above the plane on the z axis and points in the positive z direction.

Since \mathbf{r}_{PM} is perpendicular to N (cf. Figure 1), equation (6) reduces to

$$\xi(M) = - \frac{1}{2\pi} \frac{\partial \phi}{\partial n} |_s = - \frac{1}{2\pi} H_{pm} \quad (8)$$

On the conductor surface, the normal component of the primary magnetic field is

$$H_{pn} = - \frac{1}{4\pi} \frac{2h^2 - x^2 - y^2}{(x^2 + y^2 + h^2)^{5/2}} \quad (9)$$

Substituting equations (8) and (9) into (5), we obtain

$$\phi(x, y, z) = \int_{-\infty}^{+\infty} \int_{-\infty}^{+\infty} \frac{\xi(x', y', 0)}{[(x-x')^2 + (y-y')^2 + z^2]^{1/2}} dx' dy' \quad (z < 0)$$

$$\phi(0, 0, z) = \frac{1}{8\pi^2} \int_{-\infty}^{+\infty} \int_{-\infty}^{+\infty} \frac{2h^2 - x'^2 - y'^2}{(x'^2 + y'^2 + h^2)^{5/2}} \frac{dx' dy'}{(x'^2 + y'^2 + z^2)^{1/2}}$$

Let $x' = R \cos \theta$, $y' = R \sin \theta$, $dx' dy' = R d\theta dR$, then

$$\phi(0, 0, z) = \frac{1}{8\pi^2} \int_0^{+\infty} \int_0^{2\pi} \frac{2h^2 - R^2}{(R^2 + h^2)^{5/2}} \frac{R d\theta dR}{(R^2 + z^2)^{1/2}}$$

Furthermore, let $r^2 = R^2 + h^2$, $R dR = r dr$, then

$$\phi(0, 0, z) = \frac{1}{4\pi} \int_h^{+\infty} \frac{3h^2 - r^2}{r^4 (r^2 - h^2 + z^2)^{1/2}} dr$$

The above integration can be carried out and the result is as follows

$$\phi(0, 0, z) = \frac{1}{4\pi} \frac{1}{(h-z)^2} \quad (z < 0)$$

The vertical component of the secondary magnetic field on z axis is

$$H_{sz}(0, 0, z) = - \frac{\partial \phi}{\partial z} = \frac{1}{2\pi} \frac{1}{(h-z)^3} \quad (10)$$

and as required is identical to the image field.

A.2 The 2-D keel

In the 2-D case, the geometry of the ice-water interface does not change in the strike direction (y -direction here). The relief of the interface is only a function of x , i.e. $h(x,y) = h(x)$. In this case, the potential of the scattered magnetic field is given by,

$$\Phi(x, y, z) = \iint_{-\infty}^{+\infty} \frac{\xi(x', y') \sqrt{1 + [dh(x')/dx']^2}}{\sqrt{(x-x')^2 + (y-y')^2 + (z-h(x'))^2}} dx' dy' \quad (11)$$

and the surface charge density $\xi(x, y)$ satisfies

$$\begin{aligned} \xi(x, y) = & -\frac{1}{2\pi} H_{pn}(x, y) - \frac{1}{2\pi} \iint_{-\infty}^{+\infty} \xi(x', y') \frac{(x-x')dh(x')/dx' - (h(x)-h(x'))}{[(x-x')^2 + (y-y')^2 + (h(x)-h(x'))^2]^{\frac{3}{2}}} \\ & \cdot \left[\frac{1 + (dh(x')/dx')^2}{1 + (dh(x)/dx)^2} \right]^{\frac{1}{2}} dx' dy' \end{aligned} \quad (12)$$

Here $H_{pn}(x, y)$ is the normal component of the primary magnetic field at the ice-water interface.

Notice that in equations 11 and 12 the integral with regard to y' is a convolution. Taking the Fourier transform of both sides we get

$$\begin{aligned} \Phi(x, k_y, z) = & \int_{-\infty}^{+\infty} \Phi(x, y, z) e^{-ik_y y} dy \\ = & 2 \int_{-\infty}^{+\infty} \xi(x', k_y) \sqrt{1 + [dh(x')/dx']^2} K_0(\rho |k_y|) dx' \end{aligned} \quad (13)$$

and

$$\xi(x, k_y) = -\frac{1}{2\pi} H_{pn}(x, k_y) - \frac{1}{2\pi} \int_{-\infty}^{+\infty} \xi(x', k_y) f(x, x', k_y) dx' \quad (14)$$

where the kernel of the integration is

$$f(x, x', k_y) = 2 \left[\frac{1 + (dh(x')/dx')^2}{1 + (dh(x)/dx)^2} \right]^{\frac{1}{2}} \frac{(x-x')dh(x')/dx' - (h(x)-h(x'))}{[(x-x')^2 + (h(x)-h(x'))^2]^{\frac{1}{2}}} \cdot |k_y| K_1(\rho' |k_y|) \quad (15)$$

In the above equations

k_y = angular wave number in the y direction

$$\rho = \sqrt{(x-x')^2 + (z-h(x'))^2}$$

$$\rho' = \sqrt{(x-x')^2 + (h(x)-h(x'))^2}$$

$K_0()$ = modified Bessel function of the zeroth order. Second kind.

$K_1()$ = modified Bessel function of the first order. Second kind.

We have thus simplified the problem by decomposing a two dimensional integral equation into a number of integral equations in one dimension.

For the case where the source is a horizontal or vertical magnetic dipole, the normal component of the primary magnetic field can be analytically transformed into the wave-number domain (i.e. $H_{pn}(x, k_y)$) as follows.

The normal component of the primary magnetic field at the ice-water interface is

$$H_{pn}(x, y) = H_p(x, y) \cdot n(x, y) \quad (16)$$

where $n(x, y)$ is the outward normal at point (x, y) on the interface. It is given by

$$n = \left(\frac{h'(x)}{\sqrt{1 + [h'(x)]^2}}, 0, -\frac{1}{\sqrt{1 + [h'(x)]^2}} \right) \quad (17)$$

where $h'(x) = dh(x)/dx$. Thus

$$H_{pn}(x, y) = \frac{h'(x)}{\sqrt{1 + [h'(x)]^2}} H_{px} - \frac{1}{\sqrt{1 + [h'(x)]^2}} H_{pz} \quad (18)$$

(a) Horizontal magnetic dipole source located at $(x_s, y_s=0, z_s)$

$$H_{px}(x, y) = \frac{2(x - x_s)^2 - y^2 - (h(x) - z_s)^2}{4\pi r^5}$$

$$H_{pz}(x, y) = \frac{3(x - x_s)(h(x) - z_s)}{4\pi r^5}$$

Here

$$r = \sqrt{(x - x_s)^2 + y^2 + (h(x) - z_s)^2}$$

Substituting the above equations into (18) and taking the Fourier transform give

$$H_{pn}(x, k_y) = \frac{1}{2\pi \rho^2 \sqrt{1 + [h'(x)]^2}} \left\{ [h'(x)(x - x_s)^2 - (x - x_s)(h(x) - z_s)] |k_y|^2 K_0(\rho |k_y|) \right. \\ \left. - \{[(h(x) - z_s)^2 - (x - x_s)^2] h'(x) + 2(x - x_s)(h(x) - z_s)\} \frac{|k_y|}{\rho} K_1(\rho |k_y|) \right\} \quad (19)$$

where

$$\rho = \sqrt{(x - x_s)^2 + (h(x) - z_s)^2}$$

As $k_y \rightarrow 0$, the asymptotic forms of the modified Bessel functions are

$$K_0(\rho |k_y|) \rightarrow -\ln \rho |k_y|$$

$$K_1(\rho |k_y|) \rightarrow \frac{1}{\rho |k_y|}$$

Therefore

$$H_{pn}(x, k_y=0) = \frac{-1}{2\pi \rho^4 \sqrt{1 + [h'(x)]^2}} \{[(h(x) - z_s)^2 - (x - x_s)^2] h'(x) + 2(x - x_s)(h(x) - z_s)\} \quad (20)$$

(b) Vertical magnetic dipole source located at $(x_s, y_s=0, z_s)$

$$H_{px}(x, y) = \frac{3(x - x_s)(h(x) - z_s)}{4\pi r^5}$$

$$H_{pz}(x, y) = \frac{2(h(x) - z_s)^2 - y^2 - (x - x_s)^2}{4\pi r^5}$$

$$H_{pn}(x, k_y) = \frac{1}{2\pi\rho^2\sqrt{1+[h'(x)]^2}} \left\{ [-(h(x)-z_s)^2 + h'(x)(x-x_s)(h(x)-z_s)] |k_y|^2 K_0(\rho|k_y|) \right. \\ \left. - [(h(x)-z_s)^2 - (x-x_s)^2 - 2h'(x)(x-x_s)(h(x)-z_s)] \frac{|k_y|}{\rho} K_1(\rho|k_y|) \right\} \quad (21)$$

$$H_{pn}(x, k_y=0) = \frac{-1}{2\pi\rho^4\sqrt{1+[h'(x)]^2}} \{ (h(x)-z_s)^2 - (x-x_s)^2 - 2h'(x)(x-x_s)(h(x)-z_s) \} \quad (22)$$

Note here that the kernel $f(x, x', k_y)$ is independent of the source and the receiver positions. Therefore it may be calculated once for each k_y value and stored for the computation of a complete profile of AEM system response. This is quite economical but impossible in the 3-D case where the matrix is too large to store. At $x = x'$, the kernel has a singularity. But this presents no difficulty for the numerical computation because it is integrable in the sense of Cauchy principal value.

The integral equation (14) can be solved for $\xi(x, k_y)$ using successive approximation method identical to the one suggested above for the general case. This needs to be done at a number of positive k_y harmonics (including $k_y = 0$). The values of $\xi(x, k_y)$ at the negative k_y harmonics may be easily obtained by its property of symmetry. As usual, the sampling in the k_y space is done on a logarithmic scale.

Once the charge density is known, the x- and z- components of the scattered magnetic field may be directly computed from the following equations

$$\begin{aligned}
 H_{sx}(x, k_y, z) &= - \frac{\partial \phi(x, k_y, z)}{\partial x} \\
 &= 2 \int_{-\infty}^{+\infty} (x - x') \xi(x', k_y) \sqrt{1 + [dh(x')/dx']^2} \frac{|k_y|}{\rho} K_1(\rho |k_y|) dx'
 \end{aligned} \tag{23}$$

and

$$\begin{aligned}
 H_{sz}(x, k_y, z) &= - \frac{\partial \phi(x, k_y, z)}{\partial z} \\
 &= 2 \int_{-\infty}^{+\infty} (z - h(x')) \xi(x', k_y) \sqrt{1 + [dh(x')/dx']^2} \frac{|k_y|}{\rho} K_1(\rho |k_y|) dx'
 \end{aligned} \tag{24}$$

Now that the scattered magnetic field is obtained in the wave-number domain its inverse Fourier transform will yield the desired result in the space domain. But prior to performing the inverse Fourier transform, the field values at the logarithmically-spaced points in the k_y space need to be interpolated for uniformly spaced values. This is accomplished using cubic spline interpolation.

The above algorithm has been successfully implemented and its speed is more than 20 times faster than that of the general 3-D algorithm. The computation of a 20 point profile of the AEM system response takes about only 10 seconds CPU time on the IBM 3090.

A.3 Computational Check

A scale model experiment was also performed to check the numerical solution. Aluminum was used to simulate the infinitely conductive medium at a scale of 1:250. A model airborne electromagnetic system was built at the same scale and was "flown" at a field height of 10m. The system consisted of a coplanar, vertical axis transmitter and receiver, which were operated at 6 kHz. Details of the model are shown in Figure A2 which also exhibits the traversed feature.

The cross section of the indented surface is a Gaussian curve that simulates a smooth ice keel. Its relief is given by

$$t(x) = A \exp\left(-\frac{x^2}{2\tau^2}\right) \quad (25)$$

and

$$\tau = 0.425W$$

Here

x = distance from the keel center line

t = keel thickness

A = drawdown or maximum keel thickness

W = keel width at half drawdown

The shape of the keel does not change along its strike direction. For this scale model, A and W were taken to be 3.4m and 21m respectively. We chose this type of surface because its simulation on the computer is simple as there are only two input parameters. Furthermore, it is easy to adjust these two parameters to simulate any real sea ice keel. The measurements and numerical calculation results (two iterations) for this model are displayed in Figure A3, which shows an excellent agreement between the numerical and experimental data.

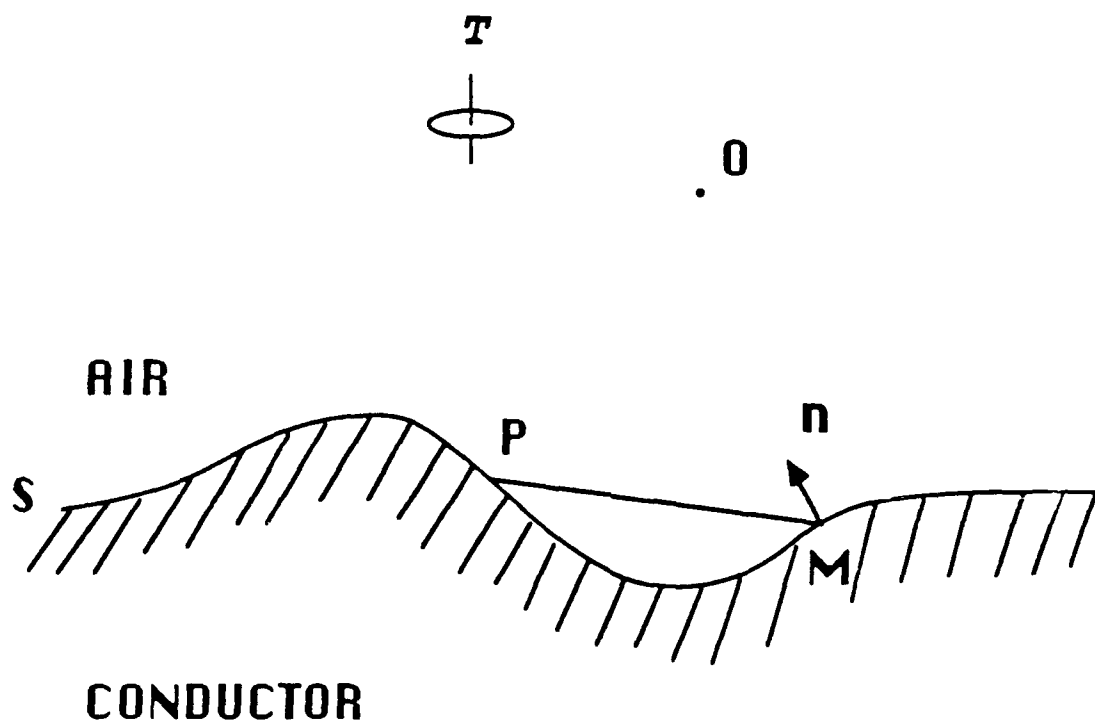


Fig.A1 The Neumann Problem

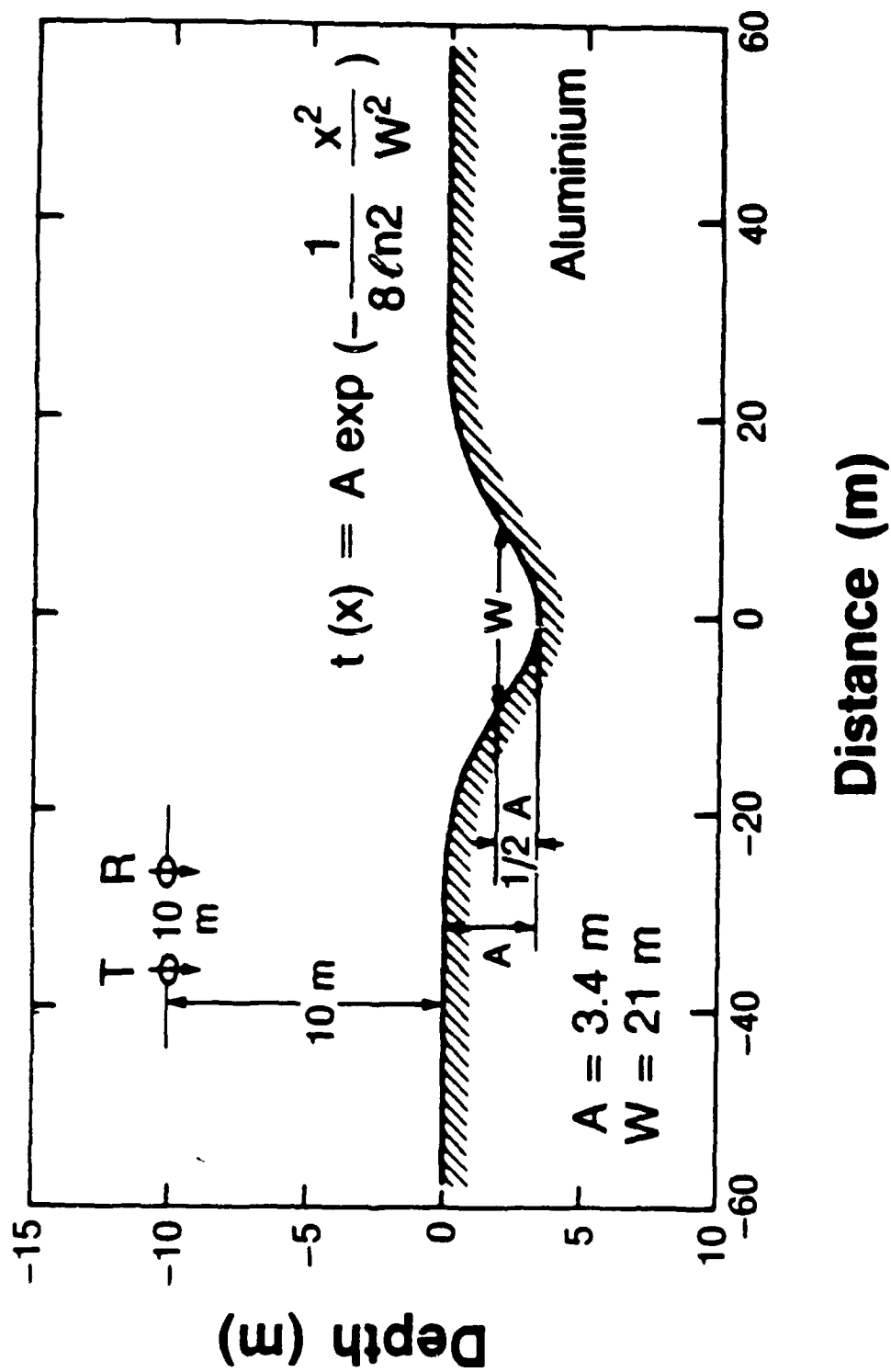


Fig.A2 Scale Model Geometry

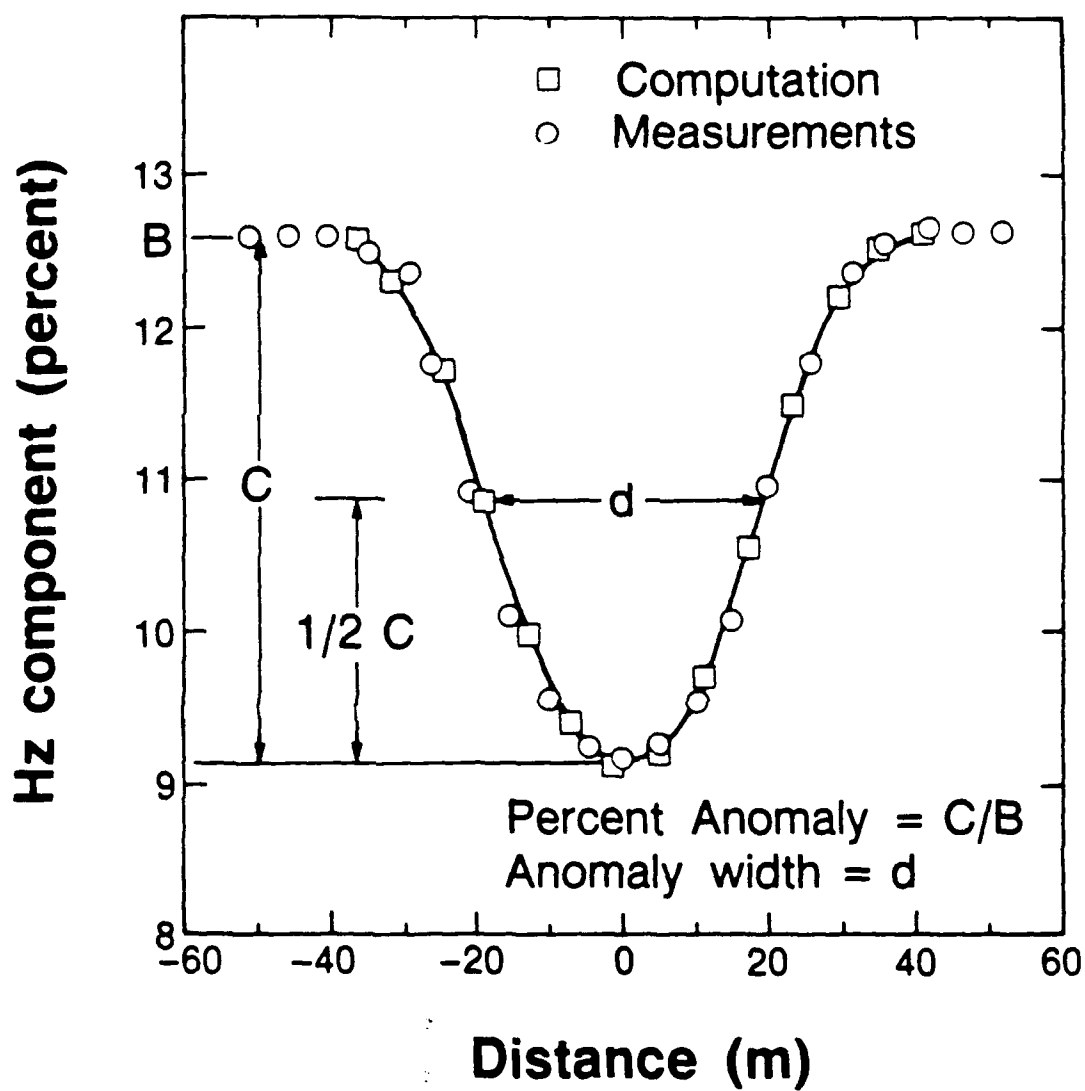


Fig.A3 Comparison of Measurements and Computation

Appendix B

This Appendix includes a listing of three Fortran programs: SURF3D, ICE2D1, and INVSM.

SURF3D is a program for computing the AEM system response for a general three-dimensional ice keel. It may also be used to calculate the surface current distribution on the ice/water interface.

ICE2D1 is a fast modeling program for the computation of AEM system response over a two-dimensional (2-D) ice keel. It is generally more than 20 times faster than using SURF3D for an identical problem.

INVSM is an inversion program for obtaining a 2-D smooth ice keel from the AEM data. It uses ICE2D1 for modeling AEM system response. Here it is acknowledged that part of this program is adapted from program OCCAM1 by Constable.


```

PROGRAM SURF3D
implicit real*8 (a-h, o-z)
*****
c Purpose....
c to compute the secondary electromagnetic response due to a mag-
c netic dipole which sits above a perfectly conductive medium.
c The secondary field is expressed in parts per million of the
c received primary field. The orientation of the dipole is arbi-
c trary and the surface of the conductor is arbitrary. When ipattn
c = 1, the program outputs the total surface current density.
c Program not optimized and can be further improved.
c Gaussian quadrature is used for the integration of the kernel.
c For fast speed, ignore the Gaussian quadrature by setting 0 in
c the IF statement.
c Author ... Guimin Liu, Engineering Geoscience, U.C.Berkeley.
c (415)642-3809 1988
*****
DIMENSION ZH(121,121),XDER(121,121),YDER(121,121),HN(121,121),
+ WZ(121,121)
DIMENSION AMPDER(121,121)
COMMON /AA/ZH/BB/XDER/CC/YDER/DD/HN/EE/W/AMP/AMPDER
COMMON /TR/XS,YS,ZS,XR,YR,ZR
COMMON /NX,NY,NX2,NY2,XDELTA,YDELTA
open (unit=3,file='surf3d.dat')
open (unit=4, file ='surf3d.out')

c WHEN NPLOT=1, THE OUTPUT IS ARRANGED FOR PLOTTING PURPOSE
c READ(3,*) NPLOT,ipattn
c ANGV = VERTICAL ANGLE. ANGH = HORIZONTAL ANGLE FROM X DIRECTION
c INORM = NORMALIZATION COMPONENT. 1 = HX, 2 = HY, 3 = HZ
c READ(3,*) ANGV, ANGH, INORM
c READ IN NUMBER OF SOURCES
c READ(3,*) NSOR
c READ IN GRID NUMBER, MAXIMUM NUMBER OF ITERATIONS
c READ(3,*) NX,NY,NLOOP
c READ IN SURFACE PARAMETERS
c GAUSSIAN DISTRIBUTION SHAPE
c READ(3,*) HEIGHT,XWIDTH,YWIDTH
c READ IN GRID SIZE
c READ(3,*) XDELTA,YDELTA
NS=0
ANGV=ANGV/180.*3.14159
ANGH=ANGH/180.*3.14159
IF (INORM.EQ.1) WRITE(4,41)
IF (INORM.EQ.3) WRITE(4,42)
41 FORMAT(4X,'HORIZONTAL MAGNETIC DIPOLE SOURCE')
42 FORMAT(4X,'VERTICAL MAGNETIC DIPOLE SOURCE')
IF (NPLOT.EQ.1) GOTO 501
WRITE(4,112) ANGV,ANGH,INORM
WRITE(4,111) HEIGHT,XWIDTH,YWIDTH
WRITE(4,200)NX,NY,XDELTA,YDELTA,NLOOP
112 FORMAT(7X,'ANGLE OF THE DIPOLE FROM VERTICAL =',F8.2,/,
+ 7X,'ANGLE OF THE DIPOLE FROM X DIRECTION =',F8.2,/,
+ 7X,'NORMALIZATION COMPONENT 1 = HX 2 = HY 3 = HZ',I5,/,
+ 7X,'ELEMENT SIZE NX =',I5,3X,NY =',I5,
+ 7X,'ELEMENT SIZE DX =',F10.5, DY =',F10.6,
+ 7X,'MAXIMUM ITERATION NUMBER', I8 ,/)
GOTO 666
501 CONTINUE
SUR00160
SUR00170
SUR00180
SUR00190
SUR00200
SUR00210
SUR00220
SUR00230
SUR00240
SUR00250
SUR00260
SUR00270
SUR00280
SUR00290
SUR00300
SUR00310
SUR00320
SUR00330
SUR00340
SUR00350
SUR00360
SUR00370
SUR00380
SUR00390
SUR00400
SUR00410
SUR00420
SUR00430
SUR00440
SUR00450
SUR00460
SUR00470
SUR00480
SUR00490

```

```

C      WRITE(4,113) ANGV,ANGH,INORM
      WRITE(4,101) HEIGHT,XWID,H,YWIDTH
      WRITE(4,201) NX,NY,XDELTA,YDELTA
101    FORMAT(5X,'H = ',F6.2,4X,'XW = ',F6.2,4X,'YW = ',F6.2)
113    FORMAT(5X,2F18.2,I8)
201    FORMAT(5X,2I8,5X,2F18.2,/)
866    CONTINUE
C      READ IN NUMBER OF RECEIVERS
      READ(3,*)NREC
C      READ IN SOURCE POSITION
      READ(3,*)XS,YS,ZS
      NR=0
111    FORMAT(7X,'SURFACE PARAMETER   HEIGHT = ',F7.1,1X,' XWIDTH = ',1X,
      * F7.1,' YWIDTH = ',F7.1)
C      GENERATING THE SURFACE OF THE WATER
      CALL SURF(HEIGHT,XWIDTH,YWIDTH)
C
C      CALCULATE THE PRIMARY FIELD AT THE SURFACE. GENERATE THE BOUNDARY COSUR0720
      FOR NEUMANN PROBLEM.
C      CALL HNPRIM ( ANGV,ANGH )
C
C      CALCULATE THE SURFACE CHARGE DENSITY BY SOLVING THE FREDHOLM INTEGRASUR0770
      EQUATION OF THE SECOND KIND.
C      CALL SIGMA(NPLOT,NLOOP)
C
C      compute the surface current pattern and then stop
C      if(ipattn.eq.1) call currnt(angv,anhv)
C
C      CALCULATE THE MAGNETIC FIELD AT A RECEIVER POINT.
555    CONTINUE
C      READ IN RECEIVER POSITION
      READ(3,*)XR,YR,ZR
      CALL FIELD(NPLOT,ANGV,ANGH,INORM)
      NR=NR+1
      IF(NR.LT.NREC) GOTO 555
      NS=N+1
      IF(NS.LT.NSOR) GOTO 666
      STOP
      END
C
C      SUBROUTINE SURF(Z0,XW,YW)
      implicit real*8 (a-h,o-z)
      DIMENSION ZH(121,121),XDER(121,121),YDER(121,121),AMPDER(121,121)
      COMMON /AA/ZH/BB/XDER/CC/YDER/AMP/AMPDER
      COMMON /TR/XS,YS,ZS,XR,YR,ZR
      COMMON  NX,NY,NX2,NY2,XDELTA,YDELTA
      NX2=(NX+1)/2
      NY2=(NY+1)/2
      TAUx=0.42466*XB

```

SUR00500
 SUR00510
 SUR00520
 SUR00530
 SUR00540
 SUR00550
 SUR00560
 SUR00570
 SUR00580
 SUR00590
 SUR00600
 SUR00610
 SUR00620
 SUR00630
 SUR00640
 SUR00650
 SUR00660
 SUR00670
 SUR00680
 SUR00690
 SUR00700
 SUR00710
 SUR00720
 SUR00730
 SUR00740
 SUR00750
 SUR00760
 SUR00770
 SUR00780
 SUR00790
 SUR00800

SUR00810
 SUR00820
 SUR00830
 SUR00840
 SUR00850
 SUR00860
 SUR00870
 SUR00880
 SUR00890
 SUR00900
 SUR00910
 SUR00920
 SUR00930
 SUR00940
 SUR00950
 SUR00960
 SUR00970
 SUR00980
 SUR00990
 SUR01000
 SUR01010
 SUR01020
 SUR01030
 SUR01040

```

333
444
TAUY=0.42466*YW
XDEV=TAUX*TAUX*2.0
YDEV=TAUY*TAUY*2.0
DO 10 I=1,NX
DO 20 J=1,NY
X=(I-NX2)*XDELTA+XS
Y=(J-NY2)*YDELTA+YS
EX=-X/X/XDEV+Y/YDEV
IF (EX.LT.(-10)) GO TO 333
RR=EXP(EX)
GO TO 444
RR=0.0
ZH(I,J)=Z0*RR
XDER(I,J)=-ZH(I,J)*X /XDEV*2.0
YDER(I,J)=-ZH(I,J)*Y /YDEV*2.0
AMPDER(I,J)=SQRT(1.0*XDER(I,J)*XDER(I,J)+YDER(I,J)*YDER(I,J))
CONTINUE
10 CONTINUE
WRITE(4,100)Z0,WIDTH,XDELTA,YDELTA,RR
C
C WRITE(4,100)((ZH(I,J),J=1,NY),I=1,NX)
C
C WRITE(4,100)((XDER(I,J),J=1,NY),I=1,NX)
C
C WRITE(4,100)((YDER(I,J),J=1,NY),I=1,NX)
100 FORMAT(3X,/,,(5E12.5))
RETURN
END
C
C
SUBROUTINE HNPRI (ANGV, ANGH)
implicit real*8 (a-h, o-z)
DIMENSION HN(121,121),ZH(121,121),XDER(121,121),YDER(121,121)
DIMENSION AMPDER(121,121)
COMMON /AA/ZH/XDER/CC/YDER/DD/HN/AMP/AMPDER
COMMON NX,NY,NX2,NY2,XDELTA,YDELTA
COMMON /TR/XS,YS,ZS,XR,YR,ZR
COSV=COS(ANGV)
SINVC=SIN(ANGV)*COS(ANGH)
SINVS=SIN(ANGV)*SIN(ANGH)
DO 10 I=1,NX
DO 20 J=1,NY
XD=(I-NX2)*XDELTA
YD=(J-NY2)*YDELTA
ZD=ZH(I,J)-ZS
XD2=XD*XD
YD2=YD*YD
ZD2=ZD*ZD
XD=XD*YD
YD=YD*ZD
ZD=ZD*XD
R5=(XD2+YD2+ZD2)**2.5
HX1=3.0*ZXD
HY1=3.0*YD
HZ1=(2*XD2 -XD2 -YD2 )
HX2=(2*XD2 -YD2 -ZD2 )
HY2=3.0*XYD
HZ2=3.0*ZXD
HX3=3.0*XYD
HY3=(2*YD2 -XD2 -ZD2 )
HZ3=3.0*YZD
HX=(HX1+COSV*HX2+SINVC*HX3+SINVS)/R5
SUR01050
SUR01060
SUR01070
SUR01080
SUR01090
SUR01100
SUR01110
SUR01120
SUR01130
SUR01140
SUR01150
SUR01160
SUR01170
SUR01180
SUR01190
SUR01200
SUR01210
SUR01220
SUR01230
SUR01240
SUR01250
SUR01260
SUR01270
SUR01280
SUR01290
SUR01300
SUR01310
SUR01320
SUR01330
SUR01340
SUR01350
SUR01360
SUR01370
SUR01380
SUR01390
SUR01400
SUR01410
SUR01420
SUR01430
SUR01440
SUR01450
SUR01460
SUR01470
SUR01480
SUR01490
SUR01500
SUR01510
SUR01520
SUR01530
SUR01540
SUR01550
SUR01560
SUR01570
SUR01580
SUR01590
SUR01600
SUR01610
SUR01620
SUR01630

```


SUR01640
 SUR01650
 SUR01660
 SUR01670
 SUR01680
 SUR01690
 SUR01700
 SUR01710
 SUR01720
 SUR01730
 SUR01740
 SUR01750
 SUR01760

 SUR01770
 SUR01780
 SUR01790
 SUR01800
 SUR01810
 SUR01820

 SUR01830
 SUR01840
 SUR01850
 SUR01860
 SUR01870
 SUR01880
 SUR01890
 SUR01900
 SUR01910
 SUR01920
 SUR01930
 SUR01940
 SUR01950
 SUR01960
 SUR01970
 SUR01980
 SUR01990
 SUR02000
 SUR02010
 SUR02020
 SUR02030
 SUR02040
 SUR02050
 SUR02060
 SUR02070
 SUR02080
 SUR02100

```

20  HY=(HY1+COSV*HY2+SINVC3*HY3+SINVSNI)/R5
10  HZ=(HZ1+COSV*HZ2+SINVC3*HZ3+SINVSNI)/R5
C   HN(I,J)=(HX*YDER(I,J)+HY*YDER(I,J)-HZ)/AMPDER(I,J)
    CONTINUE
    CONTINUE
100  WRITE(4,100)((HN(I,J),J=1,NY),I=1,NX)
    FORMAT(3X,/,/, (5E12.5))
    RETURN
    END
C
C
SUBROUTINE SIGMA (NPLOT,NLOOP)
implicit real*8 (a-h,o-z)
DIMENSION W1(121,121),ZH(121,121),YDER(121,121),YDER(121,121)
DIMENSION W2(121,121),AMPDER(121,121),HN(121,121)
DIMENSION XD(200),YD(200),XD2(200),YD2(200)
COMMON /AA/ZH/BB/XDER/CC/YDER/DD/HN/EE/W2/AMP/AMPDER
COMMON /TR/XS,YS,ZS,XR,YR,ZR
COMMON NX,NY,NX2,NY2,XDELTA,YDELTA
common /in/a,b,c,xm,ym,y1,y2,hdx,hdy
C
CXY=XDELTA*YDELTA
FAC=1.0/(2*3.1415926)
DO 10 I=1,NX
DO 10 J=1,NY
W1(I,J)=0.0
W2(I,J)=0.0
W1(I,J)=-HN(I,J)*FAC
NUM=0
NX2=NX*2
NY2=NY*2
DO 13 I=1,NX2
XD(I)=(I-NX)*XDELTA
XD2(I)=XD(I)*XD(I)
DO 14 I=1,NY2
YD(I)=(I-NY)*YDELTA
YD2(I)=YD(I)*YD(I)
CONTINUE
DO 15 I=1,NX
DO 20 J=1,NY
WS=0.0000
DO 40 I1=1,NX
DO 30 J1=1,NY
K1= I1-I*NX
K2= J1-J*NY
ZD=ZH(I1,J1)-ZH(I,J)
IF(I.EQ.I1 .AND. J.EQ.J1) GOTO 30
IF (ABS(I1-I).LE.4.AND. ABS(J1-J).LE.4) THEN
  XM=(I-NX2)*XDELTA
  YM=(J-NY2)*YDELTA
  X1=(I1-NX2-0.5)*XDELTA
  X2=(I1-NX2+0.5)*XDELTA
  Y1=(J1-NY2-0.5)*YDELTA
  Y2=(J1-NY2+0.5)*YDELTA
  HDX=XDER(I,J)
  HDY=YDER(I,J)
  a=-XDER(I1,J1)
  b=-YDER(I1,J1)
  C=-ZD-a*(I1-NX2)*XDELTA-b*(J1-NY2)*YDELTA
  CALL QGAUS(X1,X2,SS4)

```

```

      WS = WS+SS4*AMPDER(I1,J1)/AMPDER(I,J)*W1(I1,J1)
    else
      RPY2=XD2(K1)+YD2(K2)*ZD*ZD
      BT=(ZD-XDER(I,J)*XD(K1)-YDER(I,J)*YD(K2))*d*y
      WS=WS+BT*(I1,J1)*BT*AMPDER(I1,J1)/(RPY2*SQR(RPY2)*AMPDER(I,J))
    end if
  30 CONTINUE
  40 CONTINUE
  W2(I,J)=FAC*(-WS-HN(I,J))
  20 CONTINUE
  15 CONTINUE
  SUM=0.0
  IF(NPLOT.EQ.1) GOTO 501
  DO 50 I=1,NX
  DO 50 J=1,NY
    WW=W2(I,J)-W1(I,J)
  50 SUM=SUM+WW*WW
    AVER=SQR(SUM)/(NX*NY)
    WRITE(4,100) AVER
  100 FORMAT(20X, 'AVERAGE DIFFERENCE BETWEEN TWO SUCCESSIVE ITERATIONS',
    +,/,E10.5)
    NUM=NUM+1
    T1=ABS(AVER/W2(NX2,NY2))
    WRITE(4,122) NUM
  122 FORMAT(//,/,20X, 'NUM= ',IS)
    IF ( 11
      .LT.0.1E-4 .OR. NUM.GT.NLOOP) GOTO 1000
    GOTO 502
  501 NUM=NUM+1
  502 IF ( NUM.GT.NLOOP) GOTO 1000
  502 CONTINUE
  DO 44 I=1,NX
  DO 44 J=1,NY
    W1(I,J)=W2(I,J)
  44 W2(I,J)=0.0
    GOTO 999
  1000 CONTINUE
  DO 111 I=1,NX
  C111 WRITE(4,110)(W2(I,J),J=1,NY)
  C110 FORMAT(1X, //, (5E12.5))
  RETURN
  END
C
C
  SUBROUTINE FIELD(NPLOT,ANGV,ANGH,INORM)
  implicit real*8 (a-h,o-z)
  DIMENSION W(121,121),ZH(121,121),XDER(121,121),YDER(121,121)
  DIMENSION AMPDER(121,121)
  COMMON /AA/ZH,BB/XDER/CC/YDER/AMP/AMPER
  +/FE/W
  COMMON NX,NY,NX2,NY2,XDELTA,YDELTA
  COMMON /TR/XS,YS,ZS,XR,YR,ZR
  COSV=COS(ANGV)
  SINVC=SIN(ANGV)*COS(ANGH)
  SINVSN=SIN(ANGV)*SIN(ANGH)
  XD=XR-XS
  YD=YR-YS
  ZD=ZR-ZS
  XD2=XD*XD
  YD2=YD*YD

```

SUR02090
SUR02110
SUR02120

SUR02130
SUR02140
SUR02150
SUR02160
SUR02170
SUR02180
SUR02190
SUR02200
SUR02210
SUR02220
SUR02230
SUR02240
SUR02250
SUR02260
SUR02270

SUR02280
SUR02290
SUR02300
SUR02310
SUR02340
SUR02350
SUR02360
SUR02370
SUR02380
SUR02390
SUR02400
SUR02410
SUR02420
SUR02430
SUR02440
SUR02320
SUR02330
SUR02450
SUR02460
SUR02470
SUR02700
SUR02710
SUR02390

SUR02600
SUR02610
SUR02620
SUR02630
SUR02640
SUR02760
SUR02770
SUR02120
SUR02790
SUR02800
SUR02810
SUR02820
SUR02830
SUR02840
SUR02850

```

20 ZD2=ZD*ZD
10 XYD=XD*YD
   Y2D=YD*ZD
   ZD=ZD*XD
   RS=(XD2+YD2+ZD2)**.5
   HX1=3*0*ZXD
   HY1=3*0*YXD
   HZ1=(2*ZD2 - XD2 - YD2 )
   HX2=(2*XD2 - YD2 - ZD2 )
   HY2=3*0*YXD
   HZ2=3*0*ZXD
   HX3=3*0*XYD
   HY3=(2*YD2 - XD2 - ZD2 )
   HZ3=3*0*YXD
   HXP=(HX1+COSV*HX2+SINVS*HX3+SINVS)/RS
   HYP=(HY1+COSV*HY2+SINVS*HY3+SINVS)/RS
   HZP=(HZ1+COSV*HZ2+SINVS*HZ3+SINVS)/RS
   HXS=0.0
   HYS=0.0
   HZS=0.0
   DO 10 I=1,NX
   DO 20 J=1,NY
     XD=(1-NX2)*XDELTA+XS*XR
     YD=(J-NY2)*YDELTA+YS*YR
     ZD=ZH(I,J) - ZR
     RPM2=XD*XD+YD*YD+ZD*ZD
     RPM=SQRT(RPM2)
     HXS =HXS +W(I,J)*XD*AMPDER(I,J)/(RPM*RPM2)
     HYS =HYS +W(I,J)*YD*AMPDER(I,J)/(RPM*RPM2)
     HZS =HZS +W(I,J)*ZD*AMPDER(I,J)/(RPM*RPM2)
   CONTINUE
20 CONTINUE
10 CONTINUE
   HXS =-HXS *XDELTA*YDELTA
   HYS =-HYS *XDELTA*YDELTA
   HZS =-HZS *XDELTA*YDELTA
   IF (INDRM.EQ.1) GOTO 606
   IF (INDRM.EQ.2) GOTO 607
   HX=HXS/HZP*1000000
   HY=HYS/HZP*1000000
   HZ=HZS/HZP*1000000
   GOTO 608
606 HX=HXS/HXP*1000000
   HY=HYS/HXP*1000000
   HZ=HZS/HXP*1000000
   GOTO 608
607 HX=HXS/H '1000000
   HY=HYS/HYP*1000000
   HZ=HZS/HYP*1000000
608 CONTINUE
   IF (NPLOT.EQ.1) GOTO 501
   WRITE(4,200) XS,YS,ZS
200 FORMAT (
   * /, 7X, 'SOURCE POSITION ( ',F10.5,1X,F10.5,1X,F10.5,')' )
   WRITE(4,100)XR,YR,ZR,HX,HY,HZ
100 FORMAT( 7X,'RECEIVER POSITION ( ',F10.5,1X,F10.5,1X,F10.5,')' ),/ ,
   * 7X,'SECONDARY MAGNETIC FIELD IN PPM',/ ,7X,'STATIC FIELD
   * APPROXIMATION',/ ,5X,
   * 'HX = ', '5.8, ' HY = ',E15.8, ' HZ = ',E15.8)
   GOTO 502
501 WRITE(4,101) XS,YS,ZS

```

```

SUR02860
SUR02870
SUR02880
SUR02890
SUR02900
SUR02910
SUR02920
SUR02930
SUR02940
SUR02950
SUR02960
SUR02970
SUR02980
SUR02990
SUR03000
SUR03010
SUR03020
SUR02700
SUR02710
SUR02720
SUR02730
SUR02740
SUR02750
SUR02760
SUR02770
SUR02780
SUR02790
SUR02800
SUR02810
SUR02820
SUR02830
SUR02840
SUR02850
SUR02860
SUR02870
SUR03060
SUR03070
SUR03080
SUR03090
SUR03100
SUR03110
SUR03120
SUR03130
SUR03140
SUR03150
SUR03160
SUR03170
SUR03180
SUR03190
SUR03200
SUR03210
SUR03220
SUR03230
SUR03240
SUR03250
SUR03260
SUR03270
SUR03280
SUR03290
SUR03300

```

```

101 WRITE(4,201)XR,YR,ZR,HX,HY,HZ
201 FORMAT(10X,3F18.2)
301 FORMAT(10X,3F18.2,/,10X,3E18.5,/)
502 RETURN
END

```

5
5
5

the following routine compute the surface currents.

```

SUBROUTINE currnt(angv,angh)
implicit real*8 (a-h, c-z)
dimension zh(121,121),xder(121,121),yder(121,121)
dimension w2(121,121),ampder(121,121)
dimension curamp(121,121),curdir(121,121)
dimension x0(200),y0(200),x02(200),y02(200)
common /aa/zh/BB/xder/cc/yder/EE/w2/amp/ampder
common /tr/xs,ys,zs,xr,yr,zr
common nx,ny,nx2,ny2,xdelta,ydelta
common /in/a,b,c,xm,ym,y1,y2,hdx,hdy

```

N2X=NX*2

N2Y=NY*2

DXY=XDELTA*YDELTA

DO 13 I=1,N2X

X0(I)=(I-NX)*XDELTA

X02(I)=X0(I)*XD(I)

DO 14 I=1,N2Y

Y0(I)=(I-NY)*YDELTA

Y02(I)=Y0(I)*YD(I)

DO 15 I=1,NX

DO 20 J=1,NY

curx=0.0

cury=0.0

curze=0.0

DO 40 I1=1,NX

DO 30 J1=1,NY

K1= I1-I*NX

K2= J1-J*NY

ZD=ZH(I1,J1)-ZH(I,J)

IF(I.EQ.I1 .AND. J.EQ.J1) GOTO 30

IF(ABS(I1-I).LE.4 .AND. ABS(J1-J).LE.4) THEN

XW=(I-NX2)*XDELTA

YW=(J-NY2)*YDELTA

X1=(I1-NX2-0.5)*XDELTA

X2=(I1-NX2+0.5)*XDELTA

Y1=(J1-NY2-0.5)*YDELTA

Y2=(J1-NY2+0.5)*YDELTA

HDX=XDER(I,J)

HDY=YDER(I,J)

b=-XDER(I1,J1)

b=-YDER(I1,J1)

C=-ZD-A*(I1-NX2)*XDEL B*(J1-NY2)*YDEL

CALL QGAUS2(X1,X2,SS1,SS2,SS3)

WS =W2(I1,J1)*AMPDER(I1,J1)/ampder(i,j)

CURX=WS*SS1*CURX

CURY=WS*SS2*CURY

CURZ=WS*SS3*CURZ

GOTO 30

ENDIF

RPMW2=XD2(K1)*YD2(K2)+ZD*ZD

IF (RPMW2.LT.0.1) GOTO 30

SUR03310
SUR03320
SUR03330
SUR03340
SUR03350

SUR01770
SUR01780

SUR01790
SUR01800
SUR01810
SUR01820

SUR01830
SUR01920
SUR01930

SUR01940
SUR01950
SUR01960
SUR01970
SUR01980
SUR01990
SUR02010
SUR02020

SUR02040
SUR02050
SUR02060
SUR02070
SUR02080
SUR02100

SUR02090
SUR02100

SUR02110
SUR02110
SUR02110

BTX=-ZD*YDER(I,J)-YD(K2)
RTY=XD(K1)*XDER(I,J)*ZD
RTZ=-YDER(I,J)*YD(K2)+XD(K1)*YDER(I,J)
WS=W2(I,J1)*AMPDER(I1,J1)/(RPM2*SQR1(RPM2)*AMPDER(I,J))*DXY
CURX=CURX+WS*BTX
CURY=CURY+WS*BTY
CURZ=CURZ+WS*BTZ

SUR02130
SUR02140

30
40

C

C primary field calculation

COSV=COS(ANGV)
SINVC=SIN(ANGV)*COS(AHIGH)
SINVS=SIN(ANGV)*SIN(ANGH)
X1=(I-NX2)*XDELTA
Y1=(J-NY2)*YDELTA
Z1=ZH(I,J)-ZS
X2=X1*X1
Y2=Y1*Y1
Z2=Z1*Z1
XYD=X1*Y1
YZD=Y1*Z1
ZXD=Z1*X1
R5=(X2*Y2+Z2)*2.5
HX1=3.0*ZXD
HY1=3.0*YZD
HZ1=(2*Z2-X2-Y2)
HX2=(2*X2-Y2-Z2)
HY2=3.0*XYD
HZ2=3.0*7XD
HX3=3.0*YD
HY3=(2*Y2-X2-Z2)
HZ3=3.0*YZD
HX=(HX1+COSV*HX2+SINVC*HX3+SINVS)/R5
HY=(HY1+COSV*HY2+SINVC*HY3+SINVS)/R5
HZ=(HZ1+COSV*HZ2+SINVC*HZ3+SINVS)/R5
CURX=CURX+(HZ*YDER(I,J)+HY)/AMPDER(I,J)
CURY=CURY+(-HX-HZ*XDER(I,J))/AMPDER(I,J)
CURZ=CURZ+(HY*XDER(I,J)-HX*YDER(I,J))/AMPDER(I,J)
CRAMP(I,J)=SQR1(CURX**2+CURY**2+CURZ**2)
IF(ABS(CURX)/LT.1.0E-30 .AND. CURY/GE.0.0) THEN
CURDIR(I,J)=90.
else
if(abs(curx).lt.1.0e-30 .and. cury.lt.0.0) then
CURDIR(I,J)=-90.
else
CURDIR(I,J)=atan2(cury,curx)*180./3.1415928
endif
endif

SUR02160
SUR02170

20
15

100

CONTINUE
CONTINUE
DO 100 I=1,NX
write(4,101)I,(curamp(i,j),j=1,ny)
continue
DO 110 I=1,NX
write(4,102)I,(CURDIR(I,J),j=1,ny)
continue
101
101
102
FORMAT(4X,'AMPLITUDE OF SURFACE CURRENT i =',i5,'/',(5(1PE12.3)))
FORMAT(4X,'DIRECTION OF SURFACE CURRENT i =',i5,'/',(5(1PE12.3)))
stop

```

C
C
END
      subroutine ggaus2(a,b,ss1,ss2,ss3)
      implicit real*8 (a-h, o-z)
      c nine-point Gauss' quadrature
      dimension x(5),w(5)
      data x/0.0,0.324253,0.613371,0.836031,0.968160/
      data w/0.330239,0.312347,0.260611,0.180648,0.081274/
      xm=0.5*(b+a)
      xr=0.5*(b-a)
      ss1=0.
      ss2=0.
      ss3=0.
      do 11 j=2,5
        dx=xrex(j)
        ss1=ss1+w(j)*fun1(xm+dx,fun2,fun3)
        ss2=ss2+w(j)*fun2
        ss3=ss3+w(j)*fun3
        ss1=ss1+w(j)*fun1(xm-dx,fun2,fun3)
        ss2=ss2+w(j)*fun2
        ss3=ss3+w(j)*fun3
      11 continue
      ss1=xre(ss1+w(1)*fun1(xm,fun2,fun3))
      ss2=xre(ss2+w(1)*fun2)
      ss3=xre(ss3+w(1)*fun3)
      return
      END

C
C
      function fun1(xp,fun2,fun3)
      c to compute the kernel for the Gaussian quadrature
      implicit real*8 (a-h, o-z)
      common /in/a,b,c,xm,ym,y1,y2,hdx,hdy
      d=a*xp+c
      e=(xm-xp)*e2+d*d+ym*ym
      f=2.*e*(deb-ym)
      g=1.+b*b
      del=4*e*e*g-f*f
      IF (ABS(DEL) .LT. 1.E-20) EN
      SG=1./((G*SQRT(G))
      FG=F/(G+G)
      YG1=1./((Y1+f*G)
      YG2=1./((Y2+f*G)
      AIX1=abs(0.5*SG*(YG2*YG2-YG1*YG1))
      AIX2=SG*(YG2*(-1.*0.5*FG*YG2)-YG1*(-1.*0.5*FG*YG1))
      IF (YG1.LT.0.0) AIX2= -AIX2
      ELSE
        r2=1./((del+sqrt(e*(f+g*y2)*y2))
        r1=1./((del+sqrt(e*(f+g*y1)*y1))
        aix1=2.*((2.*g*y2*f)*r2-(2.*g*y1*f)*r1)
        aix2=-2.*((2.*e+f*y2)*r2-(2.*e+f*y1)*r1)
      ENDIF
      IF (AIX1.LT.0.0) THEN
        WRITE(*,*) 'XM, YM, Y1, XP, AIX1, AIX2', XM, YM, Y1, XP, AIX1, AIX2
        stop
      endif
      fun1=(d*hdxy*ym)*aix1+(b*hdxy-1.)*e*aix2
      fun2=(-(xm-xp)-d*hdxy)*e*aix1-b*hdxy*aix2
      fun3=(ym*hdxy-(xm-xp)*hdxy)*e*aix1-1*hdxy*aix2

```

```

return
end

c
c
subroutine qgaus(a,b,ss4)
implicit real*8 (a-h, o-z)
c nine point Gauss quadrature
dimension x(5),w(5)
data x/0.0,0.324253,0.613371,0.836031,0.968160/
data w/0.330239,0.312347,0.260611,0.180648,0.081274/
xm=0.5*(b+a)
xr=0.5*(b-a)
ss4=0.
do 11 j=2,5
dx=xr*x(j)
ss4=ss4+w(j)*(fun4(xm+dx)+fun4(xm-dx))
11 continue
ss4=xr*(ss4+w(1)*fun4(xm))
return
END

function fun4(xp)
implicit real*8 (a-h, o-z)
common /in/a,b,c,xm,ym,y1,y2,hdx,hdy
d=a*xp+c
e=(xm-xp)**2+d*d+ym*ym
f=2.*e*(d*b-ym)
g=1.+b*b
del=4*e*g-f*f
if (abs(del) .lt. 1.e-20 ) then
sg=1./(g*sqrt(g))
fg=f/(g+g)
yg1=1./(y1+fg)
yg2=1./(y2+fg)
aix1=abs(0.5*sg*(yg2*yg2-yg1*yg1))
aix2=sg*(yg2*(-1.+0.5*f*g*yg2)-yg1*(-1.+0.5*f*g*yg1))
if (yg1.lt.0) aix2=-aix2
else
r2=1./(del*sqrt(e*(f+g*y2)*y2))
r1=1./(del*sqrt(e*(f+g*y1)*y1))
aix1=2.*e*((2.*g*y2*f)*r2-(2.*g*y1*f)*r1)
aix2=-2.*e*((2.*g*y2)*r2-(2.*g*y1)*r1)
endif
fun4=((xm-xp)*hdx+ym*hdy-d)*aix1-(hdy+b)*aix2
return
end

```

```

PROGRAM ICE201
implicit real*8 (a-h,o-z)
C
C ... PURPOSE ...
C
C COMPUTE THE AEM SYSTEM RESPONSE OVER A 2-D ICE-WATER PROFILE
DIMENSION ZSURF(200),XDER(200),AMPOER(200),HPN(120,20)
DIMENSION AKERN(120,120,20),CHAR(120,20),XSYS(50),ZSYS(50)
COMMON /KY/ AKY(20)/KER/ AKERN/CH/CHAR/HPN/HPN
COMMON KYE,NSYS,NST,NPT,NXT,NTRUNK,XDEL,TRDIS
open (unit=3, file='ice2d1.dat')
open (unit=4, file='ice2d1.out')
READ(3,*)
READ(3,*) NSYS,NST,NPT,NXT,NRESP,NTRUNK,NLOOP
READ(3,*)
READ(3,*) XDEL,TRDIS
READ(3,*)
READ(3,*) (ZSURF(I), I=1,NPT)
READ(3,*)
READ(3,*) (XSYS(I),ZSYS(I), I=1,NRESP)
IF (NSYS.EQ.1) WRITE(4,101)
IF (NSYS.EQ.2) WRITE(4,102)
IF (NSYS.NE.1 .AND. NSYS.NE.2) PAUSE 'BAD INPUT NSYS'
WRITE(4,104) TRDIS,XDEL
WRITE(4,103) NST,NPT,NXT,NRESP,NTRUNK,NLOOP
WRITE(4,105) (ZSURF(I), I=1,NPT)
WRITE(4,106) (XSYS(I), I=1,NRESP)
WRITE(4,107) (ZSYS(I), I=1,NRESP)
CALL SURF(NST,NPT,NXT,XDEL,XDEL,ZSURF,XDER,AMPDER)
K=1
C
C ..... ASSIGN KY HARMONICS. THE FOLLOWING IS OK FOR ZR=10 - 100 METERS.
C
KYE= 15
NM=7
AKYMIN=1.0/(2.0*1000)
AKDEL=0.0006
AKLOG=0.17
AKYEX=LOG10(AKYMIN)
AKY(1)=0.0
DO 20 I=1,KYE-1
EX=AKYEX*(I-1)*AKLOG
AKY(I+1)=10**EX
20 CONTINUE
WRITE(4,202)
1001 CONTINUE
KS=(XSYS(K)-TRDIS/2.)/XDEL+2-NTRUNK/2
IF (KS.LE.0 .OR. KS.GE.NXT-NTRUNK/2) PAUSE 'BAD INPUT XSYS'
CALL HNPTRIM(K,KS,ZSURF,XDER,AMPDER,XSYS,ZSYS)
CALL KERNEL(K,KS-1,KS1,ZSURF,XDER,AMPDER)
CALL CHARGE(NTRUNK,KYE,XDEL,NLOOP)
CALL FIELD(K,KS,NM,AKDEL,HXS,HZS,XSYS,ZSYS,ZSURF,AMPDER)
WRITE(4,203) XSYS(K),ZSYS(K),HXS,HZS
K=K+1
KS1=KS
IF (K.LE.NRESP) GOTO 1001
101 FORMAT(4X,'HORIZONTAL AXIS DIPOLE SYSTEM',/)
102 FORMAT(4X,'VERTICAL AXIS DIPOLE SYSTEM',/)
103 FORMAT(4X,'NST =',I5,2X,'NPT =',I5,2X,'NXT =',I5,/,
+ 4X,'NRESP =',I5,2X,'NTRUNK =',I5,2X,'NLOOP =',I5)
104 FORMAT(4X,'T-R SEPARATION =',F7.2,' METERS',/,4X,'XDEL =',F7.2,

```

```

ICE00010
ICE00020
ICE00030
ICE00040
ICE00050
ICE00060
ICE00070

ICE00090
ICE00100
ICE00110
ICE00120
ICE00130
ICE00140
ICE00150
ICE00160
ICE00170
ICE00180
ICE00190
ICE00200
ICE00210
ICE00220
ICE00230
ICE00240
ICE00250
ICE00260
ICE00270
ICE00280
ICE00290
ICE00300
ICE00310
ICE00320
ICE00330
ICE00340
ICE00350
ICE00360
ICE00370
ICE00380
ICE00390
ICE00400
ICE00410
ICE00420
ICE00430
ICE00440
ICE00450
ICE00460
ICE00470
ICE00480
ICE00490
ICE00500
ICE00510
ICE00520
ICE00530
ICE00540
ICE00550
ICE00560
ICE00570
ICE00580

```



```

IF (NSYS.EQ.1) THEN
  GEOM1=( -XDER(J)*XD*ZD)*XD/D
  GEOM2=(- (XD*XD-ZD*ZD)*XDER(J)+2.*XD*ZD)/D
ELSE
  GEOM1=(-XDER(J)*XD*ZD)*ZD/D
  GEOM2=((ZD*ZD-XD*XD)-XDER(J)+2.*XD*ZD)/D
ENDIF
DO 20 I=1,KYE
  WK=AKY(I)*PI2
  RKY=RHO*WK
  IF (I.GT.1) THEN
    HPN(M,I)=(GEOM1*WK*BESSK0(RKY)+GEOM2*BESSK1(RKY)/RHO)*WK
  ELSE
    HPN(M,I)=GEOM2/(RHO*RHO)
  ENDIF
CONTINUE
10 WRITE(4,30) (HPN(J,1),J=1,NTR)
30 FORMAT(4X,'HPN',/, (5(1PE12.4)))
RETURN
END

SUBROUTINE KERNEL(K,KS,KS1,ZSURF,XDER,AMPDER)
implicit real*8 (a-h,o-z)
.....
COMPUTE THE KERNEL IN THE INTEGRAL EQUATION
AND SAVE IT
.....
PARAMETER (PI=3.1415926)
DIMENSION ZSURF(1),XDER(1),AMPDER(1)
DIMENSION AKERN(120,120,20)
COMMON /KER/AKERN/KY/AKY(20)
COMMON KYE,NSYS,NST,NPT,NXT,NTR,XDEL,TRDIS
PI2=PI*2.
DO 1 J=1,NTR
  DO 1 I=1,KYE
    AKERN(J,I)=0.0
  CONTINUE
  IF(K.GT.1) GOTO 30
C COMPUTE THE AKERNEL
1001 CONTINUE
DO 20 J=1,NTR
  DO 20 L=1,NTR
    IF(J.EQ.L) GOTO 20
    XD=(J-L)*XDEL
    ZD=ZSURF(J*KS)-ZSURF(L*KS)
    RHO=SQRT(XD*XD+ZD*ZD)
    GEOM=2.*(AMPDER(L*KS)/AMPDER(J*KS))*(XD*XDER(J*KS)-ZD)/RHO
    DO 10 I=1,KYE
      WK=AKY(I)*PI2
      IF (I.EQ.1) THEN
        AKERN(J,L,I)=GEOM/RHO
      ELSE
        AKERN(J,L,I)=GEOM*WK*BESSK1(RHO*WK)
      ENDIF
CONTINUE
20 CONTINUE
RETURN
END

```

```

      * , METERS')
105 FORMAT(4X,'RELIEF OF ICE-WATER INTERFACE',/, (10F7.2))
106 FORMAT(4X,'X POSITION OF THE SYSTEM',/, (10F7.2))
107 FORMAT(4X,'Z POSITION OF THE SYSTEM',/, (10F7.2))
201 FORMAT(4X,'KY HOMONICS = ',/, (5F14.4))
202 FORMAT(/,4X,' XSYS (M) HXS (PPM) HZS (PPM)')
203 FORMAT(2X,2F11.2,3X,2(IPE12.4))
      STOP
      END
C
C
C
SUBROUTINE SURF(NST,NPT,NXT,XDEL,ZSURF,XDER,AMPDER)
implicit real*8 (a-h,o-z)
C
C ..... GENERATE THE INFORMATION OF THE ICE-WATER INTERFACE, I.E.,
C ZSURF, XDER, AMPDER
C
C ..... DIMENSION ZSURF(NXT),XDER(NXT),AMPDER(NXT)
NE=NST+NPT
CALL CUBDER(NPT+2,XDEL,ZSURF,XDER)
DO 10 I=NXT,1,-1
IF (I.GE.NE.OR. I.LT.NST) THEN
    ZSURF(I)=0.0
    XDER(I)=0.
    AMPDER(I)=1.
    GOT0 10
ENDIF
ZSURF(I)=ZSURF(I-NST+1)
XDER(I)=XDER(I-NST+1)
AMPDER(I)=SQRT(1.0*XDER(I)*XDER(I))
CONTINUE
WRITE(4,50)(ZSURF(I),I=1,NXT-1)
WRITE(4,60)(XDER(I),I=1,NXT-1)
WRITE(4,70)(AMPDER(I),I=1,NXT-1)
50 FORMAT(4X,'ZSURF',/,4X,(10F7.3))
60 FORMAT(4X,'XDER',/,4X,(10F7.3))
70 FORMAT(4X,'AMPDER',/,4X,(10F7.3))
RETURN
END
C
C
SUBROUTINE HNPRIM(K,K5,ZSURF,XDER,AMPDER,XSYS,ZSYS)
C
C ..... COMPUTE THE NORMAL COMPONENT OF THE MAGNETIC FIELD
C
C ..... implicit real*8 (a-h,o-z)
PARAMETER (PI=3.1415928)
DIMENSION ZSURF(1),XDER(1),AMPDER(1),XSYS(1),ZSYS(1)
DIMENSION HPN(120,20)
COMMON /KY/ AKY(20)/HN/HPN
COMMON KYE,NSYS,NST,NPT,NXT,NTR,XDEL,TROIS
PI2=PI*.2
DO 10 J=KS,NTR+KS-1
M=J-KS+1
XD=(J-1)*XDEL-XSYS(K)+TROIS/2.
ZO=ZSURF(J)-ZSYS(K)
RHO=SQRT(XD*XD+ZO*ZO)
D=RHO*RHO*AMPDER*(J)*PI2
IF(D.EQ.0.) PAUSE'BAD HPN'

```

ICE02350
 ICE02360
 ICE02370
 ICE02380
 ICE02390
 ICE02400
 ICE02410
 ICE02420
 ICE02430
 ICE02440
 ICE02450
 ICE02460
 ICE02470
 ICE02480
 ICE02490
 ICE02500
 ICE02510
 ICE02520
 ICE02530
 ICE02540
 ICE02550
 ICE02560
 ICE02570
 ICE02580
 ICE02590
 ICE02600
 ICE02610
 ICE02620
 ICE02630
 ICE02640
 ICE02650
 ICE02660
 ICE02670
 ICE02680
 ICE02690
 ICE02700
 ICE02710
 ICE02720
 ICE02730
 ICE02740
 ICE02750
 ICE02760
 ICE02770
 ICE02780
 ICE02790
 ICE02800
 ICE02810
 ICE02820
 ICE02830
 ICE02840
 ICE02850
 ICE02860
 ICE02870
 ICE02880
 ICE02890
 ICE02900
 ICE02910
 ICE02920
 ICE02930

```

C
C
C
30  COMPUTE THE UNKNOWN PART OF THE KERNEL
    CONTINUE
    M=KS-KS1+1
    KE2=NTR-M
    IF(M.LE.0) PAUSE 'BAD INPUT XSYS'
    IF(M.GE.NTR) GOTO 1001
    DO 40 J=1,KE2
        DO 40 L=1,KE2
            DO 40 I=1,KYE
                AKERN(J,L,I)=AKERN(J+M,L+M,I)
40  CONTINUE
        DO 60 J=1,KE2
            DO 60 L=KE2+1,NTR
                XD=(J-L)*XDEL
                ZD=ZSURF(J+KS)-ZSURF(L+KS)
                RHO=SQRT(XD*XD+ZD*ZD)
                GEOM=2.*(AMPDER(L+KS)/AMPDER(J+KS))*(XD*XD*(J+KS)-ZD)/RHO
                DO 50 I=1,KYE
                    WK=AKY(I)*PI2
                    IF(I.EQ.1) THEN
                        AKERN(J,L,I)= GEOM/RHO
                    ELSE
                        AKERN(J,L,I)= GEOM*WK*BESSKI(RHO*WK)
                    ENDIF
50  CONTINUE
60  CONTINUE
        DO 80 J=KE2+1,NTR
            DO 80 L=1,NTR
                IF(J.EQ.L) GOTO 80
                XD=(J-L)*XDEL
                ZD=ZSURF(J+KS)-ZSURF(L+KS)
                RHO=SQRT(XD*XD+ZD*ZD)
                GEOM=2.*(AMPDER(L+KS)/AMPDER(J+KS))*(XD*XD*(J+KS)-ZD)/RHO
                DO 70 I=1,KYE
                    WK=AKY(I)*PI2
                    IF(I.EQ.1) THEN
                        AKERN(J,L,I)= GEOM/RHO
                    ELSE
                        AKERN(J,L,I)= GEOM*WK*BESSKI(RHO*WK)
                    ENDIF
70  CONTINUE
80  CONTINUE
    WRITE(4,90) (AKERN(40,10,I), I=1,KYE)
90  FORMAT(4X,'KERNEL',/,5(1PE12.4)))
    RETURN
    END

C
C
C
    SUBROUTINE CHARGE(NTR,KYE,XDEL,NL000)
    implicit real*8 (a-h,o-z)

C
C
C
    COMPUTE THE CHARGE DISTRIBUTION ON THE SURFACE OF
    THE SEA WATER

C
    DIMENSION CHAR(120,20),HPN(120,20),AKERN(120,120),WK(120)
    DIMENSION W2(120)
    COMMON /,ER/ AKERN/HPN/CH/CHAR
    FAC=1.0/(2*3.1415926)

```

```

ICE01760
ICE01770
ICE01780
ICE01790
ICE01800
ICE01810
ICE01820
ICE01830
ICE01840
ICE01850
ICE01860
ICE01870
ICE01880
ICE01890
ICE01900
ICE01910
ICE01920
ICE01930
ICE01940
ICE01950
ICE01960
ICE01970
ICE01980
ICE01990
ICE02000
ICE02010
ICE02020
ICE02030
ICE02040
ICE02050
ICE02060
ICE02070
ICE02080
ICE02090
ICE02100
ICE02110
ICE02120
ICE02130
ICE02140
ICE02150
ICE02160
ICE02170
ICE02180
ICE02190
ICE02200
ICE02210
ICE02220
ICE02230
ICE02240
ICE02250
ICE02260

ICE02270
ICE02280
ICE02290
ICE02300
ICE02310
ICE02320
ICE02330
ICE02340

```

```

C .....
C CUBIC SPLINE INTERPOLATION BEFORE TAKING THE
C INVERSE FOURIER TRANSFORM.
C .....
C
C DIMENSION AKY(KYE), 0(NK1) YA(KYE), Y2(20)
CALL SPLINE(AKY, YA, KYE, 1.E30, 1.E30, /2)
O(1)=YA(1)
DO 10 I=2, NK1
  XX=(I-1)*AKDEL
  KLO=1
  KHI=KYE
  IF (KHI-KLO.GT.1) THEN
    K=(KHI+KLO)/2
    IF (AKY(K).GT.XX) THEN
      KHI=K
    ELSE
      KLO=K
    ENDIF
  GOTO 1
ENDIF
H=AKY(KHI)-AKY(KLO)
A=(AKY(KHI)-XX)/H
B=(XX-AKY(KLO))/H
O(I)=A*YA(KLO)+B*YA(KHI)+(A*(A-1.)*Y2(KLO)+
  B*(B-1.)*Y2(KHI))/(H*H)/6.
*
10 CONTINUE
RETURN
END
C
C SUBROUTINE SPLINE(X,Y,N,YP1,YPN,Y2)
implicit real*8 (a-h,o-z)
C
C GIVEN ARRAYS X AND Y OF LENGTH N CONTAINING A TABULATED FUNCTION,
C I.E., Y=F(X), WITH X1<X2<X3<...<XN, THIS ROUTINE RETURNS AN ARRAY
C Y2 OF LENGTH N WHICH CONTAINS THE SECOND DERIVATIVES OF THE INTER-
C POLATING FUNCTION AT THE TABULATED POINTS XJ. NATURAL SPLINE FROM
C NUMERICAL RECIPES, PRESS AT AL.
C .....
C
C PARAMETER (NMAX=1024)
DIMENSION X(N), Y(N), Y2(N), U(NMAX)
IF (YP1.GT..99E30) THEN
  Y2(1)=0.
  U(1)=0.
ELSE
  Y2(1)=-0.5
  U(1)=(3./(X(2)-X(1)))*(Y(2)-Y(1))/(X(2)-X(1))-YP1)
ENDIF
DO 11 I=2, N-1
  SIG=(X(I)-X(I-1))/(X(I+1)-X(I-1))
  P=SIG*Y2(I-1)+2.
  Y2(I)=(SIG-1.)/P
  U(I)=(0.)*((Y(I+1)-Y(I))/(X(I+1)-X(I))-(Y(I)-Y(I-1))/
    / (X(I)-X(I-1)))/(X(I+1)-X(I-1))-SIG*U(I-1))/P
*
11 CONTINUE
IF (YPN.GT..99E30) THEN
  QN=0.
  UN=0.
ELSE

```

```

ICE03520
ICE03530
ICE03540
ICE03550
ICE03560
ICE03570
ICE03580
ICE03590
ICE03600
ICE03610
ICE03620
ICE03630
ICE03640
ICE03650
ICE03660
ICE03670
ICE03680
ICE03690
ICE03700
ICE03710
ICE03720
ICE03730
ICE03740
ICE03750
ICE03760
ICE03770
ICE03780
ICE03790
ICE03800
ICE03810
ICE03820

ICE03830
ICE03840
ICE03850
ICE03860
ICE03870
ICE03880
ICE03890
ICE03900
ICE03910
ICE03920
ICE03930
ICE03940
ICE03950
ICE03960
ICE03970
ICE03980
ICE03990
ICE04000
ICE04010
ICE04020
ICE04030
ICE04040
ICE04050
ICE04060
ICE04070
ICE04080
ICE04090
ICE04100

```

```

      AXZ=2.0*CHAR(M,I)*AMPTDER(J)/(RH0*RH0)
      E*JOIF
      AZ=(ZSYS(K)-ZSURF(J))*AXZ*AZ
      AX=(XSYS(K)-(J-1)*XDEL*XF)*AXZ*AX
      CONTINUE
      TEMP1(I)=AZ*XDEL
      TEMP2(I)=AX*XDEL
      CONTINUE
      NK=2.0*NM
      I?(NK*AKDEL.GT.AKY(KYE)) PAUSE 'BAD AKDEL OR AKY'
      CALL CUBSPL(KYE,NK,AKDEL,AKY,TEMP1,AA)
      SUM=0.0
      DO 11 I=2,NK
        SUM=SUM+AA(I)
      11 HZS=(SUM+AA(1)/2)-AKDEL*2.
      CALL CUBSPL(KYE,NK,AKDEL,AKY,TEMP2,AA)
      SUM=0.0
      DO 12 I=2,NK
        SUM=SUM+AA(I)
      12 HXS=(SUM+AA(1)/2)-AKDEL*2.
      HXS=HXS/HNORM*1000000
      HZS=HZS/HNORM*1000000
      RETURN
      END

      SUBROUTINE CUBDER(N,XDEL,YA,YD)
      implicit real*8 (a-h,o-z)
      .....
      COMPUTE THE DERIVATIVES AT EACH NODE USING
      CUBIC SPLINE.
      NOTE: N=NPT*2 ONE POINT ADDED TO EACH END.
      .....
      DIMENSION XA(50),YA(4),Y2(50),YD(N)
      DO 11 I=1,N
        XA(I)=(I-1)*XDEL
      11 DO 12 I=N-1,2,-1
        YA(I)=YA(I-1)
      12 YA(1)=0.
        YA(N)=0.
      CALL SPLINE(XA,YA,N,0.,0.,Y2)
      DO 10 I=2,N-1
        XX=XA(I)
        KLO=I
        KHI=I+1
        H=XA(KHI)-XA(KLO)
        A=(XA(KHI)-XX)/H
        B=(XX-XA(KLO))/H
        XD=XA(KHI)-XA(KLO)
        YD(I-1)=(YA(KHI)-YA(KLO))/XD-XD*((3.*A-A-1.)*Y2(KLO)
          *- (3.*B-B-1.)*Y2(KHI))/6.
      *
      10 CONTINUE
      DO 14 I=1,N-2
      14 YA(I)=YA(I+1)
      RETURN
      END

      SUBROUTINE CUBSPL(KYE,NK1,AKDEL,AKY,YA,D)
      implicit real*8 (a-h,o-z)

```

ICE04690
ICE04700
ICE04710

ICE04720
ICE04730
ICE04740

ICE04750
ICE04760
ICE04770

ICE04780
ICE04790
ICE04800

ICE04810
ICE04820
ICE04830

ICE04840
ICE04850
ICE04860

ICE04870
ICE04880
ICE04890

ICE04900
ICE04910
ICE04920

ICE04930
ICE04940
ICE04950

ICE04960
ICE04970
ICE04980

ICE04990
ICE05000
ICE05010

ICE05020
ICE05030
ICE05040

ICE05050
ICE05060
ICE05070

ICE05080
ICE05090
ICE05100

ICE05110
ICE05120
ICE05130

ICE05140
ICE05150
ICE05160

ICE05170
ICE05180
ICE05190

```

c
c      Function BESSII(x)
c      implicit real*8 (a-h,o-z)
c      ..
c      Returns the modified Bessel function I1(x) for any real x
c      ..

```

```

      real*8 y,p1,p2,p3,p4,p5,p6,p7,q1,q2,q3,q4,q5,q6,q7,q8,q9
      data p1,p2,p3,p4,p5,p6,p7/0.5d0,0.87890594d0,0.51498869d0,
      * 0.15084934d0,0.2658733d-1,0.301532d-2,0.32411d-3/
      data q1,q2,q3,q4,q5,q6,q7,q8,q9/0.39894228d0,-0.39898024d-1,
      * -0.362018d-2,0.163801d-2,-0.1031555d-1,0.2282967d-1,
      * -0.289631d-1,0.1787654d-1,-0.420059d-2/
      if (abs(x).lt.3.75) then

```

```

        y=(x/3.75)**2
        BESSII=x*(p1+y*(p2+y*(p3+y*(p4+y*(p5+y*(p6+y*p7))))))

```

```

      else
        ax=abs(x)
        y=3.75/ax

```

```

        BESSII=(exp(ax)/sqrt(ax))*(q1+y*(q2+y*(q3+y*(q4+y*(q5+

```

```

        * y*(q6+y*(q7+y*(q8+y*q9))))))
      endif
      return
      end

```

```

c
c      Function BESSKI(x)
c      implicit real*8 (a-h,o-z)
c      ..
c      Returns the modified Bessel function K1(x) for positive x
c      ..

```

```

      real*8 y,p1,p2,p3,p4,p5,p6,p7,q1,q2,q3,q4,q5,q6,q7
      data p1,p2,p3,p4,p5,p6,p7/1.0d0,0.15443144d0,-0.67278579d0,
      * -0.18158897d0,-0.1919402d-1,-0.110404d-2,-0.4686d-4/

```

```

      data q1,q2,q3,q4,q5,q6,q7/1.25331414d0,0.23498619d0,-0.3655620d-1,
      * 0.1504268d-1,-0.780353d-2,0.325614d-2,-0.68245d-3/
      if (x.le.2.0) then

```

```

        y=x*x/4.0
        BESSKI= (log(x/2.0)*BESSII(x))+(1.0/x)*(p1+y*(p2+y*(p3+

```

```

        * y*(p4+y*(p5+y*(p6+y*p7))))))
      else

```

```

        if (x.gt.4.0) then
          BESSKI=0.0

```

```

        else
          y=(2.0/x)
          BESSKI=(exp(-x)/sqrt(x))*(q1+y*(q2+y*(q3+y*(q4+y*(q5+

```

```

          * y*(q6+y*q7))))))
        endif
      endif
      return
      end

```



```

12      QN=0.5
      UN=(3./.(X(N)-X(N-1)))*(YPN-(Y(N)-Y(N-1))/(X(N)-X(N-1)))
      ENDIF
      Y2(N)=(UN-QN*U(N-1))/(QN*Y2(N-1)+1.)
      DO 12 K=N-1,1,-1
      Y2(K)=Y2(K)*Y2(K+1)+U(K)
      CONTINUE
      RETURN
      END

C
C      Function BESSIO(x)
      implicit real*8 (a-h,o-z)
C
C      RETURNS THE MODIFIED BESSEL FUNCTION IO(X) FOR ANY REAL X.
C
      real*8 y,p1,p2,p3,p4,p5,p6,p7,q1,q2,q3,q4,q5,q6,q7,q8,q9
      data p1,p2,p3,p4,p5,p6,p7/1.0d0,3.5156229d0,3.0899424d0,
      + 1.2067492d0,0.2659732d0,0.360768d-1,0.45813d-2/
      data q1,q2,q3,q4,q5,q6,q7,q8,q9/0.39894228d0,0.1328592d-1,
      + 0.225319d-2,-0.167565d-2,0.916281d-2,-0.2067706d-1,
      + 0.2635537d-1,-0.1647833d-1,0.392377d-2/
      if(abs(x).lt.3.75) then
      y=(x/3.75)**2
      BESSIO=p1+y*(p2+y*(p3+y*(p4+y*(p5+y*(p6+y*p7))))
      else
      ax=abs(x)
      y=3.75/ax
      BESSIO=(exp(ax)/sqrt(ax))*(q1+y*(q2+y*(q3+y*(q4+y*(q5+
      + y*(q6+y*(q7+y*(q8+y*q9)))))))
      endif
      return
      end

C
C      Function BESSK0(x)
      implicit real*8 (a-h,o-z)
C
C      Returns the modified Bessel function K0(x) for positive x.
C
      real*8 y,p1,p2,p3,p4,p5,p6,p7,q1,q2,q3,q4,q5,q6,q7
      data p1,p2,p3,p4,p5,p6,p7/-0.57721566d0,0.42278420d0,0.23069756d0,
      + 0.3488690d-1,0.262698d-2,0.10760d-3,0.74d-6/
      data q1,q2,q3,q4,q5,q6,q7/1.25331414d0,-0.7832358d-1,0.2189568d-1,
      + -0.10622446d-1,0.587872d-2,-0.251540d-2,0.53208d-3/
      if(x.le.2.0) then
      y=x*x/4.0
      BESSK0=(-log(x/2.0)*BESSIO(x)+(p1+y*(p2+y*(p3+
      + y*(p4+y*(p5+y*(p6+y*p7)))))
      else
      if(x.gt.40.) then
      BESSK0=0.0
      else
      y=(2.0/x)
      BESSK0=(exp(-x)/sqrt(x))*(q1+y*(q2+y*(q3+y*(q4+y*(q5+
      + y*(q6+y*q7)))))
      endif
      endif
      return
      end

```



```

IF (KK.GT.NITER) THEN
  WRITE(4,17)
  STOP
ENDIF
ENDIF
11 FORMAT(4X,'COMPUTED ICE-WATER INTERFACE',/, (5(1PE14.2)))
12 FORMAT(4X,'COMPUTED DATA',/, (5(1PE14.4)))
13 FORMAT(4X,'FIRST CONVERGENCE CRITERION SATISFIED')
14 FORMAT(4X,'SECOND CONVERGENCE CRITERION SATISFIED')
15 FORMAT(4X,'HORIZONTAL AXIS DIPOLE TRANSMITTER',/)
16 FORMAT(4X,'VERTICAL AXIS DIPOLE TRANSMITTER',/)
17 FORMAT(4X,'NPT =',16,2X,'NXT =',16,/,
18 * 4X,'NRESP =',15,2X,'NTRUNK =',15,2X,'NLOOP =',15,/,4X,'IREC =',
19 * 15,2X,'NITER =',15)
20 FORMAT(4X,'T-R SEPARATION =',F7.2,' METERS',/,4X,'XDEL =',F7.2,
21 * ' METERS',/,4X,'FIRST CONVERGENCE CRITERIA RMS ERR =',1PE12.2)
22 FORMAT(4X,'INITIAL ICE-WATER INTERFACE',/, (10F12.2))
23 FORMAT(11X,'ZSYS (M) DATA IN PPM',/, (3F17.2))
GOTO 1001
END

C
C SUBROUTINE HARMOC(KYE,NM,AKDEL,AKY)
C .....
C ASSIGN KY HARMONICS. THE FOLLOWING IS OK FOR ZR=10 - 100 METERS.
C IMPLICIT DOUBLE PRECISION (A-H, O-Z)
C DIMENSION AKY(KYE)
C KYE=15
C NM=7
C AKYMIN=1.0/(2.0*1000)
C AKDEL=0.0006
C AKLOG=0.17
C AKYEX=DLOG10(AKYMIN)
C AKY(1)=0.0
C DO 20 I=1,KYE-1
C   EX=AKYEX*(I-1)*AKLOG
C   AKY(I+1)=10**EX
C CONTINUE
20 WRITE(4,201)(AKY(I),I=1,KYE)
201 FORMAT(4X,'KY HARMONICS =',/, (5E14.4))
C .....
C RETURN
C END

C
C SUBROUTINE FORDIV(NPT,NRESP,ZH1,CALC,WJ)
C .....
C COMPUTE THE APPROXIMATE JACOBIAN MATRIX
C .....
C IMPLICIT DOUBLE PRECISION (A-H, O-Z)
C PARAMETER (NDD=40,NPP=30,NXT=200)
C DIMENSION ZH0(NXT),XSYS(NDD),ZSYS(NDD),WJ(NDD,NPP),ZH1(1)
C DIMENSION AMPDER(NXT),TEMP(20),AA(KM),ZH2(NPP),CALC2(NDD),CALC(1)
C COMMON /FCM/ZH0,XSYS,ZSYS,AMPDER,NM,IREC,AKDEL
C COMMON /KY/AKY(20)
C COMMON KYE,NSYS,NST,XDEL,TRDIS
C CALL FORMOD(NPT,NRESP,ZH1,CALC)
C K=1
1001 CONTINUE
DO 10 I=1, NPT

```

```

INV00600
INV00610
INV00620
INV00630
INV00640
INV00650
INV00660
INV00670
INV00680
INV00690
INV00700
INV00710
INV00720
INV00730
INV00740
INV00750
INV00760
INV00770
INV00780
INV00790
INV00800
INV00810
INV00820
INV00830
INV00840
INV00850
INV00860
INV00870
INV00880
INV00890
INV00900
INV00910
INV00920
INV00930
INV00940
INV00950
INV00960
INV00970
INV00980
INV00990
INV01000
INV01010
INV01020
INV01030
INV01040
INV01050
INV01060
INV01070
INV01080
INV01090
INV01100
INV01110
INV01120
INV01130
INV01140
INV01150
INV01160
INV01170
INV01180
INV01190

```

```

PROGRAM INVSM
INVERSION PROGRAM FOR IMAGING THE ICE-WATER INTERFACE FROM THE
AIRBORNE ELECTROMAGNETIC DATA.
QUADRATIC PROGRAMING APPROACH.
SMOOTH INVERSION

IMPLICIT DOUBLE PRECISION (A-H, O-Z)
PARAMETER (NXT=200,NTRUNK=100,NLOOP=8,NDD=40,NPP=30)
DIMENSION FKERN(NDD,NPP),DELZH(NDD),AMPDER(NXT),ZHO(NXT)
DIMENSION XSYS(NDD),ZSYS(NDD),CALC(NDD)
COMMON /DATA/NRESP,ZH1(NDD),SD(NDD)
COMMON /MODEL/NPT,ZH1(NPT),DM(NDD),LJUMP(NPP)
COMMON /KY/AKY(20)
COMMON /FCM/ZHO,XSYS,ZSYS,AMPDER,NM,IREC,AKDEL
COMMON KYE,NSYS,NST,XOEL,TROIS
open (unit=3, file='invhz.dat')
open (unit=4, file='invhz.out')
READ(3,*)
READ(3,*)NSYS,IREC,NST,NPT,NRESP,NITER
READ(3,*)
READ(3,*)XOEL,TROIS,ERR,PMU
READ(3,*)
READ(3,*)(ZH1(I),I=1,NPT)
READ(3,*)
READ(3,*)(XSYS(I),ZSYS(I),DAT(I),CALC(I),I=1,NRESP)
READ(3,*)
READ(3,*)(SD(I),I=1,NRESP)
READ(3,*)
READ(3,*)(LJUMP(I),I=1,NPT)
IF(IREC.EQ.2) THEN
  DO 3 I=1,NRESP
    DAT(I)=CALC(I)
  ENDIF
ENDIF

OUTPUT THE INPUT DATA

IF(NSYS.EQ.1) WRITE(4,101)
IF(NSYS.EQ.2) WRITE(4,102)
IF(NSYS.NE.1.AND.. NSYS.NE.2) PAUSE 'BAD INPUT NSYS'
IF(IREC.NE.1.AND.. IREC.NE.2) PAUSE 'BAD INPUT IREC'
WRITE(4,104)TROIS,XOEL,ERR
WRITE(4,103)NST,NPT,NXT,NRESP,NTRUNK,NLOOP,IREC,NITER
WRITE(4,105)( ZH1(I),I=1,NPT)
WRITE(4,106)(XSYS(I),ZSYS(I),DAT(I),I=1,NRESP)

ASSIGN THE KY HARMONICS

CALL HARMOC(KYE,NM,AKDEL,AKY)
KK-1
1001 CONTINUE
KK=KK+1
CALL THE SMOOTH INVERSION ROUTINE
CALL OCCAM1(1,ERR,TOST,0,NIT,STEPSZ,KONV,4,PMU)
WRITE(4,11)(ZH1(I),I=1,NPT)
WRITE(4,12)(DM(I),I=1,NRESP)
IF(TOST.LT.ERR) THEN
  WRITE(4,16)
STOP
ELSE

```

```

C TOBT = RMS MISFIT OF NEW MODEL RESPONSE.
C NIT = NUMBER OF PREVIOUS CALLS TO OCCAM1 DURING THIS INVERSION
C STEPSZ = SUM OF SQUARES OF THE CHANGES IN THE MODEL PARAMETERS
C KONV = STATUS FLAG:
C 0 = NORMAL EXIT FOR A SUCCESSFUL ITERATION.
C 1 = A PERFECTLY SMOOTH MODEL HAS BEEN FOUND FOR THE REQUIRED TOLERANCE
C 2 = CONVERGENCE PROBLEMS. UNABLE TO FIND A MODEL WITH AN R.M.S. MISFIT
C LESS THAN OR EQUAL TO THAT OF THE INITIAL MODEL.
C UM = THE MU VALUE USED AT THE MINIMUM OF THE MISFIT IN THIS ITERATION
C
C SUBROUTINES REQUIRED AND SUPPLIED:
C MAKDEL, A SUBROUTINE WHICH CREATES THE ROUGHENING MATRIX
C TOFMU(AMU), A FUNCTION WHICH RETURNS THE RMS MISFIT OF THE RESPONSE
C OF THE MODEL CONSTRUCTED USING THE LAGRANGE MULTIPLIER AMU.
C CALLS CHOLIN, CHOLSL, FORMOD, ANORM.
C INITM, TRMULT, MULT AND ANORM, SUBROUTINES FOR SIMPLE MATRIX OPERATION
C FMIN, A SUBROUTINE WHICH MINIMISES A UNIVARIATE FUNCTION
C FRONT, A SUBROUTINE WHICH FINDS THE ROOT OF A UNIVARIATE FUNCTION
C MINRK, A SUBROUTINE WHICH BRACKETS A UNIVARIATE MINIMUM
C
C SUBROUTINES WHICH MUST BE SUPPLIED BY THE USER:
C FORMOD(NP,ND,PM,DP,DM), COMPUTES THE FORWARD FUNCTION FOR MODEL PM()
C THE DATA PARAMETERS DP() AND RETURNS IT IN DM().
C FORDIV(NP,ND,PM,DP,DM,WJ), COMPUTES THE FORWARD FUNCTION AS DOES FORMOD
C BUT ALSO RETURNS THE MATRIX OF PARTIALS, WJ(ND,NP).
C
C PARAMETERS NDD AND NPP SHOULD BE SET TO THE MAXIMUM DIMENSIONS OF THE
C DATA AND PARAMETER VECTORS, RESPECTFULLY. DON'T FORGET TO ADJUST
C THEM IN TOFMU, MAKDEL, BLOCKDATA AND ANY I/O SUBROUTINES.
C
C NOTE THAT DOUBLE PRECISION IS USED THROUGHOUT. SOME COMPILERS WILL
C EXTERNAL TOFMU TO BE DECLARED IN OCCAM1'S CALLING PROGRAM.
C
C IMPLICIT DOUBLE PRECISION (A-H, O-Z)
C PARAMETER (NDD = 40, NPP = 30)
C COMMON /DATA/ ND,D(NDD),SD(NDD)
C COMMON /MODEL/ NP,PM(NPP),DM(NDD),LJMP(NPP)
C /RESULT/ IS USED TO CARRY INFO IN AND OUT OF TOFMU AND STORE LAST
C VALUE OF MU USED.
C COMMON /RESULT/ PTP(NPP,NPP),WJTWJ(NPP,NPP),WJTW2(NPP),PM2(NPP),
C * PMU,NFOR,NITER,FRAC,RLAST,IFFTOL
C DIMENSION WJ(NDD,NPP),DD(NDD),DHAT(NDD),WK(NPP)
C EXTERNAL TOFMU
C
C ON FIRST ENTRY CREATE TRANS(P),P, WHERE P IS THE ROUGHENING MATRIX OR
C ROUGHENING MATRIX SQUARED, AND SET MU TO AN ARBITRARY (LARGE) VALUE.
C
C IF (NITER.EQ.0) THEN
C   CALL MAKDEL(1RUF)
C   PMU = 10000.
C   PMU=UM
C   RLAST = 10000.
C   KONV = 0
C END IF
C
C FRAC CONTROLS THE STEP SIZE; NORMALLY WILL REMAIN AT 1.0 UNLESS WE
C CONVERGENCE PROBLEMS
C FRAC = 1.0
C CALCULATE THE MATRIX OF PARTIALS AND MODEL RESPONSE
C CALL FORDIV(NP,ND,PM,DM,WJ)
C WRITE(IOUT,11) (DM(I),I=1,ND)

```

```

INV01800
INV01810
INV01820
INV01830
INV01840
INV01850
INV01860
INV01870
INV01880
INV01890
INV01900
INV01910
INV01920
INV01930
INV01940
INV01950
INV01960
INV01970
INV01980
INV01990
INV02000
INV02010
INV02020
INV02030
INV02040
INV02050
INV02060
INV02070
INV02080
INV02090
INV02100
INV02110
INV02120
INV02130
INV02140
INV02150
INV02160
INV02170
INV02180
INV02190
INV02200
INV02210
INV02220
INV02230
INV02240
INV02250
INV02260
INV02270
INV02280
INV02290
INV02300
INV02310
INV02320
INV02330
INV02340
INV02350
INV02360
INV02370
INV02380
INV02390

```

```

10      ZH2(I) = ZH1(I)
      ZH2(K) = ZH1(K)*0.2
      CALL FORMOD(NPT,NRESP,ZH2,CALC2)
      DO 30 I=1, NRESP
        WJ(I,K) = (CALC2(I)-CALC(I))/0.2
30      CONTINUE
      K=K+1
      IF (K.LE.NPT) GOTO 1001
      DO 51 I=1,NRESP
        WRITE(4,50) (WJ(I,J), J=1,NPT)
51      CONTINUE
      FORMAT(4X, 'INVERSION KERNEL',/, (5(1PE14.4)))
      RETURN
      END
C.....
      SUBROUTINE OCCAM1(IRUF,TOLREQ,T0BT,IBUG,NIT,STEPSZ,KONV,IOUT,UM)
C
C MODIFIED VERSION OF OCCAM1
C OCCAM1 EXECUTES ONE ITERATION OF A ONE DIMENSIONAL SMOOTH MODEL FINDER
C REFERENCE: CONSTABLE, PARKER & CONSTABLE, 1987: GEOPHYSICS 52, 289-300
C
C S. CONSTABLE, MARCH 1986, S.I.O., LA JOLLA, CA 92093, U.S.A. (VERSION
C (VERSION 1987,
C
C IF YOU OBTAIN THIS CODE FROM A THIRD PERSON, PLEASE SEND YOUR NAME AND
C TO S. CONSTABLE. YOU WILL THEN RECEIVE UPDATES, NEWS ON BUGS, ETC.
C
C ON INPUT:
C /DATA/ CONTAINS
C ND = NUMBER OF DATA
C D(NDD) = VECTOR OF DATA VALUES
C SD(NDD) = VECTOR OF ABSOLUTE STANDARD ERRORS IN THE DATA
C DP(NDD,4) = MATRIX CONTAINING UP TO FOUR PARAMETERS ASSOCIATED WITH
C EACH DATUM (RANGE, FREQUENCY, DATA TYPE ETC)
C NPD = NUMBER OF PARAMETERS ASSOCIATED WITH EACH DATUM (E.G. FOR FR
C NPD = 1, FOR FREQ. AND RANGE NPD = 2)
C
C /MODEL/ CONTAINS
C NP = NUMBER OF MODEL PARAMETERS, USUALLY THE NUMBER OF LAYERS
C PM(NPP) = VECTOR OF INITIAL MODEL PARAMETERS, USUALLY LOG10(LAYER
C LJMP(NPP) = A VECTOR DESCRIBING PLACES WITHIN THE MODEL TO RELAX
C SMOOTHNESS CONSTRAINT, IN MONOTONIC ORDER FOLLOWED BY A ZERO.
C THUS LJMP = 4,10.0
C WOULD ALLOW A DISCONTINUITY BETWEEN LAYER 3 AND 4 AND LAYERS
C
C IRUF = 1 FOR FIRST DERIVATIVE MINIMIZATION
C = 2 FOR SECOND DERIVATIVE MINIMIZATION
C TOLREQ = REQUIRED RMS MISFIT
C IRUG = 1 IF A TABLE OF RMS MISFIT VERSUS LAGRANGE MULTIPLIER IS REQUIRED
C (USEFUL FOR TRACKING DOWN CONVERGENCE PROBLEMS)
C 0 OTHERWISE (LOTS FASTER)
C IOUT = FORTRAN UNIT NUMBER FOR OUTPUT, CAN BE TERMINAL OR A FILE
C UM = THE WU VALUE USED AT THE MINIMUM OF THE MISFIT IN THE LAST CALL
C TO OCCAM1
C
C ON OUTPUT:
C /MODEL/ CONTAINS
C PM(NPP) = VECTOR OF UPDATED MODEL PARAMETERS
C DM(NDD) = VECTOR CONTAINING RESPONSE OF NEW MODEL

```

```

INV01200
INV01210
INV01220
INV01230
INV01240
INV01250
INV01260
INV01270
INV01280
INV01290
INV01300
INV01310
INV01320
INV01330
INV01340
INV01350
INV01360
INV01370
INV01380
INV01390
INV01400
INV01410
INV01420
INV01430
INV01440
INV01450
INV01460
INV01470
INV01480
INV01490
INV01500
INV01510
INV01520
INV01530
INV01540
INV01550
INV01560
INV01570
INV01580
INV01590
INV01600
INV01610
INV01620
INV01630
INV01640
INV01650
INV01660
INV01670
INV01680
INV01690
INV01700
INV01710
INV01720
INV01730
INV01740
INV01750
INV01760
INV01770
INV01780
INV01790

```

```

165 WK(I) = PM2(I) - PM2(I-1)
ELSE
DO 170 I = 2, NP-1
WK(I) = PM2(I+1) - 2.*PM2(I) + PM2(I-1)
WK(NP) = 0.0
END IF
C REMOVE ENTRIES IN ROUGHNESS VECTOR WHERE JUMPS ARE ALLOWED
I = 1
175 IF (LJMP(I).NE.0) THEN
WK(LJMP(I)) = 0.0
I = I+1
GOTO 175
END IF
RUF = ANORM(NP,WK)
C IF WE HAVE ATTAINED THE INTERCEPT BUT THE MODEL IS GETTING ROUGHER
C WE HAVE PROBLEMS WITH CONVERGENCE.
C SAVE NEW MODEL AND COMPUTE STEP SIZE
DO 180 I = 1, NP
WK(I) = PM2(I) - PM(I)
PM(I) = PM2(I)
STEPSZ = ANORM(NP,WK)
STEPSZ = SQRT(STEPSZ/NP)
WRITE(IOUT,*) 'STEP SIZE IS = ', STEPSZ
WRITE(IOUT,*) 'ROUGHNESS IS = ', RUF
NITER = NITER + 1
RETURN
END
C .....
C SUBROUTINE MAKDEL(IRUF)
C MAKDEL CONSTRUCTS TRANS(DEL).DEL FOR 1ST OR 2ND DERIVATIVE ROUGHNESS
C ON INPUT:
C IRUF = 1 FOR 1ST DERIVATIVE ROUGHNESS
C 2 FOR 2ND DERIVATIVE ROUGHNESS
C /MODEL/ CONTAINS
C LJMP = ARRAY OF LAYER LOCATIONS WHERE A JUMP IN RESISTIVITY IS ALLOWED
C TERMINATED BY A ZERO
C
C IMPLICIT DOUBLE PRECISION (A-H, O-Z)
PARAMETER (NDD = 40, NPP = 30)
COMMON /MODEL/ NP, PM(NPP), DM(NDD), LJMP(NPP)
COMMON /RESULT/ PTP(NPP,NPP), WJTWJ(NPP,NPP), WJTD(NPP), PM2(NPP),
* PMJ,NFOR,NITER,FRAC,RLAST,IFFTOL
DIMENSION DEL(NPP,NPP)
C MAKE PARTIALS MATRIX
CALL INITM(NPP,NP,NP,DEL)
DO 10 I = 2, NP
DEL(I,I-1) = -1.
DEL(I,I) = 1.
10 C REMOVE ANY ENTRIES WHERE MODEL IS ALLOWED TO JUMP
I = 0
I = I+1
N = LJMP(I)
C CANNOT REMOVE AIR/EARTH INTERFACE (N=1):
IF (N.EQ.1) GOTO 20
IF (I.NE.NP+1.AND.N.NE.0) THEN

```

INV03000
 INV03010
 INV03020
 INV03030
 INV03040
 INV03050
 INV03060
 INV03070
 INV03080
 INV03090
 INV03100
 INV03110
 INV03120
 INV03130
 INV03140
 INV03150
 INV03160
 INV03170
 INV03180
 INV03190
 INV03200
 INV03210
 INV03220
 INV03230
 INV03240
 INV03250
 INV03260
 INV03270
 INV03280
 INV03290
 INV03300
 INV03310
 INV03320
 INV03330
 INV03340
 INV03350
 INV03360
 INV03370
 INV03380
 INV03390
 INV03400
 INV03410
 INV03420
 INV03430
 INV03440
 INV03450
 INV03460
 INV03470
 INV03480
 INV03490
 INV03500
 INV03510
 INV03520
 INV03530
 INV03540
 INV03550
 INV03560
 INV03570
 INV03580
 INV03590

```

11 FORMAT(4X,'COMPUTED DATA',/, (5(1PE14.4)))
C CALC MISFIT VECTOR AND MISFIT
DO 60 I = 1,ND
  DD(I) = (D(I) - DM(I))/SD(I)
  CH10 = ANORM(ND,DD)
  TOL0 = SQRT(CH10/ND)
  IF (NITER.EQ. 0) THEN
    WRITE(IOUT,*) 'STARTING R.M.S. = ',TOL0
  END IF
C WEIGHT THE PARTIALS MATRIX
DO 70 I = 1,ND
  DO 70 J = 1,NP
    WJ(I,J) = WJ(I,J)/SD(I)
C FORM W.J. TRANS(W.J)
CALL TRMULT(ND,ND,ND,NP,NP,WJ,WJ,WJTWJ)
C FORM THE WEIGHTED, TRANSLATED DATA AND PREMUL TIPLY BY TRANS(W.J)
CALL MULT(ND,ND,NP,NP,1,WJ,PM,DHAT)
DO 80 I = 1,ND
  DHAT(I) = DD(I) * DHAT(I)
  CALL TRMULT(ND,ND,NP,NP,1,WJ,DHAT,WJTD)
C PRODUCE THE MISFIT FUNCTION IF REQUIRED
  IF (IBUG.EQ. 1) THEN
    WRITE(IOUT,*) 'MISFIT AS A FUNCTION OF MU'
    DO 100 K = 18,1,-1
      AMU = 10.**(FLOAT(K)/2. - 1.)
      T = TOFMU(AMU)
      IF (T.GE. 1.0E+09) GOTO 110
      WRITE(IOUT,*) AMU,T
    END IF
  CONTINUE
  WRITE(IOUT,*) ' '
  WRITE(IOUT,*) '** ITERATION ',NITER+1,'**'
C THE NEXT BLOCK OF CODE CONTROLS THE SELECTION OF THE LAGRANGE MULTIPLIER
C PMU
120 TOLM = 0.2
  AMU1 = 0.9*PMU
  AMU2 = PMU
  NF0R = 0
  IFFTOL = 0
C FIND MINIMUM
  CALL MINBRK(AMU1,AMU2,AMU3,TAMU1,TAMU2,TAMU3,TOFMU)
  WRITE(IOUT,*) 'AMU1','AMU1','MISFIT',TAMU1
  WRITE(IOUT,*) 'AMU2','AMU2','MISFIT',TAMU2
  WRITE(IOUT,*) 'AMU3','AMU3','MISFIT',TAMU3
  TOBT = FMIN(AMU1,AMU2,AMU3,TAMU2,TOFMU,TOLM,PMU)
  PMU = AMU2
  TOBT = TAMU2
C COMPUTE THE MODEL PARAMETERS (AGAIN) AT WHICH MINIMUM MISFIT WAS
C OBTAINED. TORBDM IS DUMMY
  TORBDM=TOFMU(PMU)
  WRITE(IOUT,*) 'MINIMUM TOL IS AT MU = ',PMU
  WRITE(IOUT,*) 'AND IS = ',TOBT
  WRITE(IOUT,*) 'USING ',NF0R,' EVALUATIONS OF FUNCTION'
C IF THE NEW MINIMUM TOLERANCE IS GREATER THAN THE TOLERANCE FROM THE
C PREVIOUS MODEL, WE ARE HAVING CONVERGENCE PROBLEMS.
C **FIND LAGRANGE MULTIPLIER SELECTION
C COMPUTE ROUGHNESS
  WK(1) = 0.0
  IF (IRUF.EQ. 1) THEN
    DO 105 I = 2,NP

```

```

INV02400
INV02410
INV02420
INV02430
INV02440
INV02450
INV02460
INV02470
INV02480
INV02490
INV02500
INV02510
INV02520
INV02530
INV02540
INV02550
INV02560
INV02570
INV02580
INV02590
INV02600
INV02610
INV02620
INV02630
INV02640
INV02650
INV02660
INV02670
INV02680
INV02690
INV02700
INV02710
INV02720
INV02730
INV02740
INV02750
INV02760
INV02770
INV02780
INV02790
INV02800
INV02810
INV02820
INV02830
INV02840
INV02850
INV02860
INV02870
INV02880
INV02890
INV02900
INV02910
INV02920
INV02930
INV02940
INV02950
INV02960
INV02970
INV02980
INV02990

```



```

PD (I) = PM(I)
CVEC(I) = WJTW(I)
10 CONTINUE
CALL QUAD(PD,NPP,NPP,NP,HESS,CVEC)
DO 15 I=1,NP
PM2(I) = PD(I)
C CUT STEP SIZE IF NECESSARY
IF (FRAC.LT. 0.999) THEN
DO 30 I = 1,NP
PM2(I) = PM(I) + FRAC*(PM2(I)-PM(I))
END IF
C CALC. MODEL RESPONSE AND MISFIT
CALL FORMOD(NP,NO,PM2,DM)
DO 40 I = 1,NO
WK(I) = (D(I) - DM(I))/SD(I)
CHI = ANORM(NO,WK)
TOFNU = SQRT(CHI/NO)
RETURN
END
C
SUBROUTINE QUAD(PD,NROWH,NCOLH,N,HESS,CVEC)
IMPLICIT REAL*8 (A-H,O-Z)
PARAMETER (ITMAX=50,MSGLVL=1,NROWA=1,
1 BIGND=1.E+10,LIWORK=60,LWORK=1980,NCLIN=0,NPP=30)
REAL*8 A(1,NPP),BL(NPP),BU(NPP),CVEC(N),FEATOL(NPP),
1 HESS(NROWH,NCOLH),CLAMDA(NPP),WORK(LWORK),IWORK(LIWORK),
2 ISTATE(NPP),PD(N)
LOGICAL COLD,LP,ORTHOG
EXTERNAL QPHESS
DATA NOUT/7/
CALL X04ABF(1,NOUT)
COLD=.TRUE.
LP=.FALSE.
ORTHOG=.FALSE.
NCTOTL=N+NCLIN
DO 10 I=1,N
BL(I)=0.
BU(I)=20.
FEATOL(I)=0.02
10 CONTINUE
BU(1)=0.
BU(N)=0.
IFAIL=0
C QUADRATIC PROGRAMMING
C CALL E04NAF(ITMAX,MSGLVL,N,NCLIN,NCTOTL,NROWA,NROWH,NCOLH,
C 1 BIGND,A,BL,BU,CVEC,FEATOL,HESS,QPHESS,
C 2 COLD,LP,ORTHOG,PD,ISTATE,ITER,DEJ,
C 3 CLAMDA,IWORK,LIWORK,WORK,LWORK,IFAIL)
C CALL VE04A(N,HESS,NROWH,CVEC,BL,BU,PD,Q,IWORK,K,WORK)
IF (IFAIL.GT.0) THEN
WRITE(4,20) IFAIL
STOP
ENDIF
20 FORMAT('E04NAF TERMINATED WITH IFAIL = ',I3)
RETURN
END
SUBROUTINE QPHESS(N,NROWH,NCOLH,JTHCOL,HESS,X,HX)
IMPLICIT REAL*8 (A-H,O-Z)
INTEGER JTHCOL,N,NCOLH,NROWH
REAL*8 HESS(NROWH,NCOLH),HX(N),X(N)

```

```

INV04200
INV04210
INV04220
INV04230
INV04240
INV04250
INV04260
INV04270
INV04280
INV04290
INV04300
INV04310
INV04320
INV04330
INV04340
INV04350
INV04360
INV04370
INV04380
INV04390
INV04400
INV04410
INV04420
INV04430
INV04440
INV04450
INV04460
INV04470
INV04480
INV04490
INV04500
INV04510
INV04520
INV04530
INV04540
INV04550
INV04560
INV04570
INV04580
INV04590
INV04600
INV04610
INV04620
INV04630
INV04640
INV04650
INV04660
INV04670
INV04680
INV04690
INV04700
INV04710
INV04720
INV04730
INV04740
INV04750
INV04760
INV04770
INV04780

```

```

DEL(N,N-1) = 0.
DEL(N,N) = 0.
GOTO 20
END IF
C SQUARE MATRIX A-D COPY BACK INTO DEL IF SECOND DERIV. SMOOTHING REQUIRED
IF (IRUF.EQ.2) THEN
  CALL MULT(NPP,NP,NPP,NP,NP,DEL,DEL,PTP)
  DO 30 I = 1,NP
    DO 30 J = 1,NP
      DEL(J,I) = PTP(J,I)
    END IF
  END IF
C FORM TRANS(DEL).DEL
CALL TRMULT(NPP,NP,NPP,NP,NP,DEL,DEL,PTP)
RETURN
END

C
BLOCKDATA BLOCK
IMPLICIT DOUBLE PRECISION (A-H, O-Z)
PARAMETER (NDD = 40, NPP = 30)
COMMON /RESULT/ PTP(NPP,NPP), WJTWJ(NPP,NPP), WJTWJ(NPP), PM2(NPP),
  * PMU,NFOR,NITER,FRAC,RLAST,IFFTOL
DATA NITER /0/
END

C
C.....
FUNCTION TOFMU(AMU)
C
C FUNCTION TOFMU RETURNED THE RMS MISFIT OF THE RESPONSE OF A MODEL CONSTITUENT
C USING THE GIVEN VALUE OF LAGRANGE MULTIPLIER
C S. CONSTABLE, MARCH 1988, S.I.O., LA JOLLA, CA 92093, U.S.A.
C
C ON INPUT:
C AMU = LAGRANGE MULTIPLIER
C THE MODEL IS ALSO A FUNCTION OF THE ARRAYS PASSED IN COMMON BLOCK /RESULT/
C
C ON OUTPUT
C TOFMU = R.M.S. MISFIT OR 1.0E+10 IF CHOLESKY DECOMPOSITION FAILED
C /MODEL/ CONTAINS THE MODEL WHICH PRODUCES THE MISFIT TOFMU, AS WELL
C AS ITS RESPONSE
C SUBROUTINES USED:
C CHOLIN, CHOLSL ARE R.L. PARKER'S SUBROUTINES TO PERFORM CHOLESKY DECOMPOSITION
C AND THEN SOLVE A LINEAR SYSTEM BY BACK SUBSTITUTION.
C ANORN, FORMOD ARE EXPLAINED IN OCCAM1
C
C IMPLICIT DOUBLE PRECISION (A-H, O-Z)
PARAMETER (NDD = 40, NPP = 30)
COMMON /DATA/ ND,D(NDD),SD(NDD)
COMMON /MODEL/ NP,PM(NPP),DM(NDD),LJMP(NPP)
COMMON /RESULT/ PTP(NPP,NPP),WJTW(NPP,NPP),WJTW(NPP),PM2(NPP),
  * PMU,NFOR,NITER,FRAC,RLAST,IFFTOL
DIMENSION WK(NDD)
REAL*8 PD(NPP),HESS(NPP,NPP),CVEC(NPP)
C
C NFOR = NFOR + 1
C ADD AMU,TRANS(PARTIAL).PARTIAL TO TRANS(W,J).W.J
DO 20 I = 1,NP
  DO 20 J = 1,NP
    HESS(I,J) = AMU*PTP(I,J) + WJTWJ(I,J)
  END DO
  DO 10 I = 1,NP
    INV03600
    INV03610
    INV03620
    INV03630
    INV03640
    INV03650
    INV03660
    INV03670
    INV03680
    INV03690
    INV03700
    INV03710
    INV03720
    INV03730
    INV03740
    INV03750
    INV03760
    INV03770
    INV03780
    INV03790
    INV03800
    INV03810
    INV03820
    INV03830
    INV03840
    INV03850
    INV03860
    INV03870
    INV03880
    INV03890
    INV03900
    INV03910
    INV03920
    INV03930
    INV03940
    INV03950
    INV03960
    INV03970
    INV03980
    INV03990
    INV04000
    INV04010
    INV04020
    INV04030
    INV04040
    INV04050
    INV04060
    INV04070
    INV04080
    INV04090
    INV04100
    INV04110
    INV04120
    INV04130
    INV04140
    INV04150
    INV04160
    INV04170
    INV04180
    INV04190
  END DO
  20

```

```

12 CONTINUE
RETURN
END
C
C
C.....
SUBROUTINE TRMULT(MAD,MA,NAD,NA,NB,A,B,C)
C MULTIPLIES THE TRANSPOSE OF A 2D MATRIX BY ANOTHER MATRIX
C IMPLICIT DOUBLE PRECISION (A-H, O-Z)
C DIMENSION A(MAD,NA),B(MAD,NB),C(NAD,NB)
DO 12 I = 1,NA
DO 12 J = 1,NB
C IJ = 0.0
DO 10 K = 1,MA
C IJ = A(K,I)*B(K,J) + C IJ
C C(I,J) = C IJ
END
END
C
C
C.....
SUBROUTINE MINBRK(AX,BX,CX,FA,FB,FC,FUNC)
C MINBRK BRACKETS A UNIVARIATE MINIMUM OF A FUNCTION. TO BE USED PRIOR
C A UNIVARIATE MINIMISATION ROUTINE.
C
C ON INPUT:
C AX, BX = TWO DISTINCT ESTIMATES OF THE MINIMUM'S WHEREABOUTS
C FUNC = THE FUNCTION IN QUESTION
C ON OUTPUT:
C AX,BX,CX = THREE NEW POINTS WHICH BRACKET THE MINIMUM
C FA,FB,FC = FUNC(AX), FUNC(BX) ETC.
C
C
C IMPLICIT DOUBLE PRECISION (A - H, O - Z)
C PARAMETER (GOLD=1.618034, GLIMIT=100., TINY=1.E-21)
C FA = FUNC(AX)
C FB = FUNC(BX)
C IF (FB GT. FA) THEN
C DUM = AX
C AX = BX
C BX = DUM
C DUM = FB
C FB = FA
C FA = DUM
C ENDIF
C CX = BX + GOLD*(BX - AX)
C FC = FUNC(CX)
C IF (FB GE. FC) THEN
C R = (BX - AX)*(FB - FC)
C Q = (BX - CX)*(FB - FA)
C U = BX - ((BX-CX)*Q - (BX-AX)*R) / (2.*SIGN(MAX(ABS(Q-R),TINY),Q-R))
C ULIM = BX + GLIMIT*(CX - BX)
C IF ((BX - U)*(U - CX).GT.0.) THEN
C FU = FUNC(U)
C IF (FU LT. FC) THEN
C AX = BX
C FA = FB
C BX = U

```

```

      INTEGER I,J
      DO 80 I=1,N
      HX(I) = 0.0
      DO 100 J=1,N
      DO 80 I=1,N
      HX(I) = HX(I) + HESS(I,J) * X(J)
100 CONTINUE
      END
C
C
C
C.....
      FUNCTION ANORM(N,D)
      ANORM = 0.0
      DO 10 I=1,N
      ANORM = ANORM + D(I) * D(I)
10 CONTINUE
      RETURN
      END
C
C
C.....
      SUBROUTINE INITM(MD,M,N,A)
      C ZEROS A 2D MATRIX
      IMPLICIT DOUBLE PRECISION (A-H, O-Z)
      DIMENSION A(MD,N)
      DO 10 I=1,M
      DO 10 J=1,N
      A(I,J) = 0.0
10 RETURN
      END
C
C
C.....
      SUBROUTINE MULT(MAD,MA,NAD,NA,NB,A,B,C)
      C MULTIPLIES TWO 2D MATRICES
      IMPLICIT DOUBLE PRECISION (A-H, O-Z)
      DIMENSION A(MAD,NA), B(NAD,NB), C(MAD,NB)
      DO 12 I=1,MA
      DO 12 J=1,NB
      C(I,J) = 0.0
      DO 10 K=1,NA
      C(I,J) = A(I,K) * B(K,J) + C(I,J)
10 CONTINUE
12 RETURN
      END
C
C
C.....
      SUBROUTINE DIMULT(MAD,MA,NA,DIAG,A,B)
      C MULTIPLIES A 2D MATRIX BY A DIAGONAL MATRIX
      IMPLICIT DOUBLE PRECISION (A-H, O-Z)
      DIMENSION DIAG(MA), A(MAD,NA), B(MAD,NA)
      DO 12 J=1,NA
      DO 11 I=1,MA
      B(I,J) = DIAG(I) * A(I,J)
11 CONTINUE
12

```

```

INV04790
INV04800
INV04810
INV04820
INV04830
INV04840
INV04850
INV04860
INV04870
INV04880
INV04890
INV04900
INV04910
INV04920
INV04930
INV04940
INV04950
INV04960
INV04970
INV04980
INV04990
INV05000
INV05010
INV05020
INV05030
INV05040
INV05050
INV05060
INV05070
INV05080
INV05090
INV05100
INV05110
INV05120
INV05130
INV05140
INV05150
INV05160
INV05170
INV05180
INV05190
INV05200
INV05210
INV05220
INV05230
INV05240
INV05250
INV05260
INV05270
INV05280
INV05290
INV05300
INV05310
INV05320
INV05330
INV05340
INV05350
INV05360
INV05370
INV05380

```

```

V = BX
W = V
X = V
E = 0
FX = FBX
FV = FX
FW = FX
DO 11 ITER = 1, ITMAX
  XM = 0.5*(A + B)
  TOL1 = TOL*ABS(X) + ZEPS
  TOL2 = 2.*TOL1
  IF (ABS(X - XM).LE.(TOL2 - .5*(B - A))) GOTO 3
  IF (ABS(E).GT.TOL1) THEN
    R = (X - W)*(FX - FV)
    Q = (X - V)*(FX - FW)
    P = (X - V)*Q - (X - W)*R
    Q = 2.*(Q - R)
    IF (Q.GT.0.) P = - P
    Q = ABS(Q)
    ETEMP = E
    E = D
    IF (ABS(P).GE.ABS(.5*Q*ETEMP).OR.P.LE.Q*(A - X).OR.
      P.GE.Q*(B - X)) GOTO 1
    D = P/Q
    U = X + D
    IF (U - A.LT.TOL2 .OR. B - U.LT.TOL2) D = SIGN(TOL1,XM - X)
    GOTO 2
  ENDIF
  IF (X.GE.XM) THEN
    E = A - X
  ELSE
    E = B - X
  ENDIF
  D = CGOLD*E
  IF (ABS(D).GE.TOL1) THEN
    U = X + D
  ELSE
    U = X + SIGN(TOL1,D)
  ENDIF
  FU = F(U)
  IF (FU.LE.FX) THEN
    IF (U.GE.X) THEN
      A = X
    ELSE
      B = X
    ENDIF
  V = W
  FV = FW
  W = X
  FW = FX
  X = U
  FX = FU
  ELSE
    IF (U.LT.X) THEN
      A = U
    ELSE
      B = U
    ENDIF
  ENDIF
  IF (FU.IE.FW .OR. W.EQ.X) THEN
    V = W

```

```

INV06590
INV06600
INV06610
INV06620
INV06630
INV06640
INV06650
INV06660
INV06670
INV06680
INV06690
INV06700
INV06710
INV06720
INV06730
INV06740
INV06750
INV06760
INV06770
INV06780
INV06790
INV06800
INV06810
INV06820
INV06830
INV06840
INV06850
INV06860
INV06870
INV06880
INV06890
INV06900
INV06910
INV06920
INV06930
INV06940
INV06950
INV06960
INV06970
INV06980
INV06990
INV07000
INV07010
INV07020
INV07030
INV07040
INV07050
INV07060
INV07070
INV07080
INV07090
INV07100
INV07110
INV07120
INV07130
INV07140
INV07150
INV07160
INV07170
INV07180

```

```

FB = FU
GO TO 1
ELSE IF (FU.GT.FB) THEN
  CX = U
  FC = FU
  GO TO 1
ENDIF
U = CX + GOLD*(CX - BX)
FU = FUNC(U)
ELSE IF ((CX - U)*(U - ULIW).GT.0.) THEN
  FU = FUNC(U)
  IF (FU.LT.FC) THEN
    BX = CX
    CX = U
    U = CX + GOLD*(CX - BX)
    FB = FC
    FC = FU
    FU = FUNC(U)
  ENDIF
ELSE IF ((U - ULIW)*(ULIW - CX).GE.0.) THEN
  U = ULIW
  FU = FUNC(U)
ELSE
  U = CX + GOLD*(CX - BX)
  FU = FUNC(U)
ENDIF
AX = BX
BX = CX
CX = U
FA = FB
FB = FC
FC = FU
GO TO 1
ENDIF
IF (AX.LT.0.) AX=0.
IF (CX.LT.0.) CX=0.
RETURN
END

```

C
 C FUNCTION FMIN(AX,BX,CX,FBX,F,TOL,XMIN)
 C FMIN RETURNS THE MINIMUM VALUE OF A FUNCTION
 C
 C ON INPUT:
 C AX,BX,CX = INDEPENDENT VARIABLE WHICH BRACKET THE MINIMUM
 C FBX = F(BX) (USUALLY AVAILABLE FROM THE BRACKETING PROCEDURE)
 C F = FUNCTION IN QUESTION
 C TOL = FRACTIONAL TOLERANCE REQUIRED IN THE INDEPENDENT VARIABLE
 C ON OUTPUT:
 C XMIN = ABSCISSA OF MINIMUM
 C FMIN = F(XMIN)
 C
 C IMPLICIT DOUBLE PRECISION (A - H, O - Z)
 C PARAMETER (ITMAX=100,CGOLD=.3819660,ZEPS=1.0E - 10)
 C A = MIN(AX,CX)
 C B = MAX(AX,CX)

INV065990
 INV066000
 INV066010
 INV066020
 INV066030
 INV066040
 INV066050
 INV066060
 INV066070
 INV066080
 INV066090
 INV066100
 INV066110
 INV066120
 INV066130
 INV066140
 INV066150
 INV066160
 INV066170
 INV066180
 INV066190
 INV066200
 INV066210
 INV066220
 INV066230
 INV066240
 INV066250
 INV066260
 INV066270
 INV066280
 INV066290
 INV066300
 INV066310
 INV066320
 INV066330
 INV066340
 INV066350
 INV066360
 INV066370
 INV066380
 INV066390
 INV066400
 INV066410
 INV066420
 INV066430
 INV066440
 INV066450
 INV066460
 INV066470
 INV066480
 INV066490
 INV066500
 INV066510
 INV066520
 INV066530
 INV066540
 INV066550
 INV066560
 INV066570
 INV066580

```

CALL CUBDER(NPT+2,XDEL,ZSURF,XDER)
DO 10 I=NXT,1,-1
  IF (I.GE.NE.OR.I.LT.NST) THEN
    ZSURF(I)=0.0
    XDER(I)=0.
    AMPDER(I)=1.
    GOTO 10
  ENDIF
  ZSURF(I)=ZSURF(I-NST+1)
  XDER(I)=XDER(I-NST+1)
  AMPDER(I)=SQRT(1.0+XDER(I)*XDER(I))
CONTINUE
10 WRITE(4,60) (ZSURF(I),I=1,NXT)
C WRITE(4,60) (XDER(I),I=1,NXT)
C WRITE(4,70) (AMPDER(I),I=1,NXT)
50 FORMAT(4X,'ZSURF',/,4X,(10F7.3))
60 FORMAT(4X,'XDER',/,4X,(10F7.3))
70 FORMAT(4X,'AMPDER',/,4X,(10F7.3))
RETURN
END

C
C SUBROUTINE HNPRIM(K,KS,ZSURF,XDER,AMPDER,XSYS,ZSYS,NTR)
C
C COMPUTE THE NORMAL COMPONENT OF THE MAGNETIC FIELD
C
C IMPLICIT DOUBLE PRECISION (A-H, O-Z)
C
C PARAMETER (PI=3.1415926)
C
C DIMENSION ZSURF(1),XDER(1),AMPDER(1),XSYS(1),ZSYS(1)
C
C DIMENSION HPN(120,20)
C
C COMMON /KY/ AKY(20)/HN/HPN
C
C COMMON KYE,NSYS,NST,XDEL,TRDIS
C
C PI2=PI*2.
C
C DO 10 J=KS,NTR+KS-1
C   M=J-KS+1
C   XD=(J-1)*XDEL-XSYS(K)+TRDIS/2.
C   ZD=ZSURF(J)-ZSYS(K)
C   RHO=SQRT(XD*XD+ZD*ZD)
C   D=RHO*RHO*AMPDER(J)*PI2
C   IF (D.EQ.0.) PAUSE 'BAD HPN'
C   IF (NSYS.EQ.1) THEN
C     GEOM1=(-XDER(J)*XD+ZD)*XD/D
C     GEOM2=(-(XD*XD+ZD*ZD)*XDER(J)+2.0*(XD*ZD))/D
C   ELSE
C     GEOM1=(-XDER(J)*XD+ZD)*ZD/D
C     GEOM2=((ZD*ZD+XD*XD)-XDER(J)*2.0*(XD*ZD))/D
C   ENDIF
C   DO 20 I=1,KYE
C     WK=AKY(I)*PI2
C     RKY=RHO*WK
C     IF (I.GT.1) THEN
C       HPN(M,I)=(GEOM1*WK+BESSK0(RKY)+GEOM2*BESSK1(RKY)
C         /RHO)*WK
C     ELSE
C       HPN(M,I)=GEOM2/(RHO*RHO)
C     ENDIF
C   CONTINUE
C   CONTINUE
C   WRITE(4,30) (HPN(J,I),J=1,NTR)
C   FORMAT(4X,'HPN',/,5(1PE12.4))
30

```

INV07790
 INV07800
 INV07810
 INV07820
 INV07830
 INV07840
 INV07850
 INV07860
 INV07870
 INV07880
 INV07890
 INV07900
 INV07910
 INV07920
 INV07930
 INV07940
 INV07950
 INV07960
 INV07970
 INV07980
 INV07990
 INV08000
 INV08010
 INV08020
 INV08030
 INV08040
 INV08050
 INV08060
 INV08070
 INV08080
 INV08090
 INV08100
 INV08110
 INV08120
 INV08130
 INV08140
 INV08150
 INV08160
 INV08170
 INV08180
 INV08190
 INV08200
 INV08210
 INV08220
 INV08230
 INV08240
 INV08250
 INV08260
 INV08270
 INV08280
 INV08290
 INV08300
 INV08310
 INV08320
 INV08330
 INV08340
 INV08350
 INV08360
 INV08370
 INV08380

```

      FV = FW
      W = U
      FW = FU
      ELSE IF (FU.LE.FV .OR. V.EQ.X .OR. V.EQ.W) THEN
        V = U
        FV = FU
      ENDIF
      ENDIF
11      CONTINUE
3      WRITE(*,*) 'MAXIMUM ITERATIONS EXCEEDED IN FMIN'
      XMIN = X
      FMIN = FX
      RETURN
      END
C
C
C
C.....
      SUBROUTINE FORMOD(NPT,NRESP,ZH1,CALC)
C
C      ...PURPOSE...
C      COMPUTE THE AEM SYSTEM RESPONSE OVER A 2-D ICE-WATER PROFILE
C
      IMPLICIT DOUBLE PRECISION (A-H, O-Z)
      PARAMETER (NDD=40,NPP=30,NXT=200,NTRUNK=100,NLOOP=8)
      DIMENSION ZSURF(NXT),XDER(NXT),AMPDER(NXT),HPN(120,20)
      DIMENSION AKERN(120,120,20),CHAR(120,20)
      DIMENSION XSYS(NDD),ZSYS(NDD),ZH1(NPP),CALC(NDD)
      COMMON /KY/ AKY(20)/KER/ AKERN/CH/ CHAR/HPN/HPN
      COMMON /FCM/ ZSURF, XSYS, ZSYS, AMPDER, NM, IREC, AKDEL
      COMMON KYE, NSYS, NST, XDEL, TRDIS
      DO 1 I=1,NPT
1      ZSURF(I)=ZH1(I)
      CALL SURF(NST,NPT,NXT,XDEL,ZSURF,XDER,AMPDER)
      K=1
1001 CONTINUE
      KS=(XSYS(K)-TRDIS/2.)/XDEL*2-NTRUNK/2
      IF (KS.LE.0 .OR. KS.GE.NXT-NTRUNK/2) PAUSE 'BAD INPUT XSYS'
      CALL HNPRIM(K,KS,ZSURF,XDER,AMPDER,XSYS,ZSYS,NTRUNK)
      CALL KERNEL(K,KS-1,KS1,ZSURF,XDER,AMPDER,NTRUNK)
      CALL CHARGE(NTRUNK,KYE,XDEL,NLOOP)
      CALL FIELD(K,KS,NM,AKDEL,HXS,HZS,XSYS,ZSYS,ZSURF,AMPDER,NTRUNK)
      IF (IREC.EQ.1) CALC(K)=HXS
      IF (IREC.EQ.2) CALC(K)=HZS
      K=K+1
      KS1=KS
      IF (K.LE.NRESP) GOTO 1001
      RETURN
      END
C
C
C
      SUBROUTINE SURF(NST,NPT,NXT,XDEL,ZSURF,XDER,AMPDER)
C
C      GENERATE THE INFORMATION OF THE ICE-WATER INTERFACE, I.E.,
C      ZSURF, XDER, AMPDER
C
C      IMPLICIT DOUBLE PRECISION (A-H, O-Z)
      DIMENSION ZSURF(NXT),XDER(NXT),AMPDER(NXT)
      NE = NST+NPT

```

INV07190
 INV07200
 INV07210
 INV07220
 INV07230
 INV07240
 INV07250
 INV07260
 INV07270
 INV07280
 INV07290
 INV07300
 INV07310
 INV07320
 INV07330
 INV07340
 INV07350
 INV07360
 INV07370
 INV07380
 INV07390
 INV07400
 INV07410
 INV07420
 INV07430
 INV07440
 INV07450
 INV07460
 INV07470
 INV07480
 INV07490
 INV07500
 INV07510
 INV07520
 INV07530
 INV07540
 INV07550
 INV07560
 INV07570
 INV07580
 INV07590
 INV07600
 INV07610
 INV07620
 INV07630
 INV07640
 INV07650
 INV07660
 INV07670
 INV07680
 INV07690
 INV07700
 INV07710
 INV07720
 INV07730
 INV07740
 INV07750
 INV07760
 INV07770
 INV07780


```

WK=AKY(I)*PI2
IF (I.EQ.1) THEN
    GEOM/RHO
ELSE
    AKERN(J,L,I)=      GEOM*WK*BESSK1(RHO*WK)
ENDIF
CONTINUE
60 CONTINUE
DO 80 J=KE2+1,NTR
DO 80 L=1,NTR
IF (J.EQ.L) GOTO 80
XD=(J-L)*XDEL
ZD=ZSURF(J*KS)-ZSURF(L*KS)
RHO=SQR(XD*XD+ZD*ZD)
GEOM=2.*(AMPDER(L*KS)/AMPDER(J*KS))*( XD*XDER(J*KS)-ZD)/RHO
DO 70 I=1,KYE
WK=AKY(I)*PI2
IF (I.EQ.1) THEN
    GEOM/RHO
ELSE
    AKERN(J,L,I)=      GEOM*WK*BESSK1(RHO*WK)
ENDIF
CONTINUE
70 CONTINUE
80 CONTINUE
WRITE(4,90)( AKERN(40,I),I
          ,I=1,KYE)
FORMAT(4X,'KERNEL',/, (5(1PE12.4)))
RETURN
END
C
C
SUBROUTINE CHARGE(NTR,KYE,XDEL,NLOOP)
C
C COMPUTE THE CHARGE DISTRIBUTION ON THE SURFACE OF
C THE SEA WATER
C
C IMPLICIT DOUBLE PRECISION (A-H,O-Z)
DIMENSION CHAR(120,20),HPN(120,20),AKERN(120,120,20),W1(120)
DIMENSION W2(120)
COMMON /KER/AKERN/HN/HPN/CH/CHAR
FAC=1./((2*3.1415928)
I=1
KK=0
1001 CONTINUE
DO 10 J=1,NTR
W1(J)=HPN(J,I)*FAC
CONTINUE
999 DO 20 J=1,NTR
SUM=0.0
DO 30 L=1,NTR
SUM=SUM+W1(L)*AKERN(J,L,I)
CONTINUE
30 SUM=SUM*FAC*(-SUM*XDEL+HPN(J,I))
CONTINUE
20 DO 40 J=1,NTR
W1(J)=W2(J)
40 KK=KK+1
IF(KK.LT.NLOOP) GOTO 999
DO 50 J=1,NTR
CHAR(J,I)=W1(J)
50 I=I+1

```

```

RETURN
END

C
C
SUBROUTINE KERNEL(K,KS,KS1,ZSURF,XDER,AMPDER,NTR)
C
C.....
C COMPUTE THE KERNEL IN THE INTEGRAL EQUATION
C AND SAVE IT
C
C.....
C IMPLICIT DOUBLE PRECISION (A-H, O-Z)
C PARAMETER (PI=3.1416926)
C DIMENSION ZSURF(1),XDER(1),AMPDER(1)
C DIMENSION AKERN(120,120,20)
C COMMON /KER/AKERN/KY/AKY(20)
C COMMON KYE,NSYS,NST,XDEL,TRDIS
C PI2=PI*2.
C DO 1 J=1,NTR
C   DO 1 I=1,KYE
C     AKERN(J,J,I)=0.0
C     CONTINUE
C   IF(K.GT.1) GOTO 30
C   C COMPUTE THE AKERNEL
C   1001 CONTINUE
C   DO 20 J=1,NTR
C     DO 20 L=1,NTR
C       IF(J.EQ.L) GOTO 20
C       XD=(J-L)*XDEL
C       ZD=ZSURF(J+KS)-ZSURF(L+KS)
C       RHO=SQR(XD*XD+ZD*ZD)
C       GEOM=2.*(AMPDER(L+KS)/AMPDER(J+KS))*(XD*XDER(J+KS)-ZD)/RHO
C       DO 10 I=1,KYE
C         WK=AKY(I)*PI2
C         IF(I.EQ.1) THEN
C           GEOM/RHO
C           AKERN(J,L,I)=
C             ELSE
C               FNOIF
C             AKERN(J,L,I)= GEOM*WK*BESSKI(RHO*WK)
C           CONTINUE
C         CONTINUE
C       RETURN
C     C
C     C
C   C COMPUTE THE UNKNOWN PART OF THE KERNEL
C   CONTINUE
C   M=KS-KS1+1
C   KE2=NTR-M
C   IF(M.LE.0) PAUSE 'BAD INPUT XSYS'
C   IF(M.GE.NTR) GOTO 1001
C   DO 40 J=1,KE2
C     DO 40 L=1,KE2
C       DO 40 I=1,KYE
C         AKERN(J,L,I)=AKERN(J+M,L+M,I)
C       CONTINUE
C     DO 60 J=1,KE2
C       DO 60 L=KE2+1,NTR
C         XD=(J-L)*XDEL
C         ZD=ZSURF(J+KS)-ZSURF(L+KS)
C         RHO=SQR(XD*XD+ZD*ZD)
C         GEOM=2.*(AMPDER(L+KS)/AMPDER(J+KS))*(XD*XDER(J+KS)-ZD)/RHO
C         DO 50 I=1,KYE

```

```

C
C
SUBROUTINE CUBDER(N,XDEL,YA,YD)
.....
C      COMPUTE THE DERIVATIVES AT EACH NODE USING
C      CUBIC SPLINE.
C      NOTE: N=NPT+2 . ONE POINT ADDED TO EACH END.
.....
C
C
IMPLICIT DOUBLE PRECISION (A-H, O-Z)
DIMENSION XA(50),YA(N),Y2(50),YD(N)
DO 11 I=1,N
    XA(I)=(I-1)*XDEL
DO 12 I=N-1,2,-1
    YA(I)=YA(I-1)
    YD(I)=0.
    YD(N)=0.
CALL SPLINE(XA,YA,N,0.,0.,Y2)
DO 10 I=2,N-1
    XX=X A(I)
    KLO=I
    KHI=I+1
    H=X A(KHI)-X A(KLO)
    A=(X A(KHI)-XX)/H
    B=(XX-X A(KLO))/H
    XD=X A(KHI)-X A(KLO)
    YD(I-1)=(Y A(KHI)-Y A(KLO))/XD-XD*((3.*A-A-1.)*Y2(KLO)
        +
            - (3.*B-B-1.)*Y2(KHI))/6.
10 CONTINUE
DO 14 I=1,N-2
    YA(I)=YA(I+1)
14 RETURN
END
C
C
SUBROUTINE CUBSPL(KYE,NK1,AKDEL,AKY,YA,0)
.....
C      CUBIC SPLINE INTERPOLATION BEFORE TAKING THE
C      INVERSE FOURIER TRANSFORM.
.....
C
C
IMPLICIT DOUBLE PRECISION (A-H, O-Z)
DIMENSION AKY(KYE), 0(NK1),YA(KYE),Y2(20)
CALL SPLINE(AKY,YA ,KYE,1.E30,1.E30,Y2)
O(1)=YA(1)
DO 10 I=2,NK1
    XX=(I-1)*AKDEL
    KLO=1
    KHI=KYE
    IF (KHI-KLO.GT.1) THEN
        K=(KHI+KLO)/2
        IF (AKY(K).GT.XX) THEN
            KHI=K
        ELSE
            KLO=K
        ENDIF
GOTO 1
ENDIF
H=AKY(KHI)-AKY(KLO)

```

```

C 22 IF (I.LE.KYE) GOTO 1001
WRITE(4,22) (CHAR(J,1),J=1,NTR)
FORMAT(4X,'CHARGE',/, (5E14.4))
RETURN
END
C
C
C
C
C SUBROUTINE FIELD(K,KS,NM,AKDEL,HXS,HZS,XSYS,ZSYS,ZSURF,AMPDER,NTR)
C .....
C COMPUTE THE SECONDARY MAGNETIC FIELD, BOTH
C X AND Z COMPONENTS, EXPRESSED IN PPM OF THE
C RECEIVED PRIMARY FIELD.
C .....
C
C IMPLICIT DOUBLE PRECISION (A-H, O-Z)
C PARAMETER (PI=3.1415926)
C DIMENSION AMPDER(1),CHAR(120,20),ZSURF(1),XSYS(1),ZSYS(1),AA(513)
C DIMENSION TEMP1(20),TEMP2(20)
C COMMON /CH/CHAR/KY/ARY(20)
C COMMON KYE,NSYS,NST,XDEL,TRDIS
C R = TRDIS
C XF=R/2.
C IF (NSYS.EQ.1) THEN
C   HNORM=1./ (2.*PI*R**3)
C ELSE
C   HNORM=-1./ (4.*PI*R**3)
C ENDIF
C DO 10 I=1,KYE
C   WK=ARY(I)*PI*2.
C   AZ=0.0
C   AX=0.0
C   DO 20 J=KS,NTR+KS-2
C     M=J-KS+1
C     RHO=SQRT((XSYS(K)-(J-1)*XDEL*XF)**2+(ZSYS(K)-ZSURF(J))**2)
C     IF (1.GT.1) THEN
C       AXZ=2.0*CHAR(M,I)*AMPDER(J)*WK*BESSK1(RHO*WK)/RHO
C     ELSE
C       AXZ=2.0*CHAR(M,I)*AMPDER(J)/(RHO*RHO)
C     ENDIF
C     AZ=(ZSYS(K)-ZSURF(J))*AXZ*AZ
C     AX=(XSYS(K)-(J-1)*XDEL*XF)*AXZ*AX
C 20 CONTINUE
C   TEMP1(I)=AZ*XDEL
C   TEMP2(I)=AX*XDEL
C 10 CONTINUE
C   NK=2**N'I
C   IF (NK*AK.LEL.GT.ARY(KYE)) PAUSE 'BAD AKDEL OR ARY'
C   CALL CUB.PL(KYE,NK,AKDEL,ARY,TEMP1,AA)
C   SUM=0.0
C   DO 11 I=2,NK
C     SUM=SUM+AA(I)
C 11 HZS=(SUM*AA(1)/2.)*AKDEL*2.
C   CALL CUB.PL(KYE,NK,AKDEL,ARY,TEMP2,AA)
C   SUM=0.0
C   DO 12 I=2,NK
C     SUM=SUM+AA(I)
C 12 HXS=(SUM*AA(1)/2.)*AKDEL*2.
C   HXS=HXS/HNORM*1000000
C   HZS=HZS/HNORM*1000000

```

INV09590
 INV09600
 INV09610
 INV09620
 INV09630
 INV09640
 INV09650
 INV09660
 INV09670
 INV09680
 INV09690
 INV09700
 INV09710
 INV09720
 INV09730
 INV09740
 INV09750
 INV09760
 INV09770
 INV09780
 INV09790
 INV09800
 INV09810
 INV09820
 INV09830
 INV09840
 INV09850
 INV09860
 INV09870
 INV09880
 INV09890
 INV09900
 INV09910
 INV09920
 INV09930
 INV09940
 INV09950
 INV09960
 INV09970
 INV09980
 INV09990
 INV10000
 INV10010
 INV10020
 INV10030
 INV10040
 INV10050
 INV10060
 INV10070
 INV10080
 INV10090
 INV10100
 INV10110
 INV10120
 INV10130
 INV10140
 INV10150
 INV10160
 INV10170
 INV10180

```

if (abs(x) .lt. 3.75) then
  y=(x/3.75)**2
  BESS10=p1+y*(p2+y*(p3+y*(p4+y*(p5+y*(p6+y*p7))))
else
  ax=abs(x)
  y=3.75/ax
  BESS10=(exp(ax)/sqrt(ax))*(q1+y*(q2+y*(q3+y*(q4+y*(q5+
    + y*(q6+y*(q7+y*(q8+y*q9)))))))
endif
return
end

C
C      Function BESSK0(x)
C      ..... Returns the modified Bessel function K0(x) for positive x.
C      .....
C      IMPLICIT DOUBLE PRECISION (A-H, O-Z)
C      real*8 y,p1,p2,p3,p4,p5,p6,p7,q1,q2,q3,q4,q5,q6,q7
C      data p1,p2,p3,p4,p5,p6,p7/-0.67721566d0,0.42278420d0,0.23089756d0,
C      + 0.348859d-1,0.262098d-2,0.10760d-3,0.74d-6/
C      data q1,q2,q3,q4,q5,q6,q7/1.25331414d0,-0.7832358d-1,0.2189588d-1,
C      + -0.1052448d-1,0.687872d-2,-0.261540d-2,0.53208d-3/
C      if (x.le.2.0) then
C        y=x*x/4.0
C      BESSK0=(-log(x/2.0)*BESS10(x))+ (p1+y*(p2+y*(p3+
C      + y*(p4+y*(p5+y*(p6+y*p7))))))
C      else
C        if (x.gt.40.) then
C          BESSK0=0.0
C        else
C          y=(2.0/x)
C          BESSK0=(exp(-x)/sqrt(x))*(q1+y*(q2+y*(q3+y*(q4+y*(q5+
C      + y*(q6+y*(q7+y*(q8+y*q9))))))
C        endif
C      endif
C      return
C      end

C
C      Function BESS11(x)
C      ..... Returns the modified Bessel function I1(x) for any real x.
C      .....
C      IMPLICIT DOUBLE PRECISION (A-H, O-Z)
C      real*8 y,p1,p2,p3,p4,p5,p6,p7,q1,q2,q3,q4,q5,q6,q7,q8,q9
C      data p1,p2,p3,p4,p5,p6,p7/0.5d0,0.87890594d0,0.51498869d0,
C      + 0.15084934d0,0.2658733d-1,0.301532d-2,0.32411d-3/
C      data q1,q2,q3,q4,q5,q6,q7,q8,q9/0.39894228d0,-0.3989024d-1,
C      + -0.362018d-2,0.163801d-2,-0.1031555d-1,0.2282967d-1,
C      + -0.289631d-1,0.1787864d-1,-0.420069d-2/
C      if (abs(x) .lt. 3.75) then
C        y=(x/3.75)**2
C        BESS11=x*(p1+y*(p2+y*(p3+y*(p4+y*(p5+y*(p6+y*p7))))))
C      else
C        ax=abs(x)
C        y=3.75/ax
C        BESS11=(exp(ax)/sqrt(ax))*(q1+y*(q2+y*(q3+y*(q4+y*(q5+
C      + y*(q6+y*(q7+y*(q8+y*q9))))))
C      endif

```

INV11390
 INV11400
 INV11410
 INV11420
 INV11430
 INV11440
 INV11450
 INV11460
 INV11470
 INV11480
 INV11490
 INV11500
 INV11510
 INV11520
 INV11530
 INV11540
 INV11550
 INV11560
 INV11570
 INV11580
 INV11590
 INV11600
 INV11610
 INV11620
 INV11630
 INV11640
 INV11650
 INV11660
 INV11670
 INV11680
 INV11690
 INV11700
 INV11710
 INV11720
 INV11730
 INV11740
 INV11750
 INV11760
 INV11770
 INV11780
 INV11790
 INV11800
 INV11810
 INV11820
 INV11830
 INV11840
 INV11850
 INV11860
 INV11870
 INV11880
 INV11890
 INV11900
 INV11910
 INV11920
 INV11930
 INV11940
 INV11950
 INV11960
 INV11970
 INV11980

```

      A=(AKY(KHI)-XX)/H
      B=(XX-AKY(KLO))/H
      O(I)=A*YA(KLO)+B*YA(KHI)+(A*(A-A-1.)*Y2(KLO)+
      B*(B-B-1.)*Y2(KHI))*(H*H)/6.
*
10  CONTINUE
    RETURN
    END
C
C      SUBROUTINE SPLINE(X,Y,N,YP1,YPN,Y2)
C
C      .....
C      GIVEN ARRAYS X AND Y OF LENGTH N CONTAINING A TABULATED FUNCTION,
C      I.E., YJ=F(XJ), WITH X1<X2<X3<...<XN, THIS ROUTINE RETURNS AN ARRAY
C      Y2 OF LENGTH N WHICH CONTAINS THE SECOND DERIVATIVES OF THE INTER-
C      POLATING FUNCTION AT THE TABULATED POINTS XJ. NATURAL SPLINE FROM
C      NUMERICAL RECIPES, PRESS AT AL.
C      .....
C
C      IMPLICIT DOUBLE PRECISION (A-H, O-Z)
C      PARAMETER (NMAX=1024)
C      DIMENSION X(N),Y(N),Y2(N),U(NMAX)
C      IF (YP1.GT..99E30) THEN
C        Y2(1)=0.
C        U(1)=0.
C      ELSE
C        Y2(1)=-0.5
C        U(1)=(3./(X(2)-X(1)))*((Y(2)-Y(1))/(X(2)-X(1))-YP1)
C      ENCF
C      DO 11 I=2,N-1
C        SIG=(X(I)-X(I-1))/(X(I+1)-X(I-1))
C        F=SIG*Y2(I-1)+2.
C        Y2(I)=(SIG-1.)/P
C        U(I)=(0.*(Y(I+1)-Y(I))/(X(I+1)-X(I))-Y(I)-Y(I-1))
C          /((X(I)-X(I-1))/(X(I+1)-X(I-1))-SIG*U(I-1))/P
C      *
11  CONTINUE
    IF (YPN.GT..99E30) THEN
      UN=0.
      UN=0.
    ELSE
      QN=0.5
      UN=(3./(X(N)-X(N-1)))*(YPN-(Y(N)-Y(N-1))/(X(N)-X(N-1)))
    ENDF
    Y2(N)=(UN-QN*U(N-1))/(QN*Y2(N-1)+1.)
    DO 12 K=N-1,1,-1
      Y2(K)=Y2(K)*Y2(K+1)+U(K)
    CONTINUE
    RETURN
    END
C
C      Function BESSIO(x)
C
C      .....
C      RETURNS THE MODIFIED BESSEL FUNCTION I0(X) FOR ANY REAL X.
C      .....
C
C      IMPLICIT DOUBLE PRECISION (A-H, O-Z)
C      real*8 y,p1,p2,p3,p4,p5,p6,p7,q1,q2,q3,q4,q5,q6,q7,q8,q9
C      data p1,p2,p3,p4,p5,p6,p7/1.0d0,3.5156229d0,3.0899424d0,
C      + 1.2067492d0,0.2659732d0,0.360788d-1,0.45813d-2/
C      data q1,q2,q3,q4,q5,q6,q7,q8,q9/0.39894228d0,0.1328592d-1,
C      + 0.225319d-2,-0.167565d-2,0.916281d-2,-0.205770d-1,
C      + 0.2836637d-1,-0.1647633d-1,0.392377d-2/

```

INV10790

INV10800

INV10810

INV10820

INV10830

INV10840

INV10850

INV10860

INV10870

INV10880

INV10890

INV10900

INV10910

INV10920

INV10930

INV10940

INV10950

INV10960

INV10970

INV10980

INV10990

INV11000

INV11010

INV11020

INV11030

INV11040

INV11050

INV11060

INV11070

INV11080

INV11090

INV11100

INV11110

INV11120

INV11130

INV11140

INV11150

INV11160

INV11170

INV11180

INV11190

INV11200

INV11210

INV11220

INV11230

INV11240

INV11250

INV11260

INV11270

INV11280

INV11290

INV11300

INV11310

INV11320

INV11330

INV11340

INV11350

INV11360

INV11370

INV11380

```

IOUT=0
DEL=0.
DO 21 I=K1,N
  LI=LT(I)
  IF (X(LI).EQ.BL(LI).AND.G(I).GE.0.)GOTO21
  IF (X(LI).EQ.BU(LI).AND.G(I).LE.0.)GOTO21
  IF (G(I).LT.0.)GOTO22
  Z=X(LI)-BL(LI)
  J=1
GOTO23
22 CONTINUE
  Z=BU(LI)-X(LI)
  J=0
23 CONTINUE
  IF (G(ICAC+I).LE.0.)GOTO24
  BETA=ABS(G(I))/G(ICAC+I)
  YF(BETA.GE.Z)GOTO24
  Z=BETA
  D=.5*Z*ABS(G(I))
  J=-1
GOTO26
24 CONTINUE
  D=Z*(ABS(G(I))-5*Z*(ICAC+I))
26 CONTINUE
  IF (D.LT.DEL)GOTO21
  DEL=D
  ALPHA=Z
  IOUT=I
  IIN=I
  IF (J.LT.0)IIN=0
  LB=J
21 CONTINUE
27 CONTINUE
  IF (IOUT.NE.0)GOTO29
  Q=0.
  DO 28 I=1,N
    LI=LT(I)
    Q=Q+X(LI)*(G(I)-B(LI))
  Q=.5*Q
  RETURN
29 CONTINUE
  SIG=1.
  IF (G(IOUT).GT.0.)SIG=-1.
  LIOUT=LT(IOUT)
  LIIN=LIOUT
26 CONTINUE
  SAS=G(ICAC+IOUT)
  IF (K.EQ.0)GOTO31
  DO 30 I=1,K
    G(IIS+I)=G(ID+I)*A(IOUT,I)
31 CONTINUE
  DO 37 I=K1,N
    LI=LT(I)
    IF (LI-LIOUT)32,37,33
32 Z=A(LI,LIOUT)
    GOTO34
33 Z=A(LIOUT,LI)
34 CONTINUE
    IF (K.EQ.0)GOTO36
    DO 36 J=1,K

```

```

INV12690
INV12600
INV12610
INV12620
INV12630
INV12640
INV12650
INV12660
INV12670
INV12680
INV12690
INV12700
INV12710
INV12720
INV12730
INV12740
INV12750
INV12760
INV12770
INV12780
INV12790
INV12800
INV12810
INV12820
INV12830
INV12840
INV12850
INV12860
INV12870
INV12880
INV12890
INV12900
INV12910
INV12920
INV12930
INV12940
INV12950
INV12960
INV12970
INV12980
INV12990
INV13000
INV13010
INV13020
INV13030
INV13040
INV13050
INV13060
INV13070
INV13080
INV13090
INV13100
INV13110
INV13120
INV13130
INV13140
INV13150
INV13160
INV13170
INV13180

```

```

return
end

C
C
Function BESSK1(x)
C
C .. Returns the modified Bessel function K1(x) for positive x.
C
IMPLICIT DOUBLE PRECISION (A-H, O-Z)
real*8 y,p1,p2,p3,p4,p5,p6,p7,q1,q2,q3,q4,q5,q6,q7
data p1,p2,p3,p4,p5,p6,p7/1.d0,0,16443144d0,-0.67278679d0,
+ -0.18168897d0,-0.1919407d-1,-0.110404d-2,-0.4088d-4/
data q1,q2,q3,q4,q5,q6,q7/1.,6331414d0,0.23498619d0,-0.3656620d-1,
+ 0.1604268d-1,-0.780353d-2,0.32614d-2,-0.68245d-3/
if (x.le.2.0) then
y=x*x/4.0
BESSK1= (log(x/2.0)*BESSI1(x)+(1.0/x)*(p1+y*(p2+y*(p3+
+ y*(p4+y*(p5+y*(p6+y*p7))))))
else
if (.gt.40) then
BESSK1=0.0
else
y=(2.0/x)
BESSK1=(exp(-x)/sqrt(x))*(q1+y*(q2+y*(q3+y*(q4+y*(q5+
+ y*(q6+y*q7))))))
endif
endif
return
end
SUBROUTINE VE04A(N,A,IA,B,BL,BU,X,Q,LT,K,G)
IMPLICIT REAL*8 (A-H,O-Z)

C
C QUADRATIC PROGRAMMING FROM HARWELL LIBRARY.
C SIMPLE BOUND CONSTRAINTS.
C
DIMENSION A(IA,1),B(1),BL(1),BU(1),X(1),LT(1),G(1)
IS=N
IAS=N
IV=N
ICAC=N+N
ID=ICAC
DO 9 I=1,N
9 G(I)=-B(I)
DO 10 I=1,N
10 X(I)=0.
LT(I)=I
G(ICAC-I)=A(I,I)
IF (0..GE.BL(I).AND.0..LE.BU(I)) GO TO 10
IF (0..LT.BL(I)) X(I)=BL(I)
IF (0..GT.BU(I)) X(I)=BU(I)
DO 12 J=1,I
12 G(J)=G(J)+A(J,I)*X(I)
IF (I.EQ.N) GO TO 10
II=I+1
DO 11 J=II,N
11 G(J)=G(J)+A(I,J)*X(I)
10 CONTINUE
K=0
K1=1
20 CONTINUE

```



```

VD=V/G(ID,I1)
S1=S0*V*VD
R=S1/S0
G(ID,I1)=G(ID,I1)*R
BETA=VD/S1
IF(R.GT.4.)GOTO841
DO 81 J=I2,N
81 G(IV,J)=G(IV,J)-V*A(J,I1)
IF(I1.GT.K2)GOTO83
DO 82 J=I1,K2
J1=J+1
82 A(J,I1)=A(J1,I1)+BETA*G(IV,J1)
83 CONTINUE
A(K,I)=BETA
DO 84 J=K1,N
84 A(J,I)=A(J,I1)+BETA*G(IV,J)
GOTO849
841 CONTINUE
IF(I1.GT.K2)GOTO843
DO 842 J=I1,K2
J1=J+1
842 A(J,I1)=BETA*G(IV,J1)+A(J1,I1)/R
843 CONTINUE
A(K,I)=BETA
DO 844 J=K1,N
844 A(J,I1)=BETA*G(IV,J)+A(J,I1)/R
DO 845 J=I2,N
845 G(IV,J)=G(IV,J)-V*A(J,I1)
849 CONTINUE
LT(I)=LT(I1)
S0=S1
I1=I2
I2=I2+1
SG=1./S1
LT(K)=LIIN
G(ID,K)=SG
IF(IIN.EQ.1)GOTO361
II=IIN-1
DO 862 I=1,II
Z=A(IIN,I)
DO 863 J=IIN,K2
863 A(J,I)=A(J+1,I)
862 A(K,I)=Z
861 CONTINUE
86 CONTINUE
DO 87 I=K1,N
87 G(ICAC,I)=G(ICAC,I)+SG*G(IV,I)**2
K1=K
K=K2
IIN=0
ALPHA=1E75
SAS=G(ICAC,IOUT)
IF(SAS.GT.0.)ALPHA=ABS(G(IOUT))/SAS
IF(G(IOUT).LT.0.)GOTO898
J=1
Z=X(LIOUT)-BL(LIOUT)
GOTO899
898 CONTINUE
J=0
Z=BU(LIOUT)-X(LIOUT)

```

```

INV13790
INV13800
INV13810
INV13820
INV13830
INV13840
INV13850
INV13860
INV13870
INV13880
INV13890
INV13900
INV13910
INV13920
INV13930
INV13940
INV13950
INV13960
INV13970
INV13980
INV13990
INV14000
INV14010
INV14020
INV14030
INV14040
INV14050
INV14060
INV14070
INV14080
INV14090
INV14100
INV14110
INV14120
INV14130
INV14140
INV14150
INV14160
INV14170
INV14180
INV14190
INV14200
INV14210
INV14220
INV14230
INV14240
INV14250
INV14260
INV14270
INV14280
INV14290
INV14300
INV14310
INV14320
INV14330
INV14340
INV14350
INV14360
INV14370
INV14380

```

```

35 Z=Z-A(I,J)*G(IS*J)
36 G(IS*I)=Z
37 CONTINUE
   G(IS*IOUT)=SAS
   IF (K.EQ.0)GOTO42
   G(IS*K)=-A(IOUT,K)
   IF (K.EQ.1)GOTO42
   I=K
   DO 41 I1=2,K
   I=I-1
   Z=-A(IOUT,I)
   I1=I+1
   DO 40 J=I1,K
40 Z=Z-G(IS*J)*A(J,I)
41 G(IS*I)=Z
42 CONTINUE
   IF (SIG.EQ.1.)GOTO61
   DO 60 I1=1,N
60 G(IS*I)=-G(IS*I)
61 CONTINUE
   IF (K.EQ.0)GOTO62
   DO 61 I1=1,K
   IF (G(IS*I).EQ.0.)GOTO61
   LI=LI(I)
   J=1
   Z=BL(LI)-X(LI)
   IF (G(IS*I).LT.0.)GOTO60
   J=0
   Z=BU(LI)-X(LI)
90 CONTINUE
   Z=Z/G(IS*I)
   IF (Z.GE.ALPHA)GOTO61
   ALPHA=Z
   LB=J
   LIIN=I
   LIIN=LI
61 CONTINUE
62 CONTINUE
   X(LIOUT)=X(LIOUT)+SIG*ALPHA
   IF (K.EQ.0)GOTO71
   DO 70 I1=1,K
   LI=LI(I)
70 X(LI)=X(LI)+ALPHA*G(IS*I)
71 CONTINUE
   DO 72 I=K1,N
72 G(I)=G(I)+ALPHA*G(IAS*I)
   IF (IIN.EQ.0)GOTO90
   X(LIIN)=BL(LIIN)
   IF (LB.EQ.0)X(LIIN)=BU(LIIN)
   IF (IIN.EQ.IOUT)GOTO20
   K2=K-1
   SG=G(ID*IIN)
   I1=IIN+1
   DO 80 I1=I1,N
80 G(IV*I)=A(I,IIN)
   IF (IIN.EQ.K)GOTO86
   I2=IIN+2
   S0=1./SG
   DO 85 I=IIN,K2
   V=G(IV*I1)

```

```

INV13190
INV13200
INV13210
INV13220
INV13230
INV13240
INV13250
INV13260
INV13270
INV13280
INV13290
INV13300
INV13310
INV13320
INV13330
INV13340
INV13350
INV13360
INV13370
INV13380
INV13390
INV13400
INV13410
INV13420
INV13430
INV13440
INV13450
INV13460
INV13470
INV13480
INV13490
INV13500
INV13510
INV13520
INV13530
INV13540
INV13550
INV13560
INV13570
INV13580
INV13590
INV13600
INV13610
INV13620
INV13630
INV13640
INV13650
INV13660
INV13670
INV13680
INV13690
INV13700
INV13710
INV13720
INV13730
INV13740
INV13750
INV13760
INV13770
INV13780

```

```

DC 100 L=I1,J1
100 Z=Z+A(J,L)*A(L,I)
101 A(J,I)=-Z
102 CONTINUE
AA=1./G(ID*I1)
G(N*I1)=AA
DO 111 J=1,I
Z=A(I1,J)*AA
G(N*J)=G(N*J)+Z*A(I1,J)
IF (I.EQ.1) GOT0111
J1=J+1
DO 110 L=J1,I
110 A(L,J)=A(L,J)+A(I1,L)*Z
111 A(I1,J)=Z
RETURN
END

```

```

INV14990
INV15000
INV15010
INV15020
INV15030
INV15040
INV15050
INV15060
INV15070
INV15080
INV15090
INV15100
INV15110
INV15120
INV15130
INV15140

```

```

899 CONTINUE
  IF (Z.GE.ALPHA)GOTO26
  ALPHA=Z
  LB=J
  IIN=IOUT
  LIIN=LIOUT
  GOTO26
90 CONTINUE
  K2=K1+1
  IF (SIG.EQ.1.)GOTO91
  DO 901 I=K1,N
901  G(IAS+I)=-G(IAS+I)
91 CONTINUE
  IF (IOUT.EQ.K1)GOTO97
  LT(IOUT)=LT(K1)
  LT(K1)=LIOUT
  G(IAS+IOUT)=G(IAS+K1)
  G(ICAC+IOUT)=G(ICAC+K1)
  G(ICAC+K1)=SAS
  G(IOUT)=G(K1)
  IF (K.EQ.0)GOTO97
  DO 92 I=1,K
  Z=A(K1,I)
  A(K1,I)=A(IOUT,I)
92  A(IOUT,I)=Z
93 CONTINUE
  IF (K2.EQ.IOUT)GOTO95
  I1=IOUT-1
  DO 94 I=K2,I1
94  A(IOUT,I)=A(I,K1)
95 CONTINUE
  IF (IOUT.EQ.N)GOTO97
  I1=IOUT+1
  DO 96 I=I1,N
96  A(I,IOUT)=A(I,K1)
97 CONTINUE
  G(K1)=0.
  K=K1
  IF (K.EQ.N)GOTO27
  DO 98 I=K2,N
  Z=G(IAS+I)/SAS
  A(I,K1)=Z
98  G(ICAC+I)=G(ICAC+I)-Z*G(IAS+I)
  K1=K2
  GOTO20
C
  ENTRY VE04B(N,A,IA,G,K)
  IF (K.EQ.0)RETURN
  ID=N+N
  G(N+1)=1./G(ID+1)
  IF (K.EQ.1)RETURN
  N1=K-1
  DO 111 I=1,N1
  I1=I+1
  A(I1,I)=-A(I1,I)
  IF (I.EQ.N1)GOTO102
  I1=I+2
  DO 101 J=I1,K
  Z=A(J,I)
  J1=J-1

```

```

INV14390
INV14400
INV14410
INV14420
INV14430
INV14440
INV14460
INV14480
INV14470
INV14480
INV14480
INV14490
INV14500
INV14510
INV14520
INV14530
INV14540
INV14560
INV14560
INV14570
INV14580
INV14590
INV14600
INV14610
INV14620
INV14630
INV14640
INV14650
INV14660
INV14670
INV14680
INV14690
INV14700
INV14710
INV14720
INV14730
INV14740
INV14760
INV14780
INV14770
INV14780
INV14790
INV14800
INV14810
INV14820
INV14830
INV14840
INV14860
INV14860
INV14860
INV14870
INV14880
INV14890
INV14900
INV14910
INV14910
INV14920
INV14930
INV14940
INV14950
INV14960
INV14970
INV14970
INV14980

```

Introduction

The utilization of downhole current sources in resistivity mapping increases the resolution for detecting and delineating subsurface features. The effects of near surface inhomogeneities are immensely reduced as shown by Asch and Morrison (1988). Being sensitive to changes in resistivities, the surveys with downhole sources are well suited for monitoring surface processes such as injection or leakage of contaminants from a waste site, steam flooding for enhanced oil recovery, or production of geothermal reservoirs.

In most of these applications, the holes are steel-cased and the casing distorts the current flow in the medium. Holladay and West (1984) have shown ^{that} ^{that} the surface resistivity surveys are strongly affected by casings. Also, Kauahikaua et al. (1980) showed that if the casing itself is used as an electrode, the results are unpredictable because the current leaves the pipe irregularly due to the variability of the contact resistance between the pipe and the formation.

To study the casing effects in more detail, we have recently formulated the problem for a point source of current, either inside or outside the pipe, on the axis of a finite length metal pipe in a conductive half space. The first part of this study (Schenkel and Morrison, 1987) showed that only the region very near the pipe exerts any substantial influence on the potential fields for a point source 100 casing diameters beyond the end of the pipe (Figure 1). For a 5% or less field distortion, the surface measurements must not be closer than 1/2 the pipe's length. In cross-hole surveys, the affected area is greatly reduced; near the pipe's end, measurements as close as 1/6 the length of the pipe for a 5% or less distortion. If the pipe-source separation is sufficiently large, then the resistivity survey can be corrected for the casing effects (assuming that the target are not too close to the pipe).

This study showed that cross-hole and hole-surface studies may be conducted with very little effects: even when the pipe exerts some influence, e.g., when the current source is close to the end, time monitoring experiments could be carried out with very little reduction in the signal strength. Further, this study revealed the intriguing possibility that segments of pipe, separated by insulated couplings, could be used as electrodes.

Proposed Work

The above study was only developed for a very simple case, i.e., a pipe in a homogeneous half-space. A more complex model is required to simulate field situations. Several aims are proposed to create a realistic model and to evaluate field measurements for downhole sources in steel cased wells. These objectives are:

- 1) To determine the effects of contact resistance between the pipe and the host medium. Contact resistance is used to describe the resistance of the pipe-medium contact. If there is a large contact resistance, the results will completely change. The currents in the pipe will only leak out of the pipe in areas where the pipe has made a good contact with the host medium, thus completely changing the potential fields around the pipe. The contact resistance may be found by assuming a very thin layer between the host and pipe for each segment (Figure 2). An equivalent layer can be used to represent the effects of the contact resistance for each segment. The calculated potential field is obtained from the integral equation solution of the pipe variables. With the additional layer included to the model, the effects of pipe coating, corrosion, and cement on the potential fields can be evaluated.
- 2) To use insulated pipe segments as downhole sources and receivers. Downhole current electrodes can be created by energizing isolated segments. Likewise, insulated segments could be used as potential electrodes. By insulating several segments in the well (Figure 3), multiple

downhole source locations could be used to image a target in a hole-surface survey. A pole-pole configuration can be achieved by attaching to different segments current and potential electrodes. The isolated segments in the well can be used for an AC vertical electric dipole. By attaching to adjacent segments a positive and negative AC source, a grounded electric dipole can be produced to study EM properties of the medium. If an additional well is drilled with multiple isolated segments, then cross-hole DC and AC measurements can be acquired. Thus, cross-hole DC tomography (Daily and Morely, 1988 and Shima and Saito, 1988) could be used to reconstruct an image of a target between the two wells.

- 3) To determine the interaction between the source, pipe, and the anomalous body (Figure 4). To monitor the changes in the body, the effects of the metal pipe-body interaction must be investigated. The extent of this interaction will greatly depend on the source separation from the pipe, the distance between the pipe and the body, and the conductivity of the body. The determination of the limiting values of these parameters in which the body and pipe has very little coupling will be the main objective. For this situation, the body can be modeled alone saving computational time.
- 4) To invert for the geometric parameters for a plume-like body. An integral equation solution of an ellipsoidal model will be used to represent the plume. The parameters of the three axial lengths will be obtained by a non-linear least squares inversion which will make use of the integral equation solution. Sensitivity analysis and minimum spatial coverage will be evaluated for various acquisition array configurations.

Computer models will be required to investigate the above proposed tasks. The current algorithm is flexible so that variable source locations, segment lengths, and segment conductivities can be used. The development of an algorithm which includes an anomalous body and an outer layer is

needed. The current integral equation solution can be extended to include an additional layer and a circular disk. The circular disk is a first order approximation to a plume and will give an estimate of the pipe-body interaction.

Various lengths and separations of the insulated segments will be investigated to determine when a point approximation of the segments can be used. The outer layer will be used to evaluate the role of contact resistance on the field distortion and may be included to the pipe-body coupling phenomenon. The spatial separation of the source, pipe, and body to decouple the pipe and the body will be studied.

Field test and model verification are also required. The test would be conducted at U.C. Berkeley, Richmond Field Station where there exist several plastic-cased holes. Four additional 100 foot holes are also needed. Two of the wells will be composed of alternating steel and fiberglass segments. Another would be cased with steel with the last 20 feet perforated. The last well needs to be plastic cased and perforated at the bottom. A surface grid and/or radial arrays of potential electrodes would be installed over the area. Cross-hole and hole-surface measurements would be compared to calculated fields of various pipe models. An injection of the salt water in both the steel-cased and plastic-cased wells would be measured for hole-surface, cross-hole, and pole-pole configurations. These data would be forward modeled and inverted to determine the geometry of the plume. Lastly, other configurations for which models have been published can be field tested with this field setup.

REFERENCES

- Asch, T., and Morrison, H.F., 1988, Mapping and monitoring electrical resistivity with surface and subsurface electrode arrays: (Submitted to *Geophysics*).
- Daily, W. and Yorkey, T.J., 1988, Evaluation of cross-borehole resistivity tomography: Presented at the 58th Annual International SEG meeting in Anaheim.
- Holladay, J.S. and West, G.F., 1984, Effect of well casings on surface electrical surveys: *Geophysics*, **49**, p. 177-188.
- Kauahikaua, J., Matice, M., and Jackson, D., 1980, Mise-a-la-masse mapping of the HGP-A geothermal reservoir, Hawaii: *Geothermal Resource Council, Transactions*, **4**, p. 65-68.
- Schenkel, C.J. and Morrison, H.F., 1988, Effects of the well casing on potential field measurements: (Submitted to *Geoexploration*).
- Shima, H. and Saito, H., 1988, Application of resistivity tomography for detection of faults and evaluation of their hydraulic continuity: some numerical experiments: Presented at the 58th Annual International SEG meeting in Anaheim.